Title
Sex differences in hypothalamic responses to stress following chronic intermittent ethanol exposure

Author
Munier, Joseph J

Publication Date
2022

Peer reviewed|Thesis/dissertation

UNIVERSITY OF CALIFORNIA
Los Angeles

Sex differences in hypothalamic responses to stress following chronic intermittent ethanol exposure

A dissertation submitted in partial satisfaction of the
requirements for the degree Doctor of Philosophy
in Molecular, Cellular & Integrative Physiology

by

Joseph James Munier

2022

ABSTRACT OF THE DISSERTATION

Neurophysiological mechanisms of sex-dependent effects of chronic intermittent ethanol on hypothalamic stress-associated plasticity

by

Joseph James Munier
Doctor of Philosophy in Molecular, Cellular, and Integrative Physiology
University of California, Los Angeles, 2022
Professor Igor Spigelman, Chair

Alcohol use disorder (AUD) is a chronic, relapsing disorder that represents a substantial societal burden at a global scale. In the US alone, AUD is associated with societal and financial costs exceeding $249 billion per year. While many use alcohol for its reported anxiolytic and gregarious properties, consuming alcohol directly activates the hypothalamic stress axis. Persons with AUD, that are consistently exposed to this stressful stimulus, are known to have alterations in the acute response to alcohol. Little is known about how chronic ethanol exposure alters the plastic and metaplastic responses of stress, *per se*.

Relapse remains a main barrier in the pharmaceutical treatment of AUDs. While there are some medications currently available for AUD, none explicitly target the hypothalamic-pituitary-adrenal (HPA) axis. Further, sex is an essential variable to consider when pharmacologically targeting the HPA axis, as both acute and developmental effects of gonadal hormones can influence neuronal signaling in various brain regions. In Chapter 1, I investigate the effect of chronic intermittent vapor exposure to progressively increasing doses of ethanol (CIE) followed by protracted withdrawal on the physiological response to norepinephrine (NE; 10μM). I also investigate the mechanistic contributions of specific α adrenergic receptors (AR; α1AR & α2AR) on the CIE-induced neurophysiological effects.

The paraventricular nucleus of the hypothalamus initiates a robust glutamate signal to start the overcome tonic GABAergic inhibition and adaptively coordinate stress-associated behaviors. We have previously shown that this metaplastic feature is disrupted in gavage models of CIE due to altered function of N-methyl D-aspartate receptor. In Chapter 2, I demonstrate that the CIE_{vapor} model produces a similar impairment in hypothalamic metaplasticity. I also demonstrate how this effect is impacted by blockade of α1AR (with prazosin; 10μM).

Astrocytes and neurons undergo a complex interplay in response to changes in the chemical gradient of various neurotransmitters. Both neurons and astrocytes have distinct responses during acute alcohol intoxication and protracted withdrawal. In Chapter 3, I investigate differences in how astrocytes and/or neurons may impact the noradrenergic activation and subsequent glucocorticoid receptor mediated inhibition of the HPA axis.

The tripartite synapse is very likely involved in the regulation of stimulation-induced plasticity due to the critical role astrocytes play in glutamate shuttling, neurotransmitter release and regulation of synaptic activity. Despite this, we have not found studies evaluating the contribution of astrocytes to the metaplastic short-term glutamatergic potentiation onto CRF neurons following high-frequency stimulation. In Chapter 4, I investigate cell-specific differences to spontaneous Ca^{2+} events and event kinetics following $CIE_{vapor.}$

Various preclinical models of AUD can reliably induce anxiety-like behavior. However, AUD models fail to have full penetrance of ethanol (EtOH) preference and escalation of consumption behaviors. There are also noted genetic differences that contribute to EtOH preference. In Chapter 5, I investigate differences to stress-associated and consummatory alcohol behaviors following CIE_{vapor} treatment. I also investigate the convergence and divergence of stress-related and consummatory behaviors with neurophysiological features of *ex vivo* Ca^{2+} signals

2022

Dedication

I would like to dedicate this thesis to my grandparents, Gloria and Girolamo Altomare, who were critical in the early discovery of my love for science. I thank God for the perseverance and grace to overcome the various obstacles that came into my life over the course of my doctoral studies. I thank my mother, Diane Munier, for pushing me to strive for constant improvement. I thank my beautiful wife Laurel, who has helped me to become the best version of myself. I also thank Drs. Vincent Marty and Peixiang Zhang for their patient tutelage and mentorship for the past six years. I also thank my research mentor, Dr. Igor Spigelman, for his guidance and support on my path towards an independent scientific career and the knowledge shared of the many potential boons and pitfalls of preclinical drug development. Thank you to all my dissertational committee members for your feedback during the progress of my experiments. A special thank you to Drs. Reue, Fanselow, O'Neill, and Izquierdo for your outsized and generous support of my growth and development as a scientist through our collaborative efforts at UCLA.

TABLE OF CONTENTS

LIST OF FIGURES

Chapter 1

Chapter 2

Chapter 3

Chapter 4

Chapter 5

ACKNOWLEDGEMENTS

Portions of Chapter 1 and Chapter 2 are from a manuscript published in Alcoholism: Clinical and Experimental Research:

Munier J.J., Marty V.N., Spigelman I. (2022) Sex differences in alpha-adrenergic receptor signaling underlies maladaptive metaplasticity following chronic intermittent ethanol exposure (*Alcoholism: Clinical and Experimental Research*)

Portions of Chapter 3, 4 and 5 are from a manuscript in submission to *Neurobiology of Stress*

Munier, J.J. , Shen, S. , Hanna, A. , Marty, V.N. , O'Neal, P.R. , Fanselow, M.S. , and Spigelman, I. (2022). Chronic intermittent ethanol exposure disrupts stress-related tripartite communication to impact affect-related behavioral selection

I would also like to thank Nicole Gamboa, Sophia Shen, Anthony Hanna, Jasmine Pannu, Daniel Barrows, Megan Gomez, Mia Joseph, and Mikhail Izraylev for their contributions to this work.

Financial support for this research was provided by:

NIAAA [grant number F31AA028183] (JJM)

NIH/NIDA [grant number T32DA024635] (JJM)

NIAAA [grant number AA024527] (IS)

NIAAA [grant number R01AA026530] (IS/MSF)

VITA

Education

2018 Advanced to Candidacy, Ph.D. in Molecular, Cellular, and Integrative Physiology
University of California, Los Angeles, CA

2014 Bachelors of Science with Honors, Biochemistry
Lehigh University, Bethlehem, PA

Publications

Munier J.J., Marty V.N., Spigelman I. (2022) Sex differences in alpha-adrenergic receptor signaling underlies maladaptive metaplasticity following chronic intermittent ethanol exposure. *Alcoholism: Clinical and Experimental Research*, 46(8):1384-1396.

Munier J.J., Pank J.T., Severino, A., Wang, H., Vergnes, L., Zhang, P., Reue, K. (2022) Simultaneous monitoring of mouse grip strength and force flux distinguishes muscle physiology following surgical, pharmacologic and diet interventions (*Scientific Reports*)

Zhang P., **Munier J.J.** Ronquillo E., Reue, K. (submitted 2022) X chromosome dosage drives statin–induced dysglycemia and mitochondrial dysfunction (in peer review at *Nature Communications*)

Marty V.N., Farokhnia M., **Munier J.J.**, Mulpuri Y., Leggio L., Spigelman I. (2020) Long-Acting Glucagon-Like Peptide-1 Receptor Agonists Suppress Voluntary Alcohol Intake in Male Wistar Rats. *Front Neurosci.* Dec 23;14:599646.

Marty V.N., Mulpuri, Y., **Munier J.J.,** Spigelman I. (2020). Chronic alcohol disrupts hypothalamic responses to stress by modifying CRF and NMDA receptor function. *Neuropharmacology*. 2020;167:107991.

Mulpuri Y., Marty V.N**, Munier, J.J.,** Mackie K., Schmidt, B. L., Seltzman H. H., Spigelman I. (2018). Synthetic peripherally-restricted cannabinoid suppresses chemotherapy-induced peripheral neuropathy pain symptoms by CB1 receptor activation. *Neuropharmacology*, Volume 139, Pages 85-97, ISSN 0028-3908.

Spacek, L. a, Mudalel, M. L., Lewicki, R., Tittel, F. K., Risby, T. H., Stoltzfus, J., **Munier, J. J**. Solga, S. F. (2015). Breath ammonia and ethanol increase in response to a high protein challenge. *Biomarkers : Biochemical Indicators of Exposure, Response, and Susceptibility to Chemicals*, *0*(JUNE), 1–8.

Presentations

Munier, J. J., Marty, V. N., Gamboa, N., Spigelman, I. (2020). Chronic intermittent ethanol exposure dampens small conductance Ca^{2+}-activated K^{+} channels in magnocellular hypothalamic neurons in a sex-specific manner. Abstract. Research society on alcoholism.

Munier, J. J. (2020). Sex differences in the effect of chronic ethanol exposure on hypothalamic synaptic plasticity. Presentation. Translational neuroscience of drug abuse T32 retreat

Marty, V.N., Mulpuri, Y., **Munier, J. J.**, S. Lele, R.H. Vo, I. Yenokian, A. Liao, I. Spigelman. Synthetic peripherally-restricted cannabinoid suppresses voluntary alcohol intake in rats via non-CB1/CB2 receptor action. (2019). Abstract. Research Society on Alcoholism

Munier, J. J. (2019). Sex differences in the effect of chronic ethanol exposure on hypothalamic synaptic plasticity. Presentation. Translational neuroscience of drug abuse T32 retreat

Munier, J. J., Marty, V. N., Izraylev, M., Lele, S., Liao, A., Yenokian, I., Vo, R. H., and Spigelman, I. Norepinephrine-induced suppression of glutamatergic transmission onto parvocellular hypothalamic
neurons is impaired following chronic-intermittent ethanol exposure. (2019). Abstract. Research Society on Alcoholism.

Marty, V., Mulpuri, Y., **Munier, J.J.,** Lele, S., Spigelman, I. (2018). Effects of different modes of alcohol administration on hypothalamic synaptic plasticity and HPA axis hormonal and behavioral responses to stress. Abstract. Society for Neuroscience.

INTRODUCTION

Alcohol use disorder (AUD) is a chronic relapsing disorder that imposes a societal burden on a global scale [1]. As of 2010, it cost the American taxpayer an estimated 249 billion dollars per year. In addition to the third leading cause of preventable morbidity and mortality [2], alcohol use also causes an undue amount of harm to those around afflicted by AUD [3]. While some drugs are approved for the treatment of AUD, there remain significant gaps. For example, no drugs available for the treatment of alcohol use disorder explicitly target stress neurocircuitry [4] . This is especially important when considering that relapse, while hard to define [5], remains persistently high in patients with are high (~20-30% [6,7])

AUD is characterized a loss of intake control, a preoccupation of/craving consuming alcohol, and a negative emotional state [8,9]. Chronic, intermittent phases of alcohol intoxication and withdrawal creates a state of dependence in both animal models and humans. The allostatic load, or the altered set-point of mood below the origin [10] has been thought to play an essential role in the development of many of the characteristic behavioral impairments due to chronic intermittent ethanol (CIE) exposure [11]. However, the neural mechanisms underlying allostasis at a fundamental level remain incompletely understood.

The Paraventricular nucleus of the hypothalamus: An integrative stress nucleus

Corticotrophin-releasing factor-containing cells as effectors of the hypothalamic-pituitary-adrenal axis

The hypothalamic-pituitary-adrenal (HPA) axis is a neuroendocrine system responsible for coordinating a plethora of physiological responses to stressful stimuli [12]. Within the paraventricular nucleus of the hypothalamus (PVN), corticotropin releasing factor (CRF) cells integrate upstream brain signals and neurotransmitter cues to tightly coordinate this response adaptively [13]. After sufficient activation, release of CRF from these cells causes the HPA axis cascade negatively feeds back through action of glucocorticoids within the PVN [14]

Under normal physiological conditions, the PVN is constrained by strong GABAergic inhibition [15]. However, PVN PNCs have a unique form of metaplasticity that is believed to facilitate the rapid, appropriate response to incoming threats. In animals exposed to various

stressors (ranging from restraint to social isolation to social transfer [16–18], CRF PNCs show a short burst of potentiation at glutamate synapses following afferent stimulation [17] which enables a short window to overcome tonic GABAergic restraint [15]. This short-term plasticity has been shown to be related to the choice between flight and freezing in rodents [19], and is disrupted in models of CIE exposure [11]. If this response is indeed coupled to adaptive responding to stress, probing the molecular mechanisms that gives rise to this phenomenon can be particularly helpful for developing new treatments for stress-associated relapse in AUD.

Oxytocin and Arginine Vasopressin as modulators of adrenal sensitivity and stress-associated behaviors

The PVN also contains other magnocellular neuroendocrine neuron (MNCs), such as those that release oxytocin (OT) and/or vasopressin (AVP) [20–22] that, aside from their stand-alone physiological functions, play critical support roles to modulate HPA axis output by CRF PNCs. AVP acts on the pituitary synergistically with CRF to facilitate adrenocorticotrophic hormone (ACTH) release through V1bR [12,23], while OT acts conversely to dampen ACTH release [24]. AVP can suppress postsynaptic AMPAR function through Vasopressin 1a receptor (V1aR) [20,22] and mediates sex-dependent social transmission of STP onto PNCs through a complex mechanism involving neuro-glial crosstalk and V1aR [16]. Within the PVN, OT release causes rapid production of endocannabinoids from PVN MNCs to dampen presynaptic glutamate release onto both MNCs [20] and PNCs [25]. Collectively, AVP and OT have multi-faceted interaction with ethanol [26–28] and stress [16,23,29–38] and targeting these neurohormone signaling pathways has yielded some promising preclinical [39,40], yet mixed clinical results [41–45]. Due to their clear ability to augment stress-related changes to CRF PNC signaling, it is important to mind potential changes to these neurohormones when evaluating the neuroplastic changes of CRF neurons within the PVN.

PVN astrocytes help mediate metaplastic shifts in neurotransmission during physiological stress

Astrocytes are a sub-type of glia [46] with diverse physiological roles [47]. Astrocytes are that are essential for glutamate/glutamine shuttling [48] and cholesterol synthesis [49] which can modulate the synaptic activity of neighboring cells. Astrocytes also function as an essential component of the tripartite synapse, buffering the synapse of various ions and neurotransmitters to regulate the activity of the pre and postsynaptic neurons [47,50]. One novel hypothesized role of astrocytes is their

ability to serve as neural "circuit capacitors", by which they can transform and sustain temporally dispersed signals for a short period. Astrocytes can also protect injured neurons from further oxidative damage by transfer of healthy mitochondria [51].

Regulation of PVN CRF PNCs from afferent projections

As HPA axis effector neurons [12,52], many neural circuits directly or indirectly influence the activation of PVN CRF PNCs (reviewed in [13].) The PVN receives GABAergic, glutamatergic, and monoaminergic synapses from the bed nucleus of the stria terminalis [53], central and basolateral amygdala [54,55], parabrachial nucleus [56], nucleus tractus solitarus [57,58] and various hypothalamic nuclei [59–61]. Under normal conditions, PVN PNCs are constrained by tonic GABAergic inhibition [62–65], that is only able to be overcome following short bursts of amplified glutamate release [17,66] or noradrenergic activation [67]. Thus, these cells have the critical responsibility of broadly altering the host's physiological balance in response to many channels of temporally and spatially dispersed analog (from concentration gradient changes in ions and hormones) signals.

Efferent projections of PVN CRF PNCS

For an extended period, CRF PNCs were studied primarily for their role in regulating HPA axis activity. However, recent data show that CRF PNCs are involved in encoding important behaviors, such as grooming [11], environmental exploration [68], wakefulness [69], and positive and negative environmental valence [70]. These cells can also influence behaviors controlled by the lateral hypothalamus (LH) by forming efferent synapses onto orexin neurons [68,71,72] that are important for orchestrating arousal [69] and reward seeking [73]. CRF PNCs also coordinate stress responses with physiological modulation of the sympathetic nervous system and baroreflex through communication with CRF1R-expressing PVN pre-autonomic neurons and by relaying information to other brain regions, like the ventrolateral medulla and nucleus tractus solitarus [57,74–77].

Chronic intermittent ethanol (CIE) vapor exposure

Inbred rodent models of HPA axis sensitivity and responses to ethanol

Use of murine models for the scientific investigation of human pathophysiology stem from the ease and cost of breeding, genetic similarity to humans, and short life-span [78]. This has led to

a rapid expansion of genetic tools catered to mouse models, such as inbred strains and genetic knockouts. Inbred models have been useful to examine the specific genetic mechanisms of physiology and pathophysiology, due to their ability to reduce genetic variability as a source of statistical noise [78]. They are also more genetically and phenotypically stable than outbred strains with respect to time [78]. Previously, researchers relied heavily on forward genetic approaches [79]in inbred strains specifically developed for their sensitivity to stressors [80–82] (i.e., Lewis and Fisher), withdrawal severity [83], or EtOH preference (i.e., Sardinian Preferring) [84]. More recently, panels of >100 inbred strains have been utilized in the Hybrid Mouse Diversity Panel to make powerful forward genetics approaches to identify biochemical targets of important pathologies such as obesity, diabetes, and atherosclerosis [85].

Appropriate preclinical models of behavioral pathologies should have face validity, theoretical rationale, and predictive validity [86]. This can be particularly troublesome when attempting to model psychiatric pathologies preclinically, as researchers are often tasked to anthropomorphize instinctual behaviors in rodents without cross-conference [87]. For example, the elevated plus maze has been used extensively to measure anxiety-like behavior [87], but can also be impacted by the visual acuity of the strain of rodent at hand [88,89]. Additionally, some inbred strains can show increased intraindividual variability in phenotypes as varied from immunogenic response to vaccines [90] to ultrasonic vocalization [91]. Of behaviors particularly relevant to the study of AUD, inbred strains have shown limited phenotypic variability in terms of physiological HPA axis activation and EtOH preference/consumption, when compared with outbred strains [92]. The Long-Evans outbred strain of rat (generated with a Wistar female and wild male Grey Rat) retains many similar behaviors to wild rats [93], resulting in wide adoption by the behavioral neuroscience research community. Importantly, Long-Evans rats have a more sensitive HPA axis response to passively and actively stressful assays than albino outbred Sprague-Dawley rats, potentially due to increased amygdalar and PVN CRF expression [80]. Together, these data suggest strain should be carefully considered when investigating the biochemical intersection of EtOH and HPA axis activity.

The CIE_{vapor} model

Rats are a valuable preclinical model for both the assessment of physiological consequences of CIE and pharmaceutical interventions to remedy AUD-associated pathologies. They have a more nuanced behavioral profile than mice, which enables the use of a wide array of

behavioral assays that can be subsequently linked to biochemical and/or physiological mechanisms. Further, they show some important characteristics that are more human-like than mice. For example, rat metabolism is approximately 5x slower [94], allowing them to reach intoxicating blood ethanol concentrations (BECs) without the confounding use of pyrazole using traditional models [95]. As predators, rats have a more human-like behavioral profile when weighing threatening and predatory stimuli [96]. Therefore, studying the more sophisticated neural circuitry regulating HPA axis activation to appropriately coordinate fight, flight, or freeze behaviors in rats may be more translationally relevant than mice. However, Sprague-Dawley strains do not readily escalate intake or increase EtOH preference above 50% in intermittent access models [97], without the confounding application of weaning from sucrose or other palatable liquid [98]. Alternative methods that readily reach intoxicating BECs, such as liquid ethanol diet and gavage, have the unwanted side effect of causing aversion to ethanol (our unpublished observations).

The CIE_{vapor} model represents an improvement to all the methods described above for its translational utility. CIE administration through gradually increasing intermittent doses of EtOH through passive vapor consumption allows the rats to reach intoxicating BECs in a less aversive and etiologically relevant manner. CIE causes a host of changes to neuronal physiology through direct action of ethanol, and indirect action of its metabolites [99–102]. Following CIE_{vapor} exposure and protracted withdrawal, rats demonstrated the emergence, dynamic remission, and resurgence of anxiety-like behaviors during acute (~8 hours), early protracted withdrawal (2 weeks), and late protracted withdrawal (6-12 weeks) in male CIE_{vapor} rats, respectively [103]. Additionally, CIE rats will readily self-administer EtOH in greater quantities than air exposed controls [104]. Interestingly, despite the uniform display of anxiety behaviors, only some rat strains escalate intermittent access two bottle choice ethanol consumption following CIE_{vapor} [105]. Further, CIE_{vapor} males have key alterations to self-grooming behavior [11], which we hypothesize to be a behavioral biomarker of an inability to adequately cope with stressors.

As stress-related relapse to alcohol consumption is a major hurdle for the ongoing treatment of AUD, we specifically chose an extended period of protracted withdrawal in these studies to separate the persistent HPA axis neuroadaptations of CIE [106,107] from acute withdrawal effects.

Physiological changes of neurons in response to CIE

Ethanol can induce a plethora of changes to neuronal physiology and function. Despite its low potency (efficacious only at mM *in-vivo* concentrations), EtOH can directly modulate neuronal activity through its ability to act as a positive allosteric modulator at $GABA_A$ receptors, allowing more Cl^- ions to flow across their concentration gradient per ligand-receptor interaction. EtOH also acts as an NMDAR antagonist, preventing the depolarization-dependent flow of Ca^{2+} into the post-synaptic cell. Both pharmacological effects are inhibitory, resulting in the loss of motor coordination and respiratory function at high doses.

Persistent effects from upregulation of neuronal proteins have also been noted. Indeed, CIE has been shown to dysregulate GABAergic [108,109], glutamatergic [11,110], OTergic[111], cholinergic[112], noradrenergic [110,113] and dopaminergic [114–116] synapses throughout the brain. Some of these findings have been reflected in post-mortem human brain in individuals afflicted with AUD, such as an upregulation of α1AR [65], CRF1R, or glutamate receptor NMDA type 1 [117]. These are some of the many instances that serve to exemplify the broad neurological consequences of repeated consumption of intoxicating quantities of EtOH [113].

Physiological response of astrocytes to CIE

Chronic alcohol exposure induces robust gliosis throughout the brain[118], but particularly in the cortex and hypothalamus [119], causing lasting changes to the electrophysical properties of tripartite synaptic function. Astrocytes have shown important roles modulating anxiety and the acute sedative and intoxicating properties of EtOH *in-vivo* [120,121]. Astrocytes serve cooperative action at post-synaptic neurons expressing α1AR and GluN2B [122,123] during normal physiological states. Both proteins display increased function following CIE exposure [11,113], raising questions to how these signals may affect tripartite synaptic communication at large.

Impact of sex as a biological variable

Biological sex greatly influences the response of neurons to ethanol through both direct and indirect effects of gonadal hormones [32,124–129], as well as potentially through genetic effects [130]. While males are historically more likely to develop AUD, this gap has progressively shrunk [131]. This may be attributable in part to a large increase in hazardous drinking during adolescence[132] which synergizes with a hastened, risk-oriented path to facilitate the formation of compulsive drug

seeking in females [133,134]. Females are also more likely to drink in response to stress or to alleviate a negative emotional state [135].

Other physiological mechanisms are also at play. Female noradrenergic neurons within the locus coeruleus are more sensitive to CRF-induced firing increases [136] and females are more sensitive to alcohol reinstatement following α2AR antagonism [137]. Female astrocytes have a selective upregulation of astrocytic glutamate transporters EAAT1. On the other hand, males may be particularly vulnerable to CIE-induced effects in limbic regions, including alterations in endocannabinoid [138] and κ-opioid signaling [139] in the basolateral amygdala, and inhibitory current kinetics in the central amygdala [140]. Further, only male Long Evans rats escalate two-bottle choice intake following CIE [105]. Together, these data suggest subtle sex differences in the various mechanisms contributing to altered neuronal physiology and behavioral states following CIE treatment.

Negative affect-driven behavioral states in AUD

The drug addiction cycle model put forth by Koob and colleagues is composed of three independent stages: binge/intoxication, withdrawal/negative affect, and preoccupation/anticipation [141,142] . Patients with AUD frequently report anxiety and a negative emotional state as potent triggers of craving and relapse [143]. While initial studies focused primarily on how the extended amygdala contributes to negative affect during protracted withdrawal/abstinence (reviewed [142]), it is becoming increasingly clear that many brain regions influence various stages of addiction. PVN PNCs encode positive and negative valence to environmental stimuli [70]. Therefore, understanding how CIE alters PVN PNC synaptic excitability may help those with AUD successfully maintain abstinence.

Dissertation objectives

In Chapter 1, I investigate whether male and female hypothalamic CRF neurons show altered responses to NE following exposure to CIE$_{vapor}$ and protracted withdrawal. I also assess the receptor specificity of NE-mediated effects on CRF neurons. I hypothesize that females will be relatively protected from CIE-induced changes to NE-mediated plasticity.

In Chapter 2, I investigate how stress-dependent, high-frequency stimulation (HFS)-induced short-term potentiation (STP) of glutamate synapses is affected by CIE_{vapor}. I also investigate the role of α1AR in the formation of this plasticity. I hypothesize that CIE_{vapor} cells will show similar dysfunction in STP formation following stress. I also anticipate antagonism of α1AR with prazosin will restore this loss of STP formation in CIE male rats.

In Chapter 3, I investigate the cell-type specific (neuronal v. astrocytic) differences in calcium signals following acute exposure to a pharmacological stressor. I predict there will be cell-specific differences to both astrocytes and neurons in CIE rats that are related to functional differences in noradrenergic receptor activity.

In Chapter 4, I investigate the cell-type specific differences in frequency of suprathreshold events and event kinetics following high-frequency field stimulation during different phases of the pharmacological stress protocol. I hypothesize stimulation-induced differences to astrocytic Ca^{2+} spike kinetics underlies CIE-induced deficits to stress-dependent glutamatergic metaplasticity.

In Chapter 5, I investigate the behavioral consequences of CIE vapor exposure in outbred Long-Evans male rats, and the relationship between behaviors and physiological Ca^{2+} responses to a pharmacological stress. I hypothesize that behavioral deficits in CIE rats are correlated to signaling changes in astrocytes in response to pharmacological stress, implicating neuroendocrine regulation of PVN neuro-glial communication in maladaptive CIE-associated behaviors.

CHAPTER 1

Sex-specific impairment in multiple mechanisms of noradrenergic action following chronic intermittent ethanol exposure

Abstract

Males and females have differences in both the regulation of noradrenergic receptors and intrinsic excitability of noradrenergic neurons. The noradrenergic system is an essential component of initiating the activity of the hypothalamic-pituitary-adrenal (HPA) axis to coordinate an adaptive physiological response to stressful stimuli. Here we demonstrate how norepinephrine (NE) acts on noradrenergic receptors (α1AR, α2AR) to cause an excitatory, inward current and inhibitory reduction in glutamate transmission, respectively onto the principal neurons governing HPA axis activation. Both effects are influenced in a sex-dependent manner, with females being relatively resilient. Additionally, CIE cells were hypersensitive to α2AR antagonism. Together, this provides insight towards the mechanisms by which NE can influence HPA axis activity in both males and females.

Introduction

Alcohol use disorder (AUD) is characterized by a loss of intake control, negative emotional state, and inability to cope with acute stressors [144]. While AUD is more likely to afflict males historically, this gap has rapidly diminished in recent years [131]. Norepinephrine (NE) is an essential neurotransmitter for gating the initiation of the neuroendocrine hypothalamic-pituitary-adrenal (HPA) axis response to stress [58]. However, the mechanisms by which NE acts on corticotropin-releasing factor (CRF) containing neurons in the hypothalamus to gate activation of the HPA axis response to stress, and the influence of both sex as a biological variable and chronic intermittent exposure to ethanol (CIE) physiologically are all underexplored.

The HPA axis acts to broadly influence host physiology and behavior in response to an acute stimulus in an evolutionarily favorable manner. For example, in response to a predator-related cue, such as scent or a looming shadow, animals must choose between three main options (*i.e.* freeze, fight, or flight). The hosts physiology must also be shifted towards a state of increasing oxidizable fuel availability [145,146] if the choice of flight is to be made. Awareness must also be heightened to be able to choose an opportune time to resume movement. These broad responses are carried out by acute increases in the neuroendocrine factors released by the HPA axis, such as CRF, adrenocorticotropic hormone, and glucocorticoids (CORT) [12]. However, this response needs to be tightly regulated due to the metabolic and other costs of maintaining a hypervigilant state [10,145]. Some of these mechanisms include regulation of CRF cells through excitatory and inhibitory neurotransmitters, such as glutamate and y-aminobutyric acid (GABA), respectively [13]. There are also abundant NE afferents from the nucleus tractus solitarus that impinge directly onto CRF cells [58] that can trigger CRF release [147]. Additionally, these hypothalamic CRF neurons can positively and negatively encode valence of surroundings, due to their ability to detect and respond to aversion [70]. Thus, synaptic flexibility of these neurons is vastly complex and of critical importance to the health and wellness of the host.

NE exerts its effects through 5 main adrenergic receptor subtypes (α1, α2, and β1-3; reviewed in [148]). α1 adrenergic receptor (α1AR) is an excitatory G_q-coupled G-protein coupled receptor (GPCR) in that is present on CRF neurons and causes an increase in firing [123,149]. α2AR is a G_i GPCR that is present primarily presynaptically to negatively regulate the activity of this arousal circuit following stimulation [150]. Despite hyperactivity in noradrenergic signaling during

alcohol withdrawal [151], pharmaceutical interventions targeting this system have been neglected until recently [4,152]. Thus, we aim to uncover the mechanistic consequences of CIE on NE action at hypothalamic CRF cells to help address this important therapeutic gap.

Sex is a critical factor in the synaptic flexibility of CRF neurons. Gonadal hormone, estradiol (E_2), can influence the incorporation of α1 adrenergic receptor (α1AR) in hypothalamic neurons [153], thus limiting the sensitivity to NE throughout the estrous cycle. Female noradrenergic neurons within the locus coeruleus are more sensitive to CRF-induced firing increases [136] and females are more sensitive to alcohol reinstatement following α2AR antagonism [137]. On the other hand, males may be particularly vulnerable to CIE-induced effects in limbic regions, including alterations in endocannabinoid [138] and κ-opioid signaling [139] in the basolateral amygdala, and inhibitory current kinetics in the central amygdala [140]. Together, this suggests subtle potential sex differences in the effects of NE exerts onto CRF neurons, especially following treatment of CIE.

Others have demonstrated the emergence, dynamic remission, and resurgence of anxiety-like behaviors during acute (~8 hours), early protracted withdrawal (2 weeks), and late protracted withdrawal (6-12 weeks) in male CIE_{vapor} rats, respectively [103]. We specifically chose an extended period of protracted withdrawal to separate the persistent HPA axis neuroadaptations [107,154]from acute withdrawal effects [155] seen previously. Therefore, I have used a model of CIE through intermittent vapor access followed by protracted withdrawal in male and female rats to assess the persistent HPA neuroadaptations of CRF neurons to NE and the mechanisms that contribute to this potential disturbance through pharmacological antagonism at α1AR and α2AR.

Materials and Methods

Animals

All experiments were performed in accordance with the guidance of the National Institutes of Health on animal care and use and the University of California, Los Angeles Animal Research Committee. Male or female Sprague Dawley rats (weighing 200-225 g or 150-185 g, respectively) were pair-housed under 12-hr 6AM/6PM light/dark cycle with *ad libitum* access to food, water and environmental enrichment.

Ethanol (Decon Laboratories, King of Prussia, PA) was administered via custom-built vapor chambers (La Jolla Alcohol Research, Inc.) for 12 hour on/off cycles (on at 10PM), referred to as chronic intermittent ethanol (CIE) as previously described [104]. Animals in their home cages passively consumed ethanol in gradually increasing doses throughout the 40-day experiment (Suppl. Fig. 1). Body weight was measured weekly to monitor potential adverse effects of ethanol exposure. Tail vein blood (30-50 μl) was collected into heparinized tubes (Microvette CB300, Starstedt, Germany) immediately following 12-hr vapor exposure during the last experimental week. Blood samples were centrifuged at 2,000 g for 10 min at room temperature and the EtOH content of each sample measured in duplicate along with EtOH standards using the alcohol oxidase reaction procedure (GM7 Micro-Stat, Analox, Huntington Beach, CA). A cutoff of >150 mg/dl of ethanol in plasma was used to confirm that an intoxicating level of ethanol was reached in each rat [156]. Animals were subsequently withdrawn for a period of 30-108 days to evaluate the post-acute effects of CIE exposure on PNCs, which was employed to disentangle the persistent adaptations to the HPA axis seen previously [154,157], from the effects of acute withdrawal. Room air-exposed, weight- and age-matched rats were used as controls. In some experiments, rats were confined in a Plexiglas restrainer (Braintree Scientific, Braintree, MA) for 30 min immediately prior to euthanasia.

Electrophysiology

The investigators performing the recordings were blind to the treatment (CIE or Air) that the rats received. CIE- and Air-exposed rats were randomly counterbalanced throughout data acquisition. Following 30-108 days of protracted withdrawal, CIE-exposed rats and their air-exposed controls were deeply anesthetized with isoflurane (Patterson Veterinary, MA, USA), decapitated and brain submerged in ice cold bubbling artificial cerebrospinal fluid (ACSF) containing (in mM): 125 NaCl, 2.5 KCl, 1.25 NaH_2PO_4, 2 $CaCl_2$, 2 $MgCl_2$, 26 $NaHCO_3$, 10 glucose, saturated with 95% O_2 and 5% CO_2. Coronal brain slices (400 μM) were obtained (VT1200s, Leica, Buffalo Grove, IL) and sections containing the paraventricular nucleus of the hypothalamus (PVN) microdissected and stored in a separate incubation chamber for >1 hr prior to recordings.

Whole-cell patch clamp recordings were obtained from putative parvocellular neuroendocrine cells (PNCs) within the medial aspect of the PVN as defined by their distinct

electrophysiological characteristics [158] during perfusion with ACSF at 34 ± 0.5 °C. Borosilicate glass pipettes (TW150F-3, WPI, FL, USA) were pulled (Brown-Flemming P-87, Sutter Instruments, Novato CA) with 4-8 MΩ resistance tips when filled with an internal solution containing (in mM): 130 K-gluconate, 5 NaCl, 1.1 EGTA, 2 MgATP, 0.2 NaGTP, and 10 HEPES, pH adjusted to 7.3 with KOH. Action potential (AP) voltage threshold was measured at the beginning of the sharp rise of the depolarization phase in the first AP elicited by a depolarizing current pulse. Input-output curve was obtained by calculating the number of APs eliciting in response to depolarizing current steps (10-pA increments).

Excitatory postsynaptic currents (EPSCs) were evoked with a concentric bipolar stimulating electrode (MCE-100, Rhodes Medical Instruments, CA, USA) placed within the periventricular aspect of the PVN [11]. Stimulus was adjusted to elicit a sustained amplitude reaching ~1/2 maximal response for the first current. Paired-pulse ratio (PPR) was obtained by applying a pair of equipotent stimuli at an interval of 25 ms and a rate of 0.2 Hz, as described previously [11]. High frequency stimulation (HFS) of afferents at 100 Hz for 1 s, repeated four times with a 5 s interval [11] was performed following washout of all drugs. Access resistance was continuously monitored, and recording were accepted for analysis if changed were <30%. AMPAR-mediated EPSCs were isolated during continuous application of picrotoxin (50 μM; HelloBio, Princeton, NJ, HB0506) and holding the postsynaptic cell at -60 mV.

Electrophysiological signals acquired with the aid of pCLAMP10 Clampex software (Molecular Devices, San Jose, CA) were amplified using the Multiclamp 700B amplifier (Molecular Devices), low-pass filtered at 1kHz and digitized at 10kHz with the Digidata 1440A (Molecular Devices). Data were analyzed using Clampfit software (Molecular Devices). Amplitude of evoked EPSCs (eEPSCs), holding current, and PPR was normalized to the beginning of baseline recordings following stabilization. Effects of drugs on eEPSCs, holding current, and PPR were evaluated for the last five minutes of 8-minute steady-state drug applications.

Drugs

Noradrenaline bitartrate was dissolved in distilled water at a stock concentration of 100 mM and diluted in ACSF to 10 μM. Prazosin hydrochloride (Cayman Chemical, Ann Arbor, MI #15023) was dissolved in pure dimethyl sulfoxide at a 10 mM stock concentration and diluted to a final volume of 10 μM in ACSF. Atipamezole hydrochloride (Cayman Chemical, #9001181)

was dissolved in distilled water at a stock concentration of 50 mM, sonicated for 2 minutes, and diluted to a final concentration of 10 μM in ACSF. Recordings were performed in the continuous presence of picrotoxin (50 μM). All solutions equilibrated at 34 ± 0.5 °C prior to slice application.

Statistical analyses

Data are expressed as mean ± SEM. In all figures, n represents the number of cells for each group. Comparisons of basal membrane properties were done using two-way ANOVA with Tukey's post-hoc comparison. Interactions between variables (sex, CIE, effect of drug with respect to time) were performed using 3-way ANOVA. Post-hoc comparisons were made with Dunnett's multiple comparison test to compare the change of a single parameter from the last minute of baseline to the last minute of drug exposure. Comparison of short-term potentiation was made with pair-wise t-test of an average of one minute of eEPSCs immediately prior to, and immediately after high-frequency stimulation. All statistical analyses were performed using Prism 9 software (GraphPad). Alpha cutoff of 0.05 was used.

Results

CIE alters the excitability of hypothalamic PNCs in a sex-dependent manner

Prolonged alcohol exposure causes neuroadaptations to the HPA axis that persist following protracted withdrawal [11]. We first evaluated possible sex differences in the CIE-induced alterations of membrane properties of hypothalamic PNCs. CIE c a significant increase in the current required to hold cells at -60 mV only in PNCs from CIE males (Fig. 1-1 A), indicative of more depolarized resting membrane potentials in this group. We next conducted a voltage ramp test to detect differences in holding current across various membrane potentials. PNCs from CIE males required greater current to maintain their respective membrane potentials and there was a significant interaction of sex × ethanol (Fig. 1-1 B).

We next investigated the voltage threshold to elicit an action potential (AP) in these cells in response to depolarizing current pulses. We found a highly significant sex × ethanol interaction, by which CIE males had a higher AP voltage threshold than their air controls or CIE females, indicating greater depolarization needed to elicit an AP (Fig. 1-1 C, E). To determine the firing rate elicited by depolarizing current injection, we injected various currents in 10 pA increments and counted the frequency of APs elicited. We saw a significant effect of ethanol and sex on the

frequency of elicited APs, with air exposed females consistently eliciting the most APs at a given current injection (Fig. 1-1 D, F). CIE females were also able to elicit more APs than their CIE male counterparts at the 80-pA current injection (Fig. 1-1 F). Together, these results demonstrate that CIE has lasting sex-dependent effects on the membrane properties of PVN PNCs, even following protracted withdrawal.

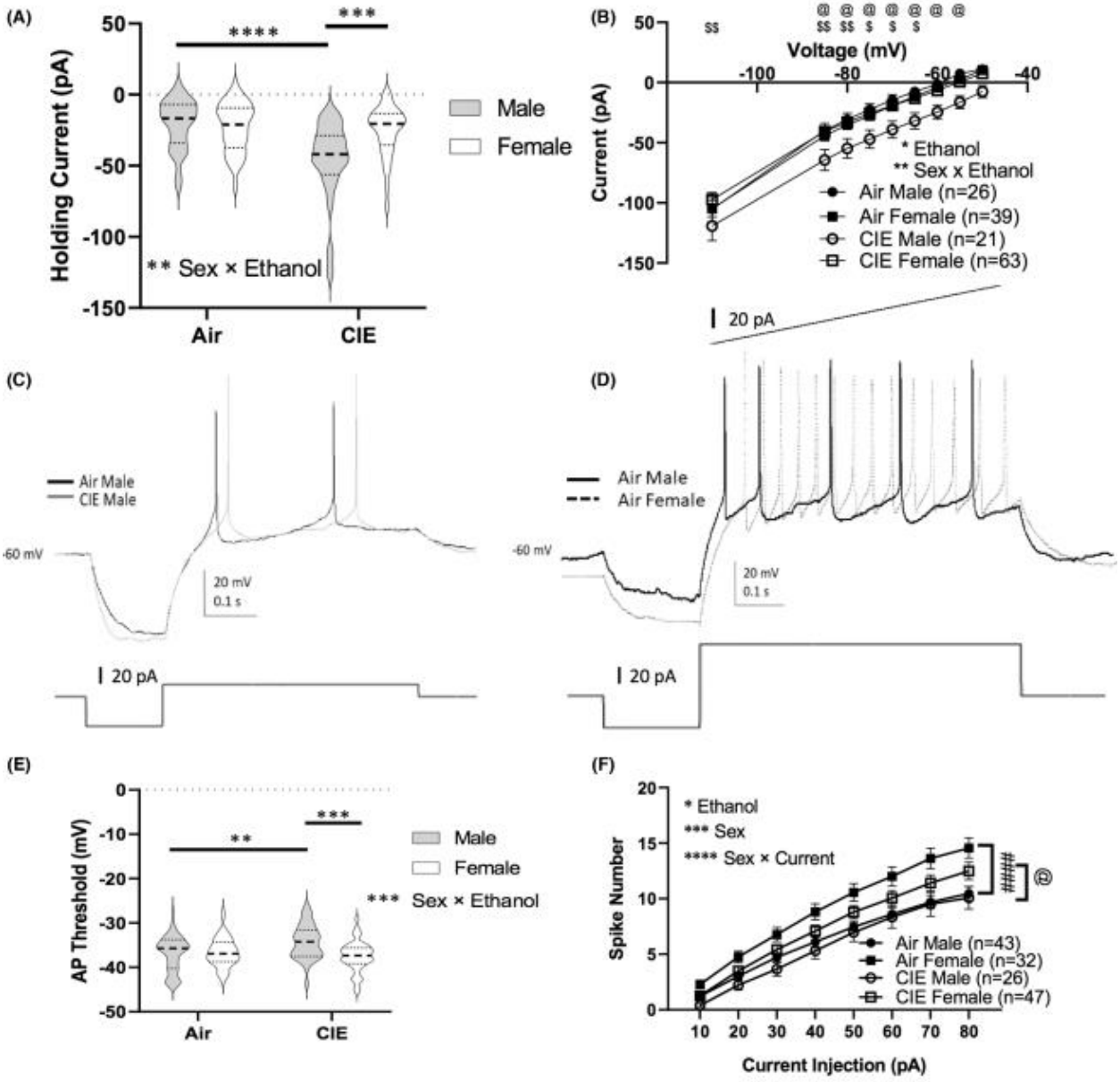

Figure 1-1: Sex-dependent effects of chronic intermittent ethanol (CIE) exposure on the membrane properties of hypothalamic parvocellular neuroendocrine cells (PNCs). **A)** CIE increases the holding current needed to maintain PNCs at -60 mV in male but not female rats. **B)** CIE increases current response to a voltage ramp only in CIE males. **C, E)** Representative traces of depolarization-induced action potentials (APs) illustrating a higher AP threshold in CIE males vs. Air males. **D, F)** Representation of depolarization-induced Aps illustrating a higher frequency of events is seen during an 80-pA current injection in air females vs. Air males. **E)** Both sex and ethanol influence AP threshold. ** $p<0.01$, *** $p<0.001$. **F)** Both sex and ethanol exposure influence spike frequency in PNCs following increasingly depolarizing current injections. * $p<0.05$, **$p<0.01$, ***$p<0.001$, ****$p<0.0001$. @ comparison between CIE males v. females; # comparison between Air males v. females. **A, E)** Two-way ANOVA. **B, F)** Three-way repeated measures ANOVA.

NE-induced inward current and suppression of eEPSC are both sex- and CIE-dependent

Noradrenergic signaling is a known regulator of the hypothalamic stress response [12,159]. Therefore, we evaluated the effects of bath application of NE (10 μM) on the excitability of PNCs. NE produced two distinct effects in recorded PNCs: a depolarizing, inward current (excitatory) and a decreased amplitude of eEPSCs (inhibitory). There was a significant interaction of sex × CIE × time for both effects. NE elicited an inward current in Air males and CIE females, but not in CIE males or Air females (Fig. 1-2 A, B). The amplitude of eEPSCs was consistently reduced following NE application in all groups when compared to baseline, except in Air females (Fig. 1-2 D, E). Interestingly, the NE-induced decreases in eEPSC amplitude were without a concomitant increase in the PPR (Fig. 1-2 F, G), suggesting a more complex mechanism than sole effects on presynaptic neurotransmitter release probability. These data suggest a dual role for NE where the excitatory effect of inward current is somewhat counterbalanced by suppression of postsynaptic glutamatergic currents. More so, these responses can be altered by CIE exposure in a sex-dependent manner.

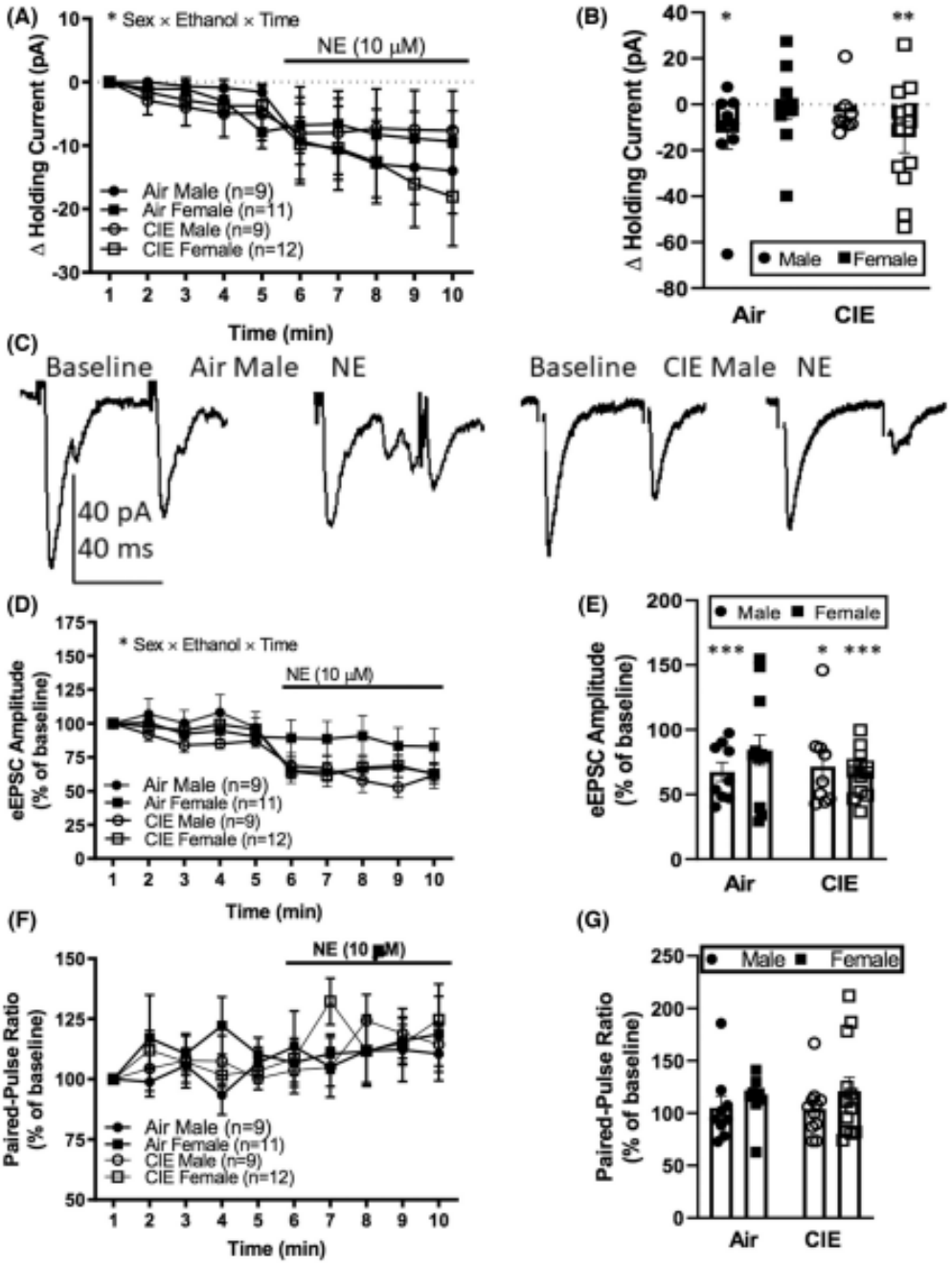

Figure 1-2: Norepinephrine (NE) elicits a dual effect on holding current and evoked excitatory postsynaptic currents in parvocellular neuroendocrine cells (PNCs). **A, B)** NE (10μM) application causes a depolarizing increase in holding current. **C)** Representative glutamatergic excitatory postsynaptic currents (eEPSCs) before and during application of NE (10μM). **D, E)** NE (10μM) suppresses glutamatergic eEPSCs in a sex and ethanol-dependent manner. **F, G**) No change in paired-pulse ratio following NE application. **A, D, F)** Three-way repeated measures ANOVA. **B, E, G)** Two-way ANOVA**;** * $p<0.05$, ** $p<0.01$, *** $p<0.001$.

Figure 1-3: Norepinephrine (NE)-induced inward current and facilitation of excitatory evoked postsynaptic currents (eEPSCs) are mediated by α1-adrenergic receptor (α1AR). **A, B)** Application of α1AR antagonist prazosin (10μM) prevents increases in holding current during concomitant NE (10μM) application. **C)** Time course showing a time × sex × ethanol interaction of prazosin and NE on eEPSC amplitude. **C, D)** Prazosin alone suppresses glutamatergic eEPSCs only in Air males, which is significantly different from Air females. **E)** Representative traces of glutamatergic eEPSCs in Air males and females before and during prazosin + NE application. **F)** Prazosin has no effect on NE's ability to suppress eEPSC amplitude. **G)** Time course showing a significant effect of sex on paired-pulse ratio following prazosin and NE application. **H)** There was a trend towards an increase in paired-pulse ratio following prazosin and NE application only in Air-exposed males. # p <0.10, * p<0.05, ** p<0.01, *** p<0.001, **** p <0.0001. **A, C, G)** Three-way repeated measures ANOVA. **B, D, F, H)** Two-way ANOVA.

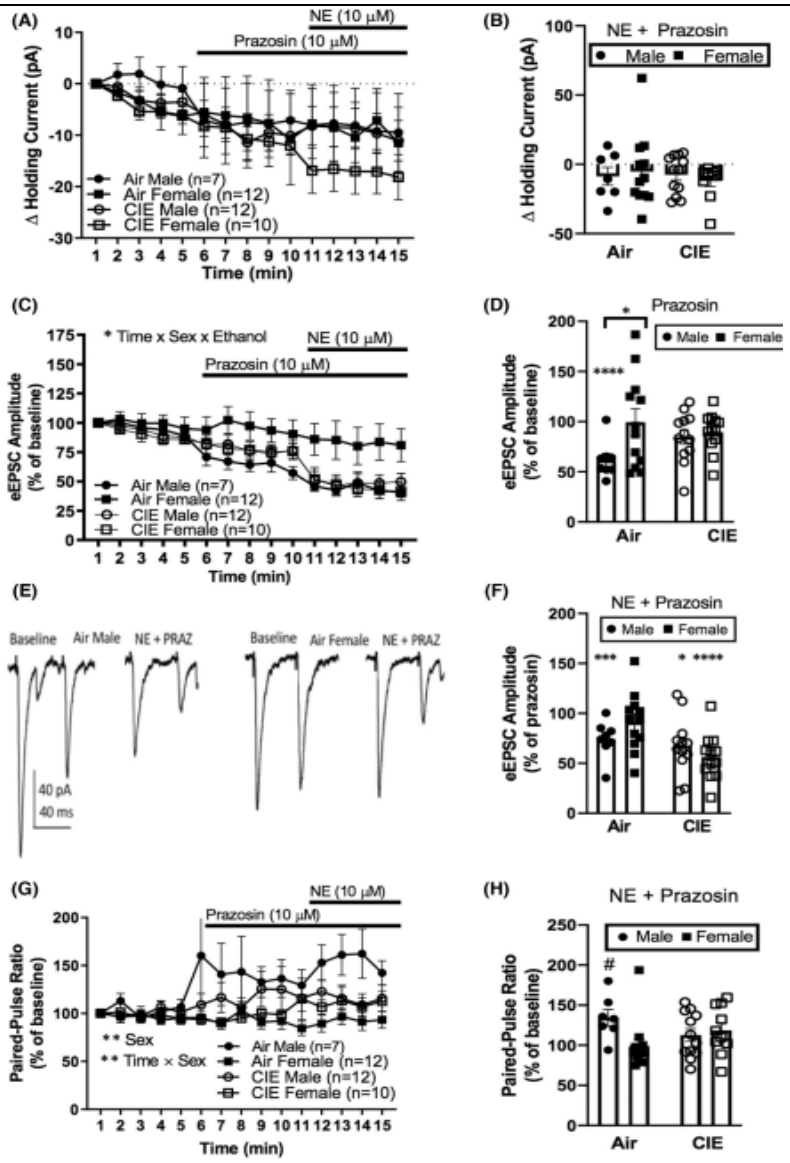

NE-induced inward current and facilitation of eEPSCs is mediated by α1AR

In the central nervous system, α1AR is a postsynaptic, G_q-coupled G-protein coupled receptor (GPCR) that causes depolarization through release of intracellular calcium stores [148]. Therefore, we evaluated the effects of bath applied selective α1AR antagonist prazosin (PRAZ; 10μM), and the effects of NE in the presence of PRAZ on hypothalamic PNCs. The ability of NE to increase holding current was lost during concomitant PRAZ application (Fig. 1-3 A, B). There was a trend towards an increase in holding current only in PNCs from CIE females during concomitant NE and PRAZ (Fig. 1-3 B). Additionally, there was a significant interaction of sex × CIE × time on eEPSCs (Fig. 1-3 C). Only Air males showed a suppression of eEPSCs with application of PRAZ alone and this was significantly different than Air females (Fig. 1-3 D). This suggests that activation of α1AR by endogenous NE contributes to basal glutamatergic transmission in males but not females. Concomitant application of NE with PRAZ shows a significant sex × CIE × time interaction and shows a suppression of eEPSCs in air males and both CIE males and females (Fig. 1-3 C, E, F). This change in eEPSCs was associated with a relative sex-dependent effect on paired-pulse ratio (Fig. 1-3 G, H). However, no significant differences in paired-pulse ratio compared to baseline were observed (Fig. 1-3 H). Taken together, our data suggests that postsynaptic α1ARs on PNCs contribute to both depolarizing, inward current and

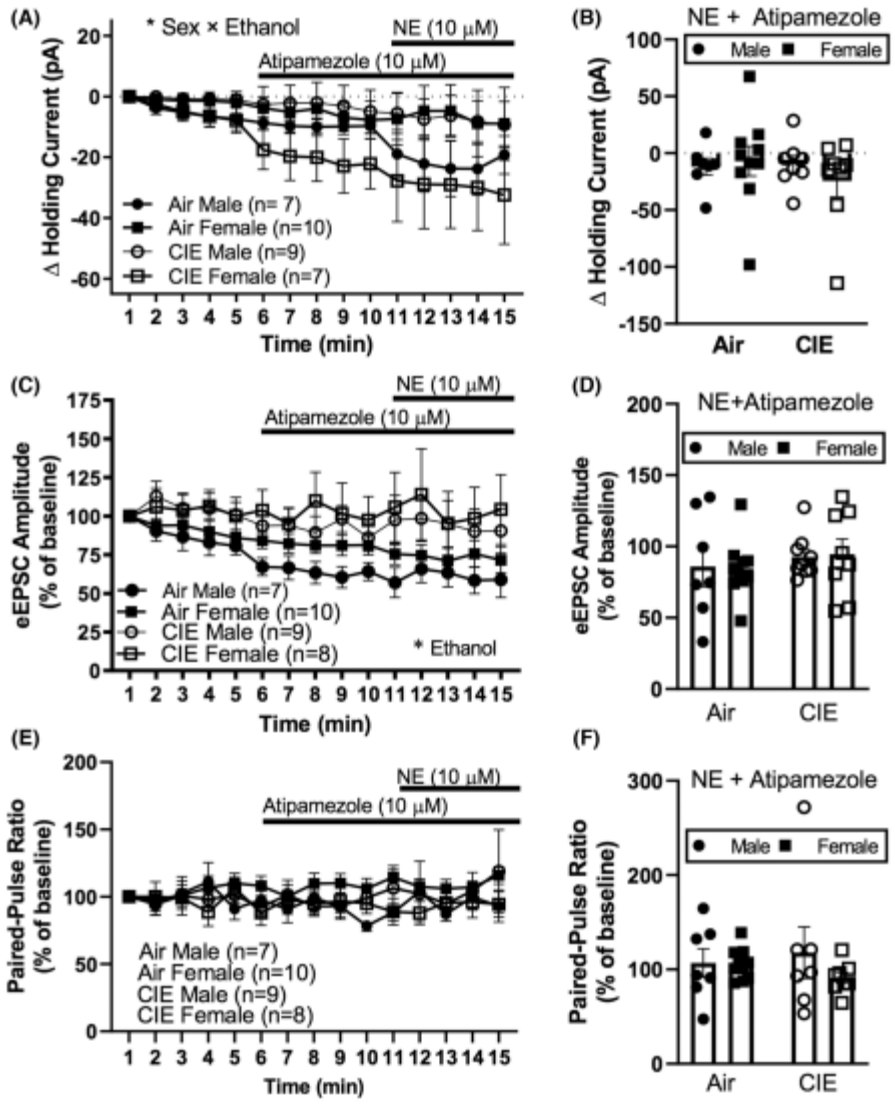

Figure 1-4: Norepinephrine acts through α2-adrenergic receptors to suppress evoked glutamatergic excitatory postsynaptic currents. **A, B)** α2-Adrenergic receptor antagonist, atipamezole (10μM) causes a significant increase to holding current in an ethanol and sex-dependent manner. **C, D)** Atipamezole alone does not affect glutamatergic evoked excitatory postsynaptic currents (eEPSCs), but blocks the ability of NE to suppress eEPSCs. There was also a significant effect of ethanol on the magnitude of eEPSCs, with ethanol groups being significantly larger. **E, F)** No effect of atipamezole was observed on paired-pulse ratio. * $p<0.05$. **A, C, E)** Three-way repeated measures ANOVA. **B, D, F)** Two-way ANOVA.

increasing eEPSCs in PNCs of male rats. Moreover, this ability of α1ARs to increase eEPSCs is selectively lost following CIE exposure.

NE-induced suppression of eEPSCs is mediated by α2AR

α2AR is a predominantly presynaptic, G_i-coupled GPCR that acts to inhibit neurotransmitter release through inhibition of adenylate cyclase [148]. As such, application of α2AR antagonists can increase synaptic release of NE [160]. Bath application of the selective α2AR antagonist, atipamezole (ATIP; 10μM) caused a sex × ethanol interaction on holding current, where there was a trend towards an increase in holding current only in CIE female cells (Fig. 1-4 A, B). Interestingly, ATIP showed an effect of ethanol exposure on eEPSC amplitude (Fig. 1-4 C). Concomitant application of NE with ATIP completely prevented the ability of NE to suppress eEPSCs (Fig. 1-4 C, D). No effect of ATIP was observed on PPR (Fig. 1-4 E, F). Altogether, these data suggest that α2AR plays a key role in the regulating PNC synaptic transmission in response to NE.

Discussion

Adaptations within central catecholaminergic circuits have been implicated for a host of substance use disorders [161]. Here we describe the adaptations in NE effects on the excitability and plasticity of glutamatergic synaptic transmission in hypothalamic PNCs induced by CIE exposure and protracted withdrawal, a validated model of alcohol dependence. CRF-releasing PNCs within the PVN are critical to the stress-induced HPA axis activation. NE, a key neurotransmitter for arousal, depolarizes PNCs through activation of α1AR and suppresses AMPAR-mediated glutamatergic neurotransmission through activation of α2AR. Both effects are influenced by sex and CIE exposure. NE also primes glutamatergic synapses in naïve males to unmask HFS-induced STP. CIE exposure dysregulates this plasticity, while blockade of α1AR restores it, highlighting the importance of targeting the NE system for the treatment of stress-induced relapse in AUD [4].

Ethanol imposes a broad range of effects on neuronal physiology, both directly and through the action of metabolites [162]. We demonstrated an increased holding current needed to stabilize cells at -60 mV selectively in CIE males. We also observed a relative decrease in the intrinsic excitability and evoked spike firing rate in CIE males. Taken together, this points to a persistent, sex-dependent neuroadaptation by CIE that may alter adaptive coordination of the neuroendocrine response to stress. While our previous research showed a lowered action potential threshold in CIE males [11], this is likely due to differences in the mode of alcohol administration (vapor v. oral gavage). Indeed, oral gavage with an intoxicating bolus of ethanol is aversive, while CIE vapor

exposure increases responding for ethanol rewards [104]. Previous evidence supports that decreases in the excitability of PVN PNCs encode differences in the valence of consummatory rewards [163]. Thus, continued research with CIE_{vapor} models should facilitate more translationally applicable insight when investigating the physiological mechanisms by which CIE disrupts stressor resiliency.

NE is a critical component of the initiation of the HPA axis response to stress [164]. NE-evoked inward currents in PNCs are excitatory and lead to increased neuronal firing. PRAZ was effective at preventing increases in the holding current following NE application. No group differences were observed in response to PRAZ + NE on holding current. This confirms that the NE-evoked excitatory inward current in PVN PNCs is mediated through postsynaptic α1AR.

NE can also affect excitatory glutamatergic signaling onto PNCs through two mechanisms. First, α1AR activation causes astrocytic ATP release to amplify presynaptic glutamate release [123]. Interestingly, we only observed this effect of α1AR in air males, where PRAZ alone was sufficient to reduce eEPSC amplitudes. This sex difference is no longer present following CIE, suggesting that CIE inhibits the ability of NE to amplify presynaptic glutamate release through α1AR selectively in males. Gonadal hormones are known to influence the incorporation of α1AR [165], which may contribute to the sex differences in air-exposed controls. Second, presynaptic and astrocytic [166] α2AR can also be activated to suppress glutamate release. We show that NE-induced decreases in postsynaptic eEPSC amplitude can be eliminated in the presence of α2AR antagonism with ATIP. CIE altered ATIP's effect on eEPSCs, leading to increased amplitude of eEPSCs. This suggests that CIE may alter the activity or incorporation of α2AR as a potential opponent process. These opposing effects of α1AR and α2AR activation on glutamate release may be responsible for the lack of significant differences in paired-pulse ratio of eEPSCs in the presence of NE.

Our findings of sex differences in CIE effects on PNCs agree with previously identified sex differences in CIE_{vapor} exposure, such as females being relatively resilient to higher blood ethanol concentrations (BECs) [167], which may be due to accelerated clearance kinetics [168]. The fact that female PNCs maintained synaptic flexibility despite consistently higher BECs (due to lower body weights; Suppl. Fig 1.) is consistent with previous data showing that female rats following CIE_{vapor} appear resistant to both CIE-induced changes to biochemical physiology [138–140] and

behavioral escalation of voluntary intake [105]. Certain sex differences, such as prevention of ethanol-induced changes in endocannabinoid signaling appear to be mediated through ovarian hormones [138], which may have contributed to the variability in female data displayed in Figure 1-2 & Supplemental Figure 2. Our study therefore expands on the reservoir of emerging data by uncovering some of the divergent mechanisms which may contribute to persistence of AUD in males and females.

The persistence of sex-specific alterations on NE-induced current following CIE is notable. As noted, we specifically chose an extended period of protracted withdrawal to separate the persistent HPA axis neuroadaptations from acute withdrawal effects. Supplemental Fig. 2 shows that the effects of NE-induced current persist up to 108 days following last ethanol exposure, which is the lifespan-adjusted equivalent of ~10.3 human years [169]. Thus, medical interventions ameliorating these effects of CIE may be able to specifically impact quality-adjusted life years in a clinical setting.

We have shown here how NE acts on isolated glutamate currents onto and depolarizes hypothalamic CRF neurons. However, our study is limited in that we only recorded from putative CRF neurons based on their response to a hyperpolarizing current pulse [158]. Future studies should examine other cellular populations of the PVN in response to NE, such as oxytocin and arginine-vasopressin-expressing magnocellular neuroendocrine cells, pre-autonomic neurons, and astrocytes, are modulated following CIE treatment. While we believe that estrous cycle influenced the variability in the sensitivity of female neurons to action at α1AR, we were unable to evaluate estrous stage from vaginal smears collected in this experiment. Experiments rigorously testing this hypothesis may be more useful in models of ovariectomized rats with or without E_2 replacement to eliminate the confounding step of interpreting vaginal smears and unhelpful data on 1/4 estrous days collected. Further, future studies should determine whether sex differences in sensitivity at αARs following CIE can augment responding for ethanol rewards in operant assays.

In summary, it was previously known that signaling flexibility in PVN PNCs is essential for the encoding of aversive and rewarding valence to incoming stimuli [70]. We show here that CIE imposes sex-specific limitations on multiple ways (α1AR-mediated excitation, α2AR-mediated suppression of glutamatergic eEPSCs) by which NE acts to dynamize or constrain the synaptic flexibility in PNCs. This may provide mechanistic support to previous findings that female CIE

rats fail to escalate drinking following two-bottle choice [105]. We hope these studies can enable the future development of novel therapeutics targeting noradrenergic dysfunction following CIE.

Supplementary Figure 1

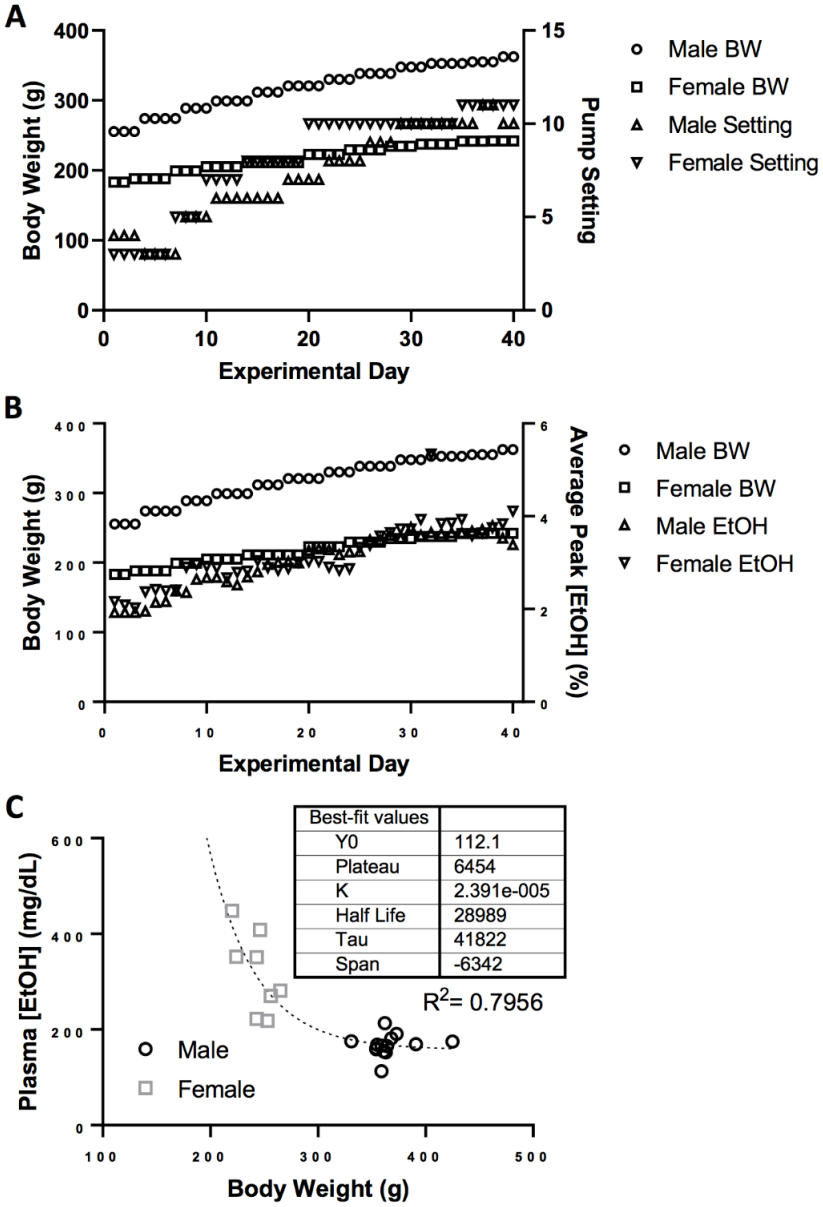

Supplemental Figure 1: **A)** Body weight and ethanol pump setting across the experimental paradigm. **B)** Body weight and peak ethanol vapor concentrations across the experimental paradigm. **C)** Non-linear trend in plasma ethanol concentrations across body weights. Female ethanol vapor concentrations were not titrated by body-weight.

Supplementary Figure 2

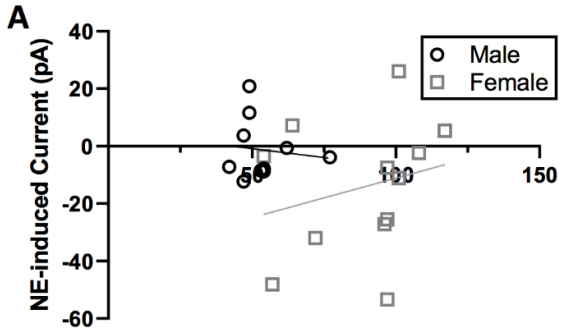

<u>Supplemental Figure 2:</u> Sex-specific alterations to hypothalamic plasticity persist throughout protracted withdrawal. **A)** Norepinephrine (NE)-induced current has no significant linear correlation to number of days post-CIE exposure in either sex.

CHAPTER 2

Chronic intermittent ethanol exposure imposes dysfunction in hypothalamic metaplasticity in male rats

Abstract

Stressful stimuli require rapid, precise, and dramatic behavioral responses to maximize host survival odds. Selection options include freezing, darting, or increasing aggression and fighting. This behavioral response to stress has been increasingly linked to HFS-STP within the PVN. We have shown that this metaplasticity is disrupted in male CIE rats, but potential sex differences have yet to be rigorously evaluated. Here, we describe how this stress and stimulation-dependent plasticity is affected in male and female rats and the influence of CIE exposure followed by protracted withdrawal. Stress neurotransmitter NE was sufficient to unmask STP in male, but not female stress-naïve rats, independent of previous CIE treatment. Further, pretreatment with α1AR antagonist PRAZ unmasked STP in CIE male and female rats, while blocking STP formation in Air males. In stressed CIE males, NE was insufficient to unmask STP, while pretreatment with prazosin restored STP. Collectively, this demonstrates that metaplastic dysfunction in hypothalamic synapses following CIE is sex- and α1ar activity dependent.

Introduction

Envision yourself as a rat. In a summer field approaching dusk, looking to scrounge some seed and grain to feed yourself and rest before having to nurse your young for the rest of the night. You see some discarded wheat in a field only a few meters out! However, after getting half-way out, you notice an ominous, dark shadow.

Suddenly, your lax and chipper attitude turns dire. What will you do? Dart towards the wheat and hope to hide in it? Freeze and hope whatever is casting that shadow misses your line of sight? Perhaps get on your hind legs and stick out your teeth and claws menacingly?

The sudden and drastic behavioral and physiological responses to an imminent threat are vastly complex and intimately involve action from various components of the hypothalamic-pituitary-adrenal (HPA) axis. PNCs exhibit a unique stress- and CRF receptor 1 (CRF1R)-dependent short-term glutamatergic plasticity (STP) following high-frequency afferent stimulation [17]. CRF1R activation suppresses postsynaptic N-methyl D-aspartate receptors (NMDARs) to prevent the release of a retrograde messenger to consequently gate STP formation [11,17]. Freezing in response to a threatening stimulus is related to STP formation in PVN PNCs [19], which highlights the importance of this glutamatergic plasticity in coordinating adaptive behavior.

Acute exposure to intoxicating concentrations of EtOH is sufficient to activate the PVN CRF neurons [26,170,171]. As such, CIE exposure puts sufficient strain to limit the plasticity of PNCs through binge intoxication and withdrawal cycles [141,172–174]. We have previously demonstrated the disruption of PVN CRF neuron STP following an oral gavage model of CIE in male rats through an upregulation in function of GluN2B NMDAR subunits which can bypass CRF1R-dependent suppression [11]. We believe this is one of the mechanisms by which CIE alters the synaptic flexibility of hypothalamic neurons, rendering the host incapable of appropriately being able to cope with exposure to repetitive stress.

Norepinephrine (NE) is a monoamine neurotransmitter involved in behavioral arousal following exposure to a stressor [164,175]. While application of NE has been shown to trigger CRF release in some *in vitro* models [147], the ability of NE to gate hypothalamic metaplasticity has not been evaluated rigorously. Hyperactivity of noradrenergic signaling is αa hallmark of alcohol

withdrawal. Evaluation of novel applications for well-known noradrenergic drugs could address a critical therapeutic gap [4].

We used a CIE_{vapor} model of exposure followed by protracted withdrawal to investigate potential sex differences in metaplastic STP formation through direct application of NE. We also evaluated if we could restore the loss of stress induced STP in male CIE rats through pharmacological blockade of α1ARs. Electrophysiological recordings from PNCs were obtained during following application of NE and selective αAR antagonists to study pharmacologically isolated α-amino-3-hydroxy-5-methyl-4-isoxazolepropionic acid receptor (AMPAR)-mediated synaptic currents before and after applying HFS.

Materials and Methods

Animals

All experiments were performed in accordance with the guidance of the National Institutes of Health on animal care and use and the University of California, Los Angeles Institutional Animal Care and Use Committee. Male or female Sprague Dawley rats (weighing 200-225 g or 150-185 g, respectively) were pair-housed under 12-hr 6AM/6PM light/dark cycle with *ad libitum* access to food, water and environmental enrichment.

Ethanol (Decon Laboratories, King of Prussia, PA) was administered via custom-built vapor chambers (La Jolla Alcohol Research, Inc.) for 12 hour on/off cycles (on at 10PM), referred to as chronic intermittent ethanol (CIE) as previously described [104]. Animals in their home cages passively consumed ethanol in gradually increasing doses throughout the 40-day experiment (Suppl. Fig. 1). Body weight was measured weekly to monitor potential adverse effects of ethanol exposure. Tail vein blood (30-50 μl) was collected into heparinized tubes (Microvette CB300, Starstedt, Germany) immediately following 12-hr vapor exposure during the last experimental week. Blood samples were centrifuged at 2,000 g for 10 min at room temperature and the EtOH content of each sample measured in duplicate along with EtOH standards using the alcohol oxidase reaction procedure (GM7 Micro-Stat, Analox, Huntington Beach, CA). A cutoff of >150 mg/dl of ethanol in plasma was used to confirm that an intoxicating level of ethanol was reached in each rat [156]. Animals were subsequently withdrawn for a period of 30-108 days to evaluate the post-acute effects of CIE exposure on PNCs, which was employed to disentangle the persistent adaptations

to the HPA axis seen previously [154,157], from the effects of acute withdrawal. Room air-exposed, weight- and age-matched rats were used as controls. In some experiments, rats were confined in a Plexiglas restrainer (Braintree Scientific, Braintree, MA) for 30 min immediately prior to euthanasia.

Electrophysiology

The investigators performing the recordings were blind to the treatment (CIE or Air) that the rats received. CIE- and Air-exposed rats were randomly counterbalanced throughout data acquisition. Following 30-108 days of protracted withdrawal, CIE-exposed rats and their air-exposed controls were deeply anesthetized with isoflurane (Patterson Veterinary, MA, USA), decapitated and brain submerged in ice cold bubbling artificial cerebrospinal fluid (ACSF) containing (in mM): 125 NaCl, 2.5 KCl, 1.25 NaH_2PO_4, 2 $CaCl_2$, 2 $MgCl_2$, 26 $NaHCO_3$, 10 glucose, saturated with 95% O_2 and 5% CO_2. Coronal brain slices (400 μM) were obtained (VT1200s, Leica, Buffalo Grove, IL) and sections containing the paraventricular nucleus of the hypothalamus (PVN) microdissected and stored in a separate incubation chamber for >1 hr prior to recordings.

Whole-cell patch clamp recordings were obtained from putative parvocellular neuroendocrine cells (PNCs) within the medial aspect of the PVN as defined by their distinct electrophysiological characteristics [158] during perfusion with ACSF at 34 ± 0.5 °C. Borosilicate glass pipettes (TW150F-3, WPI, FL, USA) were pulled (Brown-Flemming P-87, Sutter Instruments, Novato CA) with 4-8 MΩ resistance tips when filled with an internal solution containing (in mM): 130 K-gluconate, 5 NaCl, 1.1 EGTA, 2 MgATP, 0.2 NaGTP, and 10 HEPES, pH adjusted to 7.3 with KOH. Action potential (AP) voltage threshold was measured at the beginning of the sharp rise of the depolarization phase in the first AP elicited by a depolarizing current pulse. Input-output curve was obtained by calculating the number of APs eliciting in response to depolarizing current steps (10-pA increments).

Excitatory postsynaptic currents (EPSCs) were evoked with a concentric bipolar stimulating electrode (MCE-100, Rhodes Medical Instruments, CA, USA) placed within the periventricular aspect of the PVN [11]. Stimulus was adjusted to elicit a sustained amplitude reaching ~1/2 maximal response for the first current. Paired-pulse ratio (PPR) was obtained by applying a pair of equipotent stimuli at an interval of 25 ms and a rate of 0.2 Hz, as described previously [11].

High frequency stimulation (HFS) of afferents at 100 Hz for 1 s, repeated four times with a 5 s interval [11] was performed following washout of all drugs. Access resistance was continuously monitored, and recording were accepted for analysis if changed were <30%. AMPAR-mediated EPSCs were isolated during continuous application of picrotoxin (50 μM; HelloBio, Princeton, NJ, HB0506) and holding the postsynaptic cell at -60 mV.

Electrophysiological signals acquired with the aid of pCLAMP10 Clampex software (Molecular Devices, San Jose, CA) were amplified using the Multiclamp 700B amplifier (Molecular Devices), low-pass filtered at 1kHz and digitized at 10kHz with the Digidata 1440A (Molecular Devices). Data were analyzed using Clampfit software (Molecular Devices). Amplitude of evoked EPSCs (eEPSCs), holding current, and PPR was normalized to the beginning of baseline recordings following stabilization. Effects of drugs on eEPSCs, holding current, and PPR were evaluated for the last five minutes of 8-minute steady-state drug applications. The magnitude of short-term potentiation (STP) was calculated as the average amplitude of 12 eEPSCs immediately following HFS and was expressed as a % of baseline.

Drugs

Noradrenaline bitartrate was dissolved in distilled water at a stock concentration of 100 mM and diluted in ACSF to 10 μM. Prazosin hydrochloride (Cayman Chemical, Ann Arbor, MI #15023) was dissolved in pure dimethyl sulfoxide at a 10 mM stock concentration and diluted to a final volume of 10 μM in ACSF. Atipamezole hydrochloride (Cayman Chemical, #9001181) was dissolved in distilled water at a stock concentration of 50 mM, sonicated for 2 minutes, and diluted to a final concentration of 10 μM in ACSF. Recordings were performed in the continuous presence of picrotoxin (50 μM). All solutions equilibrated at 34 ± 0.5 °C prior to slice application.

Statistical analyses

Data are expressed as mean ± SEM. In all figures, n represents the number of cells for each group. Comparisons of basal membrane properties were done using two-way ANOVA with Tukey's post-hoc comparison. Interactions between variables (sex, CIE, effect of drug with respect to time) were performed using 3-way ANOVA. Post-hoc comparisons were made with Dunnett's multiple comparison test to compare the change of a single parameter from the last minute of baseline to the last minute of drug exposure. Comparison of short-term potentiation was made with pair-wise t-test of an average of one minute of eEPSCs immediately prior to, and immediately after

high-frequency stimulation. All statistical analyses were performed using Prism 9 software (GraphPad). Alpha cutoff of 0.05 was used.

Results

α1AR activation facilitates short-term synaptic plasticity in Air male, but not Air female PNCs

Previous studies have demonstrated the ability of PVN PNCs to undergo short-term potentiation (STP) of glutamatergic inputs through a corticotropin releasing-factor (CRF) receptor 1 (CRF1R)-dependent mechanism [17]. Since NE contributes to initiating the HPA axis cascade [12,164], we sought to determine whether bath application of NE can unmask STP in PNCs. We found that NE application unmasked HFS-induced STP in PNCs from stress-naïve males, but not females, regardless of CIE treatment (Fig. 2-1 A, B, E).

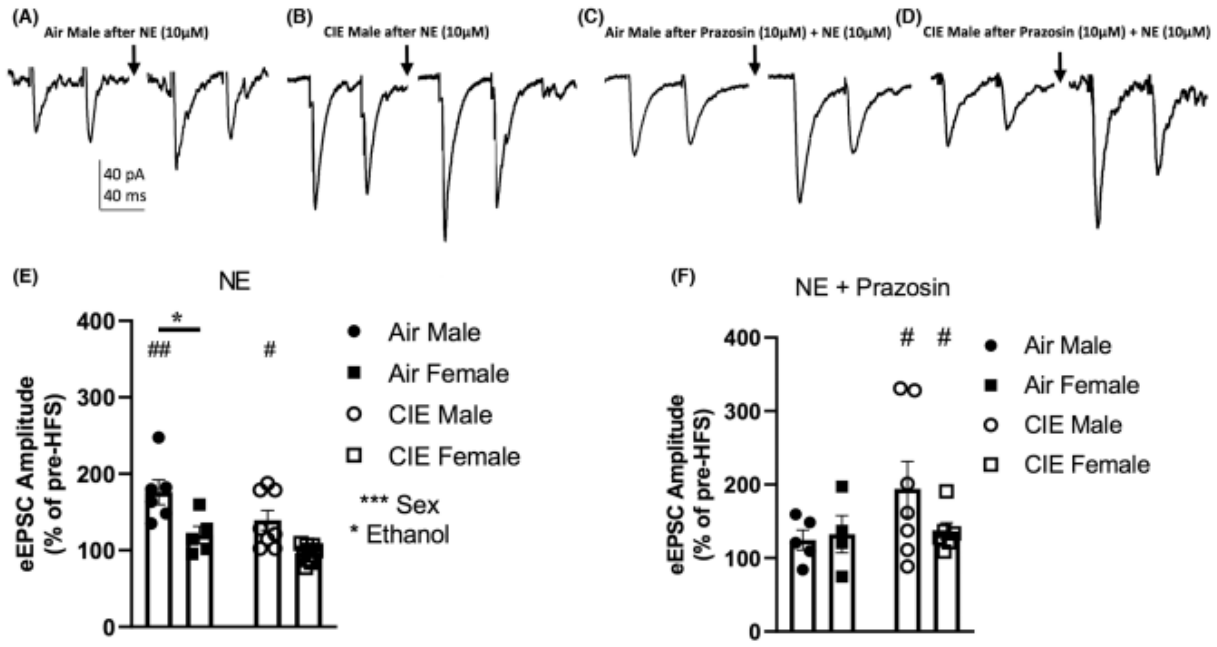

Figure 2-1: The ability for norepinephrine (NE) to gate short-term plasticity is sex-dependent. **A, B)** Representative glutamatergic evoked excitatory postsynaptic currents (eEPSCs) before and after high-frequency stimulation (HFS, black arrow). **C, D)** Representative eEPSCs in response to HFS after NE (10μM) and prazosin (10μM) application. **E)** Males, regardless of chronic intermittent ethanol (CIE) exposure show STP, while STP is blocked in females. **F)** Prazosin blocks NE's ability to unmask STP in air exposed males, while facilitating the formation in chronic intermittent ethanol-exposed (CIE) females. * p<0.05, *** p<0.001, # p<0.05 (comparison from pre-to post-HFS), ## p<0.01. **E, F)** Two-way ANOVA.

Interestingly, application of NE + PRAZ blocked STP formation in stress-naïve Air males, but had no effect on NE-induced STP in stress-naïve CIE males (Fig. 2-1 C, D, F), suggesting an alteration in the mechanism of STP induction following CIE exposure. Importantly, NE + PRAZ facilitated unmasking of STP induction in stress-naïve CIE females (Fig. 2-1 F). These data suggest that CIE induced neuroadaptive changes lead to alterations in the mechanisms mediating NE-induced STP in males and females. Altogether, these findings illustrate the sex-dependent mechanisms that gate STP induction in stress-naïve air and CIE rats.

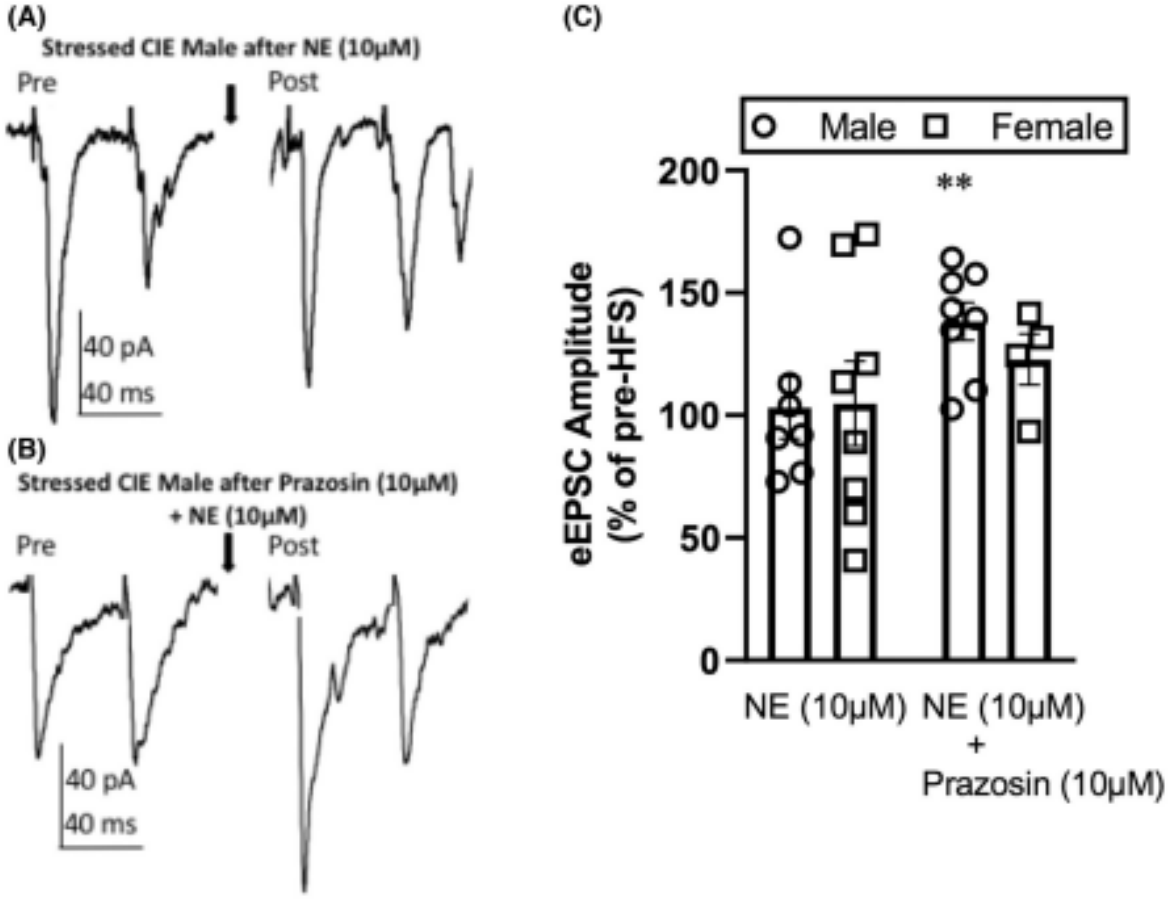

Figure 2-2: Prazosin restores the ability to form stress-dependent STP lost following ethanol exposure in a sex-dependent manner. **A)** Representative evoked excitatory postsynaptic currents (eEPSCs) in stressed CIE exposed rats showing no change in STP following high-frequency stimulation (HFS; black arrow). **B)** Representative eEPSCs showing STP following HFS after application of NE (10μM) + prazosin (10μM). **C)** Regardless of sex, CIE animals are unable to undergo STP following 30-min restraint stress and NE (10μM) application. Stressed CIE males, but not females can undergo STP after concomitant prazosin (10μM) and NE (10μM) application. ** $p<0.01$ relative to pre-HFS. **C)** Two-way ANOVA.

PRAZ restores CIE-induced loss of stress-induced metaplasticity only in males

Our previous reports showed a disrupted STP induction in stressed CIE males [11]. Since we noted that NE can unmask STP in stress-naïve CIE males, we sought to examine the effect of NE following an acute exposure to a 30-minute restraint in CIE animals. Consistent with our previous reports, application of NE was not able to unmask STP in stressed CIE rats (Fig. 2-2 A, C). However, application of NE + PRAZ restored STP in stressed CIE males (Fig. 2-2 B, C). Stress-induced metaplasticity was not observed in the female groups (Fig. 6C). These data suggest that α1AR blockade allows for NE-induced STP in CIE males, likely via other adrenergic receptors [19,176].

STP is a critical mechanism that enables PVN PNCs to maintain signaling flexibility in response to real or perceived threats through amplified glutamatergic signaling [17]. This physiological response has been subsequently related to behavioral outcomes [19]. Sex differences in stress-induced STP within PNCs have been demonstrated previously, where only socially-exposed females show a vasopressin 1a receptor-dependent blockade of STP formation [16]. This is consistent with the lack of STP in our socially exposed (pair-housed) females, independent of ethanol treatment. We note that non-stressed CIE_{vapor} males also show STP in the absence of exogenous drug application (Suppl. Fig. 2). Further, PRAZ application only prevented NE-induced STP formation in air-exposed, non-stressed males, suggesting that the STP seen in non-stressed CIE_{vapor} males may not be due to action at α1AR. This is contrasted by the finding that PRAZ + NE unmasked STP formation in non-stressed CIE females, suggesting that the vasopressin 1a receptor-mediated blockade of NE-induced STP in CIE females may be dependent on α1AR activation.

Given NE's ability to directly facilitate CRF release [147], we investigated whether bath application of NE was sufficient to unmask (stress or CRF1R-activation-dependent)-STP formation in male and female stress-naïve rats. Interestingly, CIE males show normally stress-dependent STP in stress-naïve subjects in the absence of any exogenous drug application. We found also male, but not female rats, independent of ethanol treatment, showed NE-induced STP formation. This was simultaneously blocked in Air males and facilitated in CIE females following pretreatment with PRAZ. Together, we take this data to demonstrate the STP seen in non-stressed CIE_{vapor} males may not be due to action at α1AR. This is contrasted by the finding that PRAZ + NE unmasked STP formation in non-stressed CIE females, suggesting that the vasopressin 1a

receptor-mediated blockade of NE-induced STP in CIE females may be dependent on α1AR activation.

We previously reported a loss of stress-induced STP following CIE_{og} [11]. When we evaluated the effect of NE on HFS-induced STP in restraint-stressed rats exposed to CIE_{vapor} we found that NE was insufficient to unmask stress-induced STP. We next tested whether selective α1AR antagonism can augment HFS-induced STP. To our surprise, PRAZ + NE selectively restored stress-induced STP formation in CIE males. This is consistent with a previous study showing that PRAZ reduces stress-induced anxiety in alcohol-preferring male rats during acute withdrawal [177]. Thus, while the mechanisms by which CIE_{og} and CIE_{vapor} impair STP remain incompletely understood, there is convergence in this loss of function in stress-induced metaplasticity. We believe this neurophysiological phenomenon to be a conserved mechanism underlying stress-induced relapse to ethanol consumption and thus may be impactful translationally. This insight may inform future clinical evaluations of PRAZ, as while the drug showed limited efficacy in a randomized, double-blinded study for AUD, there was improved efficacy in those with higher drinks per week [178]. It remains to be seen whether the effect size seen could be improved by the selective inclusion of men.

Our findings of sex differences in CIE effects on PNCs agree with previously identified sex differences in CIE_{vapor} exposure, such as females being relatively resilient to higher blood ethanol concentrations (BECs) [167], which may be due to accelerated clearance kinetics [168]. The fact that female PNCs maintained synaptic flexibility despite consistently higher BECs (due to lower body weights; Suppl. Fig 1.) is consistent with previous data showing that female rats following CIE_{vapor} appear resistant to both CIE-induced changes to biochemical physiology [138–140] and behavioral escalation of voluntary intake [105]. Certain sex differences, such as prevention of ethanol-induced changes in endocannabinoid signaling appear to be mediated through ovarian hormones [138], which may have contributed to the variability in female data displayed in Figure 2 & Supplemental Figure 3. Our study therefore expands on the reservoir of emerging data by uncovering some of the divergent mechanisms which may contribute to persistence of AUD in males and females.

The persistence of sex-specific alterations in NE-induced current and stress-induced STP formation imposed by CIE is notable. Others have demonstrated the emergence, dynamic remission, and resurgence of anxiety-like behaviors during acute (~8 hours), early protracted withdrawal (2 weeks), and late protracted withdrawal (6-12 weeks) in male CIE_{vapor} rats, respectively [103]. We specifically chose an extended period of protracted withdrawal to separate the persistent HPA axis neuroadaptations from acute withdrawal effects. Supplemental Fig. 3 shows that both the effects PRAZ-mediated restoration of stress-induced STP persist up to 108 days following last ethanol exposure, which is the lifespan-adjusted equivalent of ~10.3 human years [169]. Thus, medical interventions ameliorating these effects of CIE may be able to specifically impact quality-adjusted life years in a clinical setting.

Our data on the sex differences in STP formation suggests a role for βARs in the loss of stress induced STP in CIE. For example, βAR-mediated activation of downstream effectors (*i.e.* protein kinase A) can be inhibited by tonic activation of downstream α1AR signaling pathways (such as protein kinase C) [179]. Additionally, mediators of intracellular biochemical events known to impair STP formation (such as activity of protein phosphatase 2A (PP2A) [11]) negatively regulate the sensitivity of βARs [180]. As incorporation of βARs are influenced by estrogens [181], this may explain why α1AR-antagonism is only sufficient to facilitate this βAR signal to gate STP in stressed CIE males. Interestingly, the cellular integrated stress response [182] can be negatively modulated by PP2A [183] and activated by βARs [184]. As activators of the integrated stress response can restore metaplastic signaling deficits required for memory formation imposed by acute ethanol exposure in the hippocampus [185], our data suggest an unexpected convergence of NE signaling and integrated stress response pathways that may contribute to CIE-induced changes in hypothalamic synaptic plasticity.

In summary, it was previously known that signaling flexibility in PVN PNCs is essential for the encoding of aversive and rewarding valence to incoming stimuli [70]. We show here that CIE imposes sex-specific limitations on multiple ways (α1AR-mediated excitation, α2AR-mediated suppression of glutamatergic eEPSCs, and STP formation) by which NE acts to dynamize the synaptic flexibility in PNCs. Thus, CIE leads to a reciprocal narrowing [186] of the available physiological and behavioral profile to make animals particularly prone to respond with negative reinforcement behaviors, such as stress-induced ethanol seeking [187]. While STP formation has

been related to the choice between freezing and flight [19], it has yet to be determined how STP formation relates to drinking behavior in preclinical models of AUD. We suspect that STP is related to the ability of animals to cope and act favorably when encountering relapse-inducing stressors, but this should be validated in an operant assay (such as touch screen). Despite these limitations, investigations into the mechanisms underlying this metaplastic stress signaling in cells that regulate HPA axis activation should prove to be an impactful avenue of research for the future clinical treatment of AUD.

Supplementary Figure 1

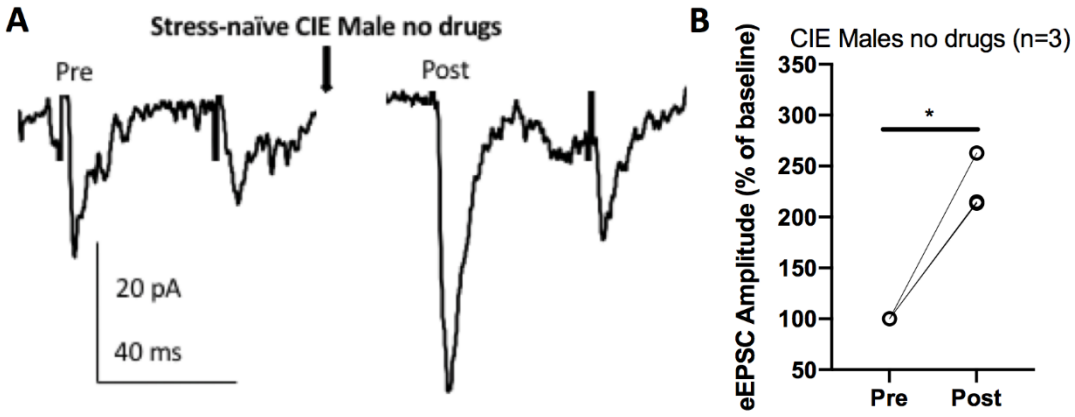

Supplemental Figure 1: **A)** Representative trace showing excitatory postsynaptic currents (eEPSCs) in non-stressed CIE male rats undergo short-term potentiation (STP) following high-frequency stimulation (HFS, black arrow). **B)** Non-stressed CIE males show STP following HFS in the absence of exogenous drug application. * $p<0.05$, Student's t-test.

Supplementary Figure 2

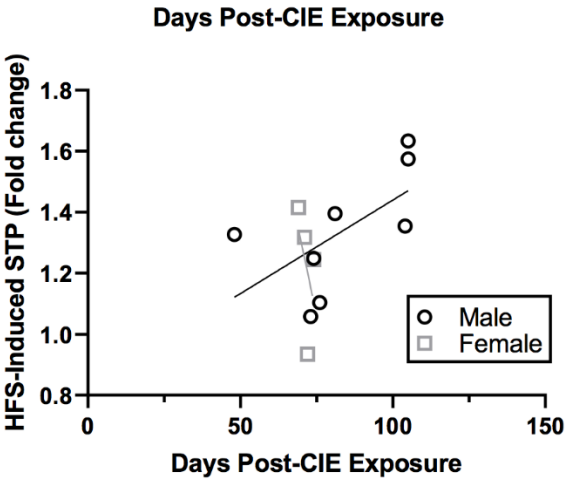

Supplemental Figure 2: Sex-specific alterations to hypothalamic plasticity persist throughout protracted withdrawal. Fold change response to high-frequency stimulation (HFS)-induced short-term potentiation (STP) has no significant linear correlation to number of days post-CIE exposure in either sex.

CHAPTER 3

CIE imposes cell-specific differences in Ca^{2+} signaling frequency during exposure to a pharmacological stressor

Abstract

Ethanol acutely activates the HPA axis despite its widely reported anxiolytic properties. Astrocytes have emerged as important cellular components for mediation of neuronal signal transduction, ethanol metabolism, and response to metabolic stressors. Astrocytes and neurons within the PVN respond cooperatively to neuroendocrine cues, such as rapid increases in extracellular [NE], to gate activation of the HPA axis. Subsequently, HPA axis activity causes release of CORT by the adrenals acts on hypothalamic GRs to suppress excitatory neurotransmission through negative feedback. Neuronal signaling in the hypothalamus is altered following CIE_{vapor} exposure and protracted withdrawal, but the underlying mechanisms remain enigmatic. We therefore employed a model of CIE_{vapor} exposure to perform Ca^{2+} imaging in *ex-vivo* slices of PVN in response to pharmacological application of NE and GR agonist, DEX, with or without selective glutamate or NE receptor antagonists. By exploiting cell-specific differences to K^+ buffering capacity, we were able to putatively differentiate between neuronal and astrocytic cell populations. Both neurons and astrocytes of CIE rats show less synaptic flexibility in response to a pharmacological stress. This effect was reversed by application of α1AR antagonist, Praz, and partially reversed by application of GluN2B-specific N-methyl D-aspartate receptor (NMDAR) antagonist, Ro 25-6981. Our results suggest tripartite synaptic dysfunction underlies previously identified deficits in PVN neurotransmission following CIE. This also shows promising preclinical validation for one mechanism by which Praz may restore synaptic PVN function following CIE.

Introduction

Alcohol misuse is a persistent global health concern which is associated with societal and financial costs exceeding $249 billion per year [188,189]. Attempts to pharmacologically treat AUD are hindered by both reluctances to seek treatment [190] and interindividual differences in the underlying mechanisms [178,191]. Establishment of behavioral biomarkers as predictors of pharmacological efficacy can help clinicians understand the underlying mechanisms that contribute to variance in drug treatments and provide improved personalized treatment plans [191].

The HPA axis is a coordinated neuroendocrine system that allows the host to adaptively respond to threatening stimuli [12]. This axis is initiated through the activation of PNCs containing CRF within the PVN by glutamatergic and noradrenergic inputs. Ultimately, HPA axis activation results in the release of CORT that negatively regulates the activity of these CRF cells [12]. Additionally, CRF cells must coordinate upstream afferent signals from the locus coeruleus, amygdala, and other regions of the hypothalamus [13]. Thus, PVN CRF cells must integrate upstream and downstream signals to positively and negatively gate their activity to allow the host to adaptively respond to stress [70]. Relapse rates in those with AUD are high (~20-30% [6,7]) and are greatly influenced by stress [8,9]. Despite this knowledge, no currently approved medications for AUD explicitly target the HPA axis [4] or noradrenergic circuitry.

CIE exposure in rodents imposes behavioral changes which include loss of control over EtOH intake, anxiety-like behavior, and disruption of stress-coping behaviors [104,105]. Increased stress-induced grooming, which helps calm an animal after exposure to a stressor, is also lost following CIE [11]. However, even gold-standard preclinical models of AUD (such as CIE vapor exposure followed by protracted withdrawal) often result in a heterogeneity of drinking preference within each experimental group. While exciting discoveries have started to uncover the neuronal underpinnings that contribute to compulsive alcohol escalation leading to AUD [192], little is known about the broad consequences contributing to cellular dysfunction within the PVN following protracted withdrawal. This may have important implications for treating AUDs, as PRAZ was found to be most efficacious in those with higher numbers of heavy drinking days [178].

CRF cells within the PVN are essential for both the conduct of the HPA axis and the gating of complex behaviors in response to environmental cues. For example, optogenetic inhibition of these cells results in increased rearing (an exploratory behavior) and decreased grooming (a stress-

coping behavior) [68]. Astrocytes have critical roles in potassium buffering [193,194], regulating synaptic strength [122], glutamate/glutamine shuttling [48], amongst others [46], that can dramatically influence the excitability of pre-and postsynaptic neurons. As such, the cooperative function between astrocytes, presynaptic axon terminal, and postsynaptic soma, termed the "tripartite synapse, " function in response to action by the other to coordinate and spatially amplify signals. Norepinephrine release in response to stressful stimuli gates a complex ATP-dependent neuronal-astrocytic crosstalk within the PVN to rapidly amplify glutamate transmission [123] specifically in males, which may be disrupted by CIE [110]. However, the mechanisms by which astrocytic-neuronal crosstalk is impaired from CIE are currently not well understood.

Ca^{2+} imaging as a technique has gained significant traction over the past decade due to its ability to obtain large, rich data sets on many cell types with minimally disruptive techniques [195,196], due to Ca^{2+} flux's relation to intracellular second messenger signaling pathways and action potentials [197,198]. There has been a recent shift to the collection of Ca^{2+} imaging in the form of two-photon recordings using chronically implanted mini-scopes to visualize neuronal or astrocytic Ca^{2+} events *in vivo* due to the rapid expansion and facilitation of relevant resources [199]. However, obtaining reliable recordings of this nature is typically limited to dorsal areas of the brain. Further, *ex-vivo,* single photon Ca^{2+} imaging can be obtained in high fidelity [200], with the added advantage of being able to rapidly apply various electrical stimulation and pharmacological manipulations in a tightly controlled setting. Thus, we performed *ex-vivo,* single photon Ca^{2+} imaging in PVN slices subjected to a pharmacological stress protocol. Utilizing this strategy, we were able to determine unique CIE-induced alterations in astrocytic and neuronal Ca^{2+} spike kinetics in response to a pharmacological stress. We also used selective antagonists of α1AR, α2AR, and Glun2B-containing NMDAR, to determine the CIE-induced alterations and HFS-sensitivity of frequency of Ca^{2+} event, proportion of excited cells, and Ca^{2+} spike kinetics in PVN slices from air and CIE rats. Finally, we determined the similarities in differences between the relations of measured Ca^{2+} signaling profiles with behaviors associated with AUD.

Materials and Methods

Animals

All experiments were performed in accordance with the guidance of the National Institutes of Health on animal care and use and the University of California, Los Angeles Animal Research Committee. Male Long-Evans rats (weighing 200-225 g) were pair-housed under 12-hr 6AM/6PM light/dark cycle with *ad libitum* access to food, water and environmental enrichment.

EtOH (Decon Laboratories, King of Prussia, PA) was administered via custom-built vapor chambers (La Jolla Alcohol Research, Inc.) for 12 hour on/off cycles (on at 10PM), referred to as CIE, as previously described [110] . Animals in their home cages passively consumed EtOH in gradually increasing doses throughout the 40-day experiment. Body weight was measured weekly to monitor potential adverse effects of EtOH exposure. Tail vein blood (30-50 μl) was collected into heparinized tubes (Microvette CB300, Starstedt, Germany) immediately following 12-hr vapor exposure during the last experimental week. Blood samples were centrifuged at 2,000 g for 10 min at room temperature and the EtOH content of each sample measured in duplicate along with EtOH standards using the alcohol oxidase reaction procedure (GM7 Micro-Stat, Analox, Huntington Beach, CA). A cutoff of >150 mg/dl of EtOH in plasma was used to confirm that an intoxicating level of EtOH was reached in each rat [156]. Animals were subsequently withdrawn for a period of 30 days prior to behavioral assessment, which was employed to disentangle the persistent adaptations to the HPA axis seen previously [154,157], from the effects of acute withdrawal. Room air-exposed, weight- and age-matched rats were used as controls.

Ca^{2+} imaging

CIE-exposed rats and their air-exposed controls were deeply anesthetized with isoflurane (Patterson Veterinary, MA, USA), decapitated and brain submerged in ice cold bubbling slicing artificial cerebrospinal fluid (ACSF) containing (in mM): 62 NaCl, 3.5 KCl, 1.25 NaH_2PO_4, 62 choline chloride, 0.5 $CaCl_2$, 3.5 $MgCl_2$, 26 $NaHCO_3$, 5 N-acetyl L-cysteine, and 5 glucose, pH adjusted to 7.3 with KOH. Acutely microdissected PVN slices (300 μM thick) were obtained (VT1200s, Leica, Buffalo Grove, IL) and transferred to room temperature normal ACSF containing (in mM): 125 NaCl, 2.5 KCl, 1.25 NaH_2PO_4, 2 $CaCl_2$, 2 $MgCl_2$, 26 $NaHCO_3$, 10 glucose, pH adjusted to 7.3 with KOH, and allowed equilibrate for >1 hr prior to experimentation. Slices were then incubated in a 5-mL chamber containing ACSF with cell-permeable Ca^{2+}-indicating dye, Calbryte 520AM (AAT Biosciences), DMSO (0.3% w/v) and pluronic acid (0.02%

w/v) for 45-60 min and allowed to wash in another normal ACSF solution for >5 min prior to imaging. Calbryte 520AM is an esterified dye that, following cleavage after passive transport into the cytosol, exhibits greatly enhanced cellular retention without the need for additional pharmaceutical intervention [201].

Imaging was performed on a Scientifica SliceScope, with imaging components built on an Olympus BX51 upright fluorescence microscope equipped with an sCMOS camera (Hamamatsu Orca Flash 4.0v3). Anatomical regions in brain sections for Ca^{2+} imaging were first identified by brightfield imaging with 780nm LED (Scientifica) illumination. Ca^{2+} imaging was performed using a 40x, 0.80NA water immersion objective (Olympus), continuous 470nm LED illumination (ThorLabs), and a filter cube suitable for Calbryte 520AM imaging: Excitation: Brightline 466/40, Dichroic: Semrock FF495-Di03, Emission: Brightline 525/50. Images were acquired continually with 20ms exposure time.

Electric field stimulation was applied at 110 mV (twin pulse every 5s). At the end of each experiment, slices were washed with high [K^+] ACSF, (containing in mM: 86 NaCl. 55.4 KCl, 1 $MgCl_2$, 0.33 NaH_2PO_4, 10 D-Glucose, 10 HEPES, 2 $CaCl_2$) to putatively discriminate between neuronal and astrocytic cell populations [202]. Temperature of ACSF during the recorded sessions was held at 28° C to minimize bubble formation.

Drugs

Norepinephrine bitartrate (Tocris Biosciences, Minneapolis, MN, #5169) was dissolved in distilled water at a stock concentration of 100 mM and diluted in ACSF to 10 μM. Selective α1AR antagonist, Praz (Cayman Chemical, Ann Arbor, MI #15023) was dissolved in DMSO at a 10 mM stock concentration and diluted to a final volume of 10 μM in ACSF. Selective α1AR antagonist Atipamezole hydrochloride (Atip; Cayman Chemical, #9001181) was dissolved in distilled water at a stock concentration of 50 mM, sonicated for 2 minutes, and diluted to a final concentration of 10 μM in ACSF. Selective GluN2b antagonist, Ro 25-6981 (Ro; Hellobio, Ann Arbor, MI #15023) was sonicated and dissolved in DMSO at a 5 mM stock concentration and diluted to a final volume of 5 μM in ACSF. Glucocorticoid receptor (GR) agonist, dexamethasone (DEX) was dissolved in DMSO at a 5 mM stock concentration and diluted to a final volume of 5 μM in ACSF. Recordings

were performed in the continuous presence of picrotoxin (50 μM). All solutions equilibrated at 28 ± 0.5 °C prior to slice application.

To mimic a pharmacologically mediated stress response, multiple PVN slices from the same animal were washed with normal ACSF for 3 minutes, then NE, with or without selective antagonists (Praz, Atip, Ro) for a period of 8 minutes prior to imaging. Subsequently, slices were washed with DEX for 8 minutes. Finally, slices were washed with high [K^+] ACSF, (containing in mM: 86 NaCl. 55.4 KCl, 1 $MgCl_2$, 0.33 NaH_2PO_4, 10 D-Glucose, 10 HEPES, 2 $CaCl_2$) to putatively discriminate between neuronal and astrocytic cell populations [202].

Data Extraction

Blinded scorers semi-manually curated regions of interest (ROIs) using Python-based Suite2P software [203]. ROI fluorescence was subtracted from the annual surround fluorescence, low-pass filtered, and transformed to dF/F_0 as previously described [200], where F_0 is calculated with a boxcar filter with a 200-frame lookback window. dF/F0 values were clipped between 0 and 9000 to eliminate negative changes. Area under the curve and event frequency of each cell was calculated for each drug treatment. A threshold of 0.15 dF/F was used to determine significant events, which is lower than the dF/F of a single *ex-vivo* action potential, but significantly above signal to noise in our recorded traces [204].

Data Analysis

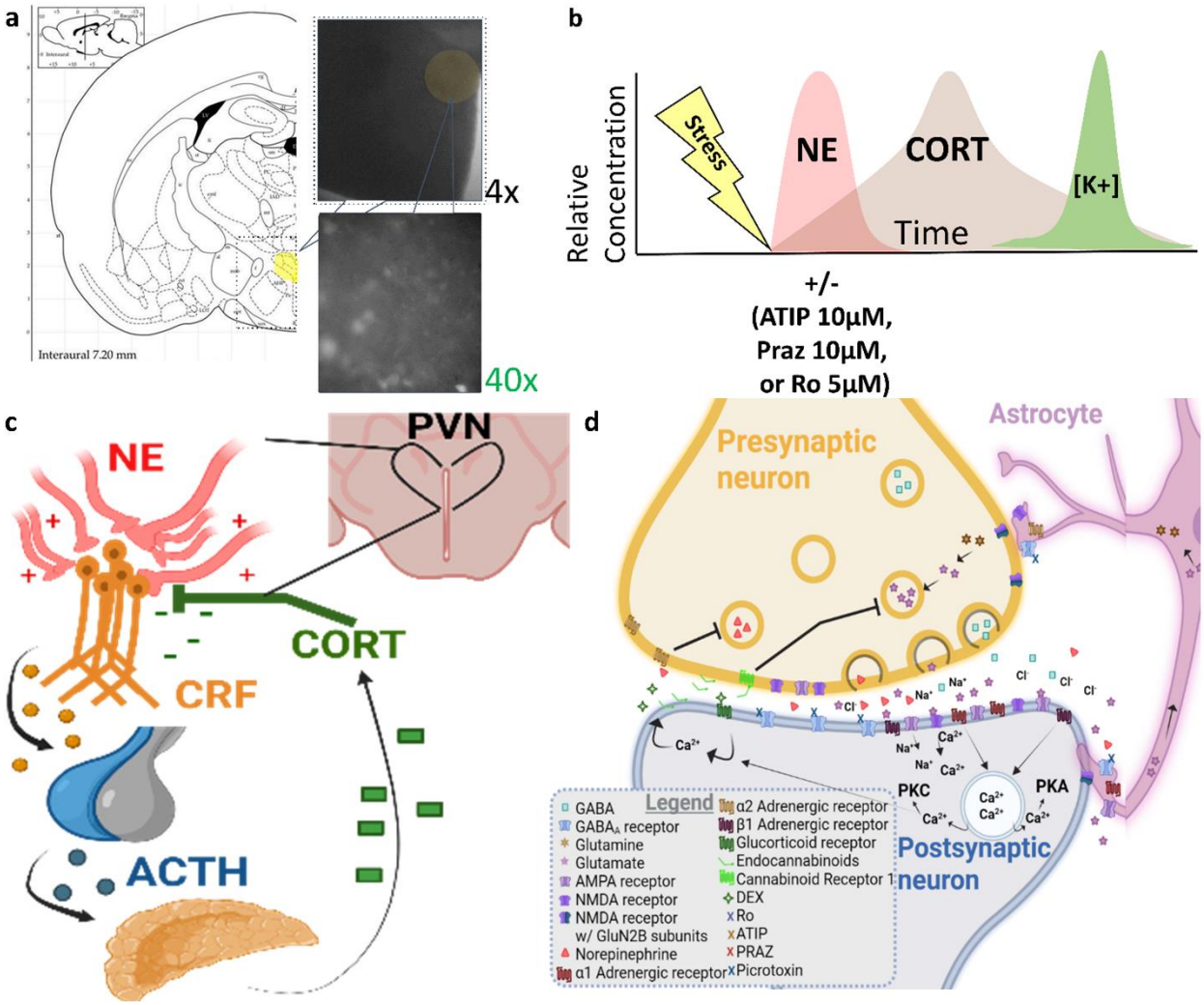

Figure 3-1: Schematic representation of *ex-vivo* pharmacological stress protocol. A Paxinos atlas diagram, showing PVN (yellow), along with 4x (brightfield) and 40x (GFP) screen captures of a representative micro-dissected PVN slice. **B** In response to stressful stimuli, NE and subsequently, CORT concentrations rise in a serial manner to regular PVN CRF neurons. Following our pharmacological stress protocol, we applied 52mM KCl to putatively discriminate between astrocytic and neuronal populations. **C** Schematic representation of positive and negative modulation of HPA axis through NE and CORT. **D** Graphical summary depicting our pharmacological manipulations to investigate tripartite synaptic communication.

All data are expressed as mean ± SEM. For basal event frequency data, student's t-test was used to evaluate differences between CIE and Air groups. GraphPad Prism 9 and Python Jupyter notebook was used for all data analyses. Alpha cutoff of 0.05 was used.

Results

Pharmacological stress protocol to assess the cellular mechanisms underlying CIE-induced HPA axis dysfunction in astrocytes and neurons

To evaluate how NE and CORT can affect the frequency and kinetics of Ca^{2+} signals in neuronal and astrocytic populations, we obtained *ex-vivo* micro-dissected PVN slices (300µM) in carbogenated, ice-cold ACSF containing N-acetyl cysteine to preserve astrocyte function. Using this technique, we were able to obtain 6-8 PVN hemispheres to be incubated in unidirectionally, cell permeable Ca^{2+} indicator, Calbryte 520AM (Fig 3-1A). We then exposed each slice to a different iteration of pharmacological stress to evaluate interindividual differences in physiological Ca^{2+} handling. Finally, we briefly applied 52mM KCl ACSF to exploit physiological differences in K^+ buffering capacity between astrocytes and neurons, as previously described (Fig. 3-1 b) [202].

NE and CORT are essential for the positive and negative gating of HPA axis activation, respectively. Here we show a simplified schematic displaying the action of NE and CORT to gate the output of this axis positively and negatively by the PVN (**Fig. 3-1 c**). A simplified diagram displaying the known biochemical mechanisms underlying tripartite glutamate signaling in the PVN during various phases of HPA activation (Fig. 3-1 d) is also provided to justify our pharmacological interventions.

CIE exposure alters the basal Ca^{2+} signaling and sensitivity to α1AR ligands in PVN neurons

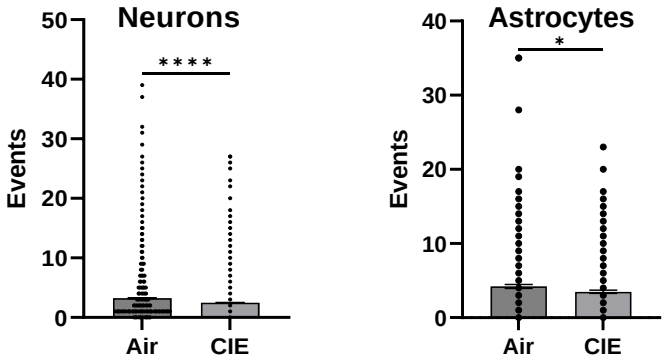

Figure 3-2: Basal Ca^{2+} signaling dysfunction in CIE neurons and astrocytes. Lower Ca^{2+} events in **A** neurons and **B** astrocytes of CIE rats**.** * p<0.05, **** p<0.0001.

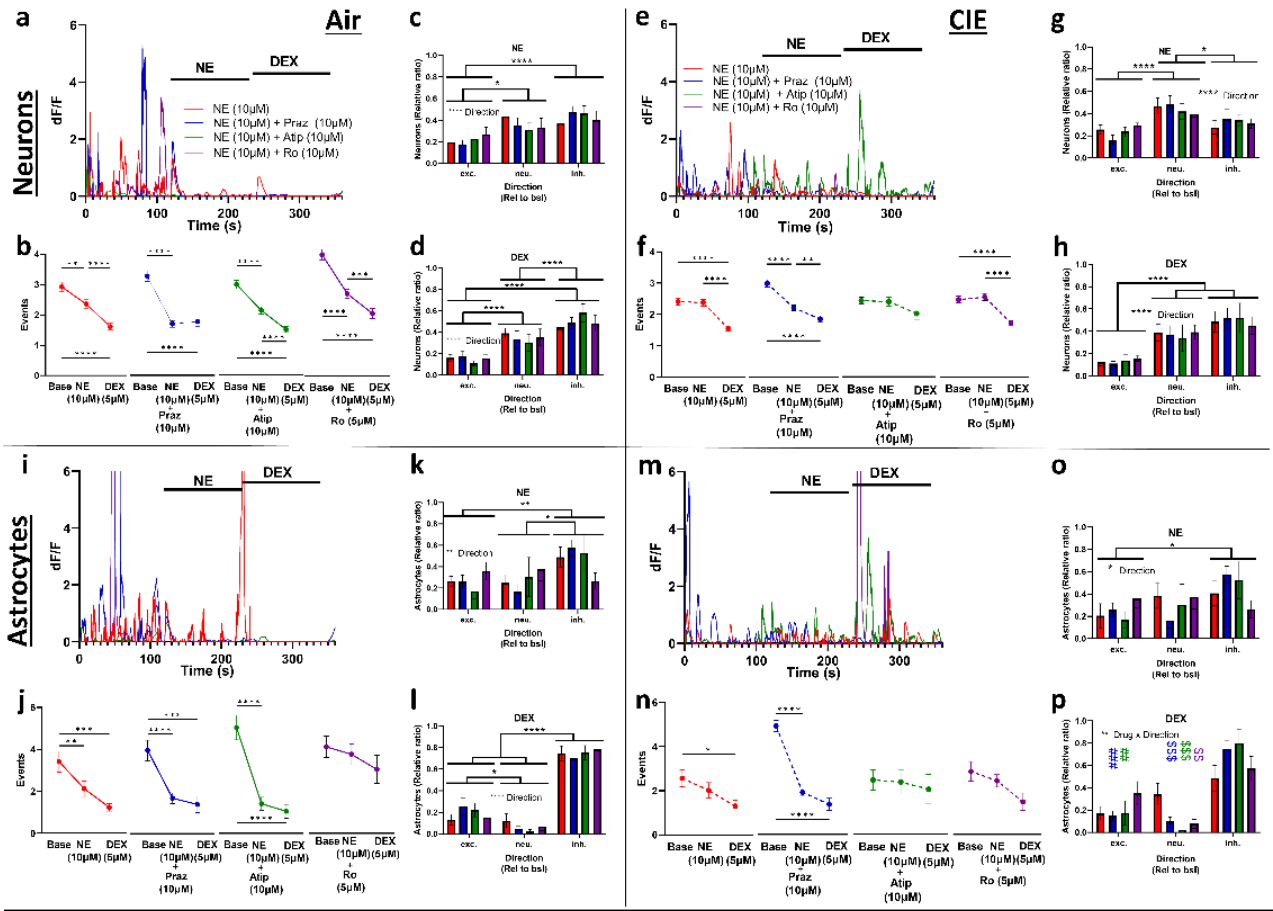

Figure 3-3: CIE exposure alters the basal Ca^{2+} signaling and sensitivity to α1AR ligands in PVN neurons and astrocytes to alter tripartite communication. **A** Representative traces of Air neurons during a pharmacological stress. **B** NE reduces the frequency of neuronal Ca^{2+} events. Neurons are largely inhibited in response to **C** NE and **D** DEX. **E** Representative traces of CIE neurons during a pharmacological stress. **F** NE is only able to reduce Ca^{2+} event frequency in CIE neurons during Praz co-application. CIE neurons are largely neutralized in response to **G** NE, while being inhibited by **H** DEX. **I** Representative traces Air astrocytes during a pharmacological stress **B** Air astrocytes reduction in Ca^{2+} event frequency is GluN2b-dependent. Air astrocytes are largely inhibited in response to **K** NE and **L** DEX. **M** Representative traces of CIE neurons during a pharmacological stress. **N** Loss of CIE astrocyte responsivity to NE is α1AR-dependent. CIE astrocytes are largely inhibited in response to **O** NE and **P** DEX. Line and bar graphs represent mean +/- SEM. * p <0.05, ** p<0.01, *** p<0.001, **** p<0.0001.

CIE exposure alters the basal Ca^{2+} signaling and sensitivity to α1AR ligands in PVN neurons

AUD is characterized by inability to cope with relapse-inducing stressors. Previously we have shown using electrophysiological methods, that CIE alters the basal excitability and responsivity to NE in PNCs within the PVN [110]. Thus, we sought to use single-photon Ca^{2+} imaging in *ex-vivo* PVN slices to visualize the basal excitability of neurons and their responsivity to NE application with and without co-application of selective αAR antagonists. CIE significantly

decreased the frequency of suprathreshold Ca^{2+} events during the baseline phase (Fig. 3-2 a). In Air neurons, NE consistently reduced the event frequency, independent of which drug NE was co-applied with (Fig. 3-3 a, b, c). Additionally, Air neurons showed a further decrease following treatment with the glucocorticoid receptor agonist, dexamethasone (DEX; 5µm) in all groups (Fig. 3-3 a, b, d) except those co-treated with Praz (Fig. 3-3 b). By contrast, CIE neurons failed to decrease their suprathreshold events in the presence of NE (Fig. 3-3 e, f, g) in all groups except in those co-treated with Praz (Fig. 3-3 f). DEX was able to reduce event frequency relative to NE treatment in all groups (Fig. 3-3 e, f, h) except following atipamezole (Atip; 10µm) co-treatment (Fig. 3-3 f). Together, these data suggest a selective dysfunction in α1AR signaling in CIE male neurons during protracted withdrawal.

CIE exposure alters astrocytic Ca^{2+} signaling in response to NE

Astrocytes have complex roles in influencing neuronal signaling in a plethora of ways [46]. Astrocytes are also known to influence both neuronal PVN signaling [123] and acute [102,121] and post-acute [205] effects of EtOH exposure. However, the contribution of astrocytes to CIE-induced alterations in neuronal signaling in response to NE [110] are not well-defined.

Under basal conditions, CIE astrocytes showed decreased Ca^{2+} events (Fig. 3-2 b). Following NE-treatment, Air astrocytes showed a consistent decrease in signaling frequency during NE application (Fig. 3-3 i, j, k), except those co-treated with Ro (Fig. 2j). DEX showed a trend towards a further reduction in signaling frequency in the same astrocytes (Fig. 2i, j, l) but this was not statistically different than NE treatment. On the other hand, astrocytes from CIE-treated rats only showed a decrease in events following NE + Praz (Fig 3-3 m, n, o). DEX also only decreased event frequency in NE and NE + Praz treated cells (Fig. 3-3 m, n, p). Atip and Ro failed to alter frequency of astrocytes in CIE-treated rats (Fig. 3-3 m-p).

Air astrocytes were more inhibited than neutral during NE application with concomitant treatment of Atip and Ro (Fig. 3-3 k). Air astrocytes treated with NE + Ro also showed a greater proportion that were excited by NE + Ro treatment, compared to neutral (Fig. 3-3 k). DEX showed an ability to shift the bulk of astrocytes towards a decrease in event frequency, regardless of pretreatment (Fig. 3-3 l). DEX was ineffective at increasing the proportion of inhibited astrocytes without any pretreatment in CIE-treated slices (Fig. 3-3 n, p). Interestingly, pretreatment with Atip,

Praz, or Ro facilitated a DEX-mediated increase in the proportion of inhibited astrocytes (Fig. 3-3 p). This data informs our understanding of the mechanisms by which NE can modulate the frequency of Ca^{2+} events in astrocytes that may underlie altered stress-related behaviors seen in CIE.

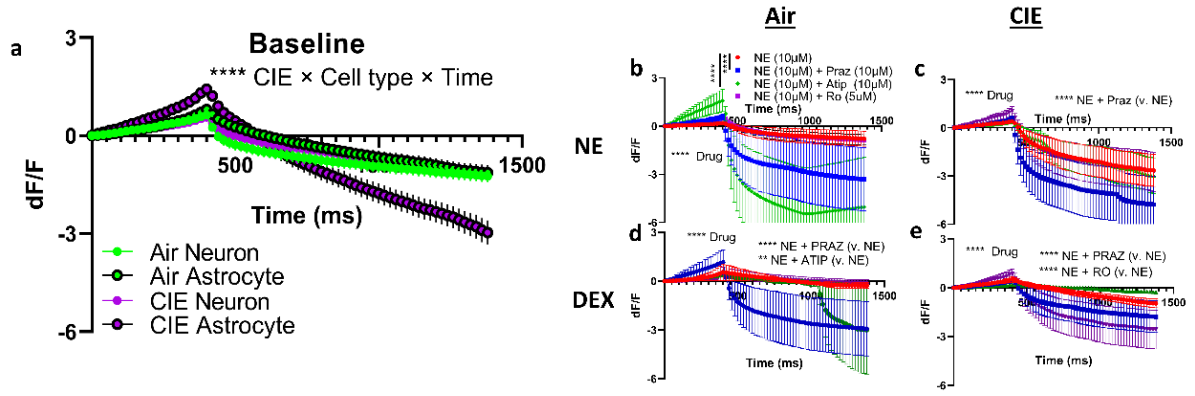

Figure 3-4: PVN astrocyte Ca^{2+} kinetics are robustly influenced by stimulation and neuroendocrine stress signaling in CIE rats. **A** CIE astrocytes have significantly elevated peaks and anti-peaks under basal conditions. **B** αARs influence the peak and anti-peak of Ca^{2+} events in Air astrocytes. **C** Kinetics of CIE astrocytes are normalized by α1AR blockade. **D,E** GR activation augments the anti-peak in an EtOH and drug-dependent manner. **A-E** Mean +/- SEM. * p <0.05, ** p<0.01, *** p<0.001, **** p<0.0001.

Discussion

NE and glucocorticoids are essential for the positive and negative regulation of the PVN CRF neuron activity, respectively [206,207]. Visualization of dynamic regulation of [Ca^{2+}] can be an appropriate proxy for monitoring neuronal and astrocytic activity and intracellular second messenger cascades [198,208,209] . Here, we show that CIE limits Ca^{2+} signaling in hypothalamic neurons in response to NE. This supports previous findings that the ability of NE to suppress glutamatergic transmission is lost in CIE males [110]. We also show that Praz blockade of α1AR normalizes neuronal Ca^{2+} responses to NE. This further supports our previous finding that Praz normalizes noradrenergic hyperactivity due to increased α1AR function in PVN CRF neurons of CIE males [110]. By contrast, the synthetic GR agonist, DEX, was able to lower events from baseline in all groups except CIE males pretreated with Atip, suggesting that GR remains functional in CIE males. This also suggests that Atip and DEX reduce the frequency of Ca^{2+} events through redundant mechanisms to suppress presynaptic glutamatergic transmission.

Previous studies have detailed that NE causes complex neuronal-astrocytic crosstalk to alter glutamatergic signaling in mouse PVN CRF neurons [123]. Astrocytes orchestrate critical roles in the acute effects of EtOH intoxication [102], escalation of EtOH consumption [121], and the post-acute effects of EtOH exposure, through astrocyte remodeling [210]. However, it is not known how CIE influences this neuronal-astrocytic crosstalk in the PVN, or how this may underlie the changes we saw to neuronal signaling in response to pharmacological stress. Interestingly, like neurons, astrocytes from Air rats largely showed decreased Ca^{2+} event frequency in the presence of NE. The lone exception to this was in the co-presence of GluN2B antagonist, Ro. Previous studies showed that secreted factors from astrocytes can amplify the synaptic activity of GluN2B-subunit containing NMDA receptors [122]. Our data that selective blockade of GluN2B eliminates the NE-mediated reduction in astrocytic Ca^{2+} event frequency, suggesting that tonic neuronal GluN2B signaling is required to suppress astrocytic Ca^{2+} event frequency in response to neuroendocrine stress signals. This mechanism by which NE acts to suppress astrocytic Ca^{2+} signals may be upstream of GluN2B signaling, as astrocytes typically don't express this NMDAR subunit [211,212]. Like CIE neurons, only CIE astrocytes co-treated with Praz were able to decrease their event frequency in response to NE. Together, our data suggest that CIE causes a shift in reactivity of both neurons and astrocytes in response to excitatory and inhibitory neuroendocrine signals.

There are important limitations of our study that should be noted. First, while visualizing Ca^{2+} signaling can be a suitable assay for assessing changes to synaptic activity [198], it can also be directly affected by many other intracellular signaling cascades [198], such as on-demand synthesis of endocannabinoids [208]. Future studies could simultaneously record local field potentials to help differentiate between action potential-dependent and independent Ca^{2+} signals [213] in both neurons and astrocytes. Other incremental features could be added to the described methods, such as addition of two-photon microscopy systems, especially those that can automatedly survey multiple depths of an *ex-vivo* slice [200]. Another limitation of the described study is that we gathered very little information regarding how cell-specific genotypes may differentially respond to pharmacological stressors in different groups. However, future studies could couple this technique with subsequent histological processes like CLARITY [214] to gain a richer biochemical dataset.

In conclusion, we demonstrate the tripartite cooperation involved in the regulation of HPA axis function by neuroendocrine factors, such as NE and CORT. Increased function of neuronal

α1AR and GluN2B-containing NMDARs following CIE likely contribute to this dysfunction, since their pharmacological antagonism ameliorated action of NE to reduce neuronal and astrocytic Ca^{2+} events. Furthering knowledge of the mechanisms by CIE can alter hypothalamic tripartite synapses may be an important step in developing novel pharmaceuticals that are able to mitigate stress-induced relapse in those afflicted with AUD.

CHAPTER 4

Chronic intermittent ethanol exposure disrupts the tripartite cooperative gating of metaplastic glutamate signaling by neuroendocrine stress cues

Abstract

Hypothalamic plasticity is an essential component of coordinating appropriate behavioral responses to stressful stimuli. CIE impairs the plasticity of PVN PNCs, which we believe mechanistically underlies the high relapse rates seen clinically in AUD patients. While CIE-induced dysfunction of α1AR activity has been implicated in this altered plasticity, mechanisms underlying CIE-induced changes the unmasking of this plasticity in response to afferent stimulation are poorly understood. Astrocytes and neurons cooperate for a vast number of physiological processes. Here, we used *ex-vivo* Ca^{2+} imaging in PVN slices exposed to a pharmacological stress protocol (NE 10uM followed by 5uM DEX) and evaluated the effects of HFS on Ca^{2+} event frequency and Ca^{2+} spike kinetics. We show here that HFS-STP involves cooperative function between astrocytes and neurons. Following antagonism of either α1 adrenergic receptor or GluN2B subunit of N-Methyl D-aspartate receptor, CIE astrocytes showed a complete loss of afterhyperpolarization current, suggesting neuronal signaling through these receptors augments the astrocytic response to afferent stimulation. This data may provide a groundwork for future pharmacotherapies for alcohol use disorder involving tripartite synaptic dysfunction in CIE.

Introduction

The cooperative function between astrocytes, presynaptic axon terminal, and postsynaptic soma, termed the "tripartite synapse", has garnered significant attention in the biomedical community over the past 30 years. All three parts of the synapse function in response to action by the other to coordinate and spatially amplify signals [46,123] . Astrocytes recycle neurotransmitters to allow for re-release by presynaptic terminals and buffer ionic concentrations of the synapse. Astrocytes can release various paracrine agents to alter synaptic activity [122,166]. However, the mechanisms by which astrocytic-neuronal crosstalk is impaired from CIE are currently not well understood.

CRF cells within the PVN are essential for both the function of the HPA axis and the gating of complex behaviors in response to environmental cues. For example, optogenetic inhibition of these cells results in increased rearing (an exploratory behavior) and decreased grooming (a stress-coping behavior) [68]. Additionally, high frequency stimulation-evoked short-term glutamatergic plasticity (HFS-STP) within the PVN [17] has been shown to correlate with an animal's freezing response to a threatening stimulus [19]. We have previously demonstrated that CIE-induced loss of stress-induced HFS-STP within the PVN was due to increased N-methyl D-aspartate receptor (NMDA) subunit 2B (GluN2B) function and decreased CRF receptor 1 function [11]. We have also shown that CIE-induced loss of stress-induced STP could be recovered by application of Praz in PNC recordings from male, but not female rats [110]. Thus, furthering the understanding of the complex cellular mechanisms of PVN PNCs has potential to positively impact development of future pharmacotherapies for those afflicted with AUD.

STP is believed to be the neurophysiological mechanism that ensures a fitted "fight, flight, or freeze" response to a real or perceived threat. Previous studies have documented a stress-dependent plasticity in PVN CRF neurons, whereby stimulation of afferents with 100Hz produces a short-term burst of glutamatergic signaling [17], which has been shown to be related to escape mechanisms in response to a looming shadow *in-vivo* [19]. This metaplastic response in glutamate signaling is known to be disrupted following models of CIE exposure [11,110]. However, it remains unclear how unmasking this metaplastic response affects acute Ca^{2+} signals in neurons and astrocytes. On one hand, it has been shown that postsynaptic Ca^{2+} chelation through BAPTA

unmasked HFS-induced STP in PNCs [17]. Seemingly paradoxically, both local glutamatergic signaling, and action potentials increase intracellular [Ca^{2+}] of the postsynaptic cell [204].

Materials and Methods

Animals

All experiments were performed in accordance with the guidance of the National Institutes of Health on animal care and use and the University of California, Los Angeles Animal Research Committee. Male Long-Evans rats (weighing 200-225 g) were pair-housed under 12-hr 6AM/6PM light/dark cycle with *ad libitum* access to food, water and environmental enrichment.

EtOH (Decon Laboratories, King of Prussia, PA) was administered via custom-built vapor chambers (La Jolla Alcohol Research, Inc.) for 12 hour on/off cycles (on at 10PM), referred to as CIE, as previously described [110] . Animals in their home cages passively consumed EtOH in gradually increasing doses throughout the 40-day experiment. Body weight was measured weekly to monitor potential adverse effects of EtOH exposure. Tail vein blood (30-50 μl) was collected into heparinized tubes (Microvette CB300, Starstedt, Germany) immediately following 12-hr vapor exposure during the last experimental week. Blood samples were centrifuged at 2,000 g for 10 min at room temperature and the EtOH content of each sample measured in duplicate along with EtOH standards using the alcohol oxidase reaction procedure (GM7 Micro-Stat, Analox, Huntington Beach, CA). A cutoff of >150 mg/dl of EtOH in plasma was used to confirm that an intoxicating level of EtOH was reached in each rat [156]. Animals were subsequently withdrawn for a period of 30 days prior to behavioral assessment, which was employed to disentangle the persistent adaptations to the HPA axis seen previously [154,157], from the effects of acute withdrawal. Room air-exposed, weight- and age-matched rats were used as controls.

Ca^{2+} imaging

CIE-exposed rats and their air-exposed controls were deeply anesthetized with isoflurane (Patterson Veterinary, MA, USA), decapitated and brain submerged in ice cold bubbling slicing artificial cerebrospinal fluid (ACSF) containing (in mM): 62 NaCl, 3.5 KCl, 1.25 NaH_2PO_4, 62 choline chloride, 0.5 $CaCl_2$, 3.5 $MgCl_2$, 26 $NaHCO_3$, 5 N-acetyl L-cysteine, and 5 glucose, pH adjusted to 7.3 with KOH. Acutely microdissected PVN slices (300 μM thick) were obtained

(VT1200s, Leica, Buffalo Grove, IL) and transferred to room temperature normal ACSF containing (in mM): 125 NaCl, 2.5 KCl, 1.25 NaH_2PO_4, 2 $CaCl_2$, 2 $MgCl_2$, 26 $NaHCO_3$, 10 glucose, pH adjusted to 7.3 with KOH, and allowed equilibrate for >1 hr prior to experimentation. Slices were then incubated in a 5-mL chamber containing ACSF with cell-permeable Ca^{2+}-indicating dye, Calbryte 520AM (AAT Biosciences), DMSO (0.3% w/v) and pluronic acid (0.02% w/v) for 45-60 min and allowed to wash in another normal ACSF solution for >5 min prior to imaging. Calbryte 520AM is an esterified dye that, following cleavage after passive transport into the cytosol, exhibits greatly enhanced cellular retention without the need for additional pharmaceutical intervention [201].

Imaging was performed on a Scientifica SliceScope, with imaging components built on an Olympus BX51 upright fluorescence microscope equipped with an sCMOS camera (Hamamatsu Orca Flash 4.0v3). Anatomical regions in brain sections for Ca^{2+} imaging were first identified by brightfield imaging with 780nm LED (Scientifica) illumination. Ca^{2+} imaging was performed using a 40x, 0.80NA water immersion objective (Olympus), continuous 470nm LED illumination (ThorLabs), and a filter cube suitable for Calbryte 520AM imaging: Excitation: Brightline 466/40, Dichroic: Semrock FF495-Di03, Emission: Brightline 525/50. Images were acquired continually with 20ms exposure time.

Electric field stimulation was applied at 110 mV (twin pulse every 5s). HFS was applied (100 Hz for 1 s, repeated four times with a 5 s interval) as previously described, except with field stimulation as opposed to a bipolar concentric stimulating electrode [110]. At the end of each experiment, slices were washed with high $[K^+]$ ACSF, (containing in mM: 86 NaCl. 55.4 KCl, 1 $MgCl_2$, 0.33 NaH_2PO_4, 10 D-Glucose, 10 HEPES, 2 $CaCl_2$) to putatively discriminate between neuronal and astrocytic cell populations [202]. Temperature of ACSF during the recorded sessions was held at 28° C to minimize bubble formation.

Drugs

Norepinephrine bitartrate (Tocris Biosciences, Minneapolis, MN, #5169) was dissolved in distilled water at a stock concentration of 100 mM and diluted in ACSF to 10 μM. Selective α1AR antagonist, Praz (Cayman Chemical, Ann Arbor, MI #15023) was dissolved in DMSO at a 10 mM stock concentration and diluted to a final volume of 10 μM in ACSF. Selective α1AR antagonist Atipamezole hydrochloride (Atip; Cayman Chemical, #9001181) was dissolved in distilled water

at a stock concentration of 50 mM, sonicated for 2 minutes, and diluted to a final concentration of 10 μM in ACSF. Selective GluN2b antagonist, Ro 25-6981 (Ro; Hellobio, Ann Arbor, MI #15023) was sonicated and dissolved in DMSO at a 5 mM stock concentration and diluted to a final volume of 5 μM in ACSF. Glucocorticoid receptor (GR) agonist, dexamethasone (DEX) was dissolved in DMSO at a 5 mM stock concentration and diluted to a final volume of 5 μM in ACSF. Recordings were performed in the continuous presence of picrotoxin (50 μM). All solutions equilibrated at 28 ± 0.5 °C prior to slice application.

To mimic a pharmacologically mediated stress response, multiple PVN slices from the same animal were washed with normal ACSF for 3 minutes, then NE, with or without selective antagonists (Praz, Atip, Ro) for a period of 8 minutes prior to imaging. Slices were then washed with normal ACSF again for 3 minutes prior to HFS of four trains at 100Hz every 5 seconds to unmask STP of specific glutamatergic synapses onto PNCs. Subsequently, slices were washed with DEX for 8 minutes and then washed with normal ACSF for 3 minutes to perform another round of HFS. Finally, slices were washed with high [K^+] ACSF, (containing in mM: 86 NaCl. 55.4 KCl, 1 $MgCl_2$, 0.33 NaH_2PO_4, 10 D-Glucose, 10 HEPES, 2 $CaCl_2$) to putatively discriminate between neuronal and astrocytic cell populations [202].

Data Extraction

Blinded scorers semi-manually curated regions of interest (ROIs) using Python-based Suite2P software [203]. ROI fluorescence was subtracted from the annual surround fluorescence, low-pass filtered, and transformed to dF/F_0 as previously described [200], where F_0 is calculated with a boxcar filter with a 200-frame lookback window. dF/F0 values were clipped between 0 and 9000 to eliminate negative changes. Area under the curve and event frequency of each cell was calculated for each drug treatment. A threshold of 0.15 dF/F was used to determine significant events, which is lower than the dF/F of a single *ex-vivo* action potential, but significantly above signal to noise in our recorded traces [204].

Data Analysis

All data are expressed as mean ± SEM. For behavioral and basal event frequency data, student's t-test was used to evaluate differences between CIE and Air groups. Correlation was determined between behavioral variables using Pearson's correlation test. Correlation of

behavioral variables with Ca^{2+} imaging parameters was evaluated using Spearman's correlation test. GraphPad Prism 9 and Python Jupyter notebook was used for all data analyses. Alpha cutoff of 0.05 was used.

Results

Figure 4-1: PVN astrocyte Ca^{2+} kinetics are robustly influenced by stimulation and neuroendocrine stress signaling in CIE rats. **A** CIE astrocytes have significantly elevated peaks and anti-peaks under basal conditions. **B** αARs influence the peak and anti-peak of Ca^{2+} events in Air astrocytes. **C** Kinetics of CIE astrocytes are normalized by α1AR blockade. **D,E** CIE unmasks a greatly increased peak and anti-peak following α1AR and GluN2B blockade. **F,G** GR activation augments the anti-peak in an EtOH and drug-dependent manner. **H,I** GR activation blocks HFS-induced peak and anti-peak increases in CIE astrocytes. **J** Imbalance of PKC/PKA activity in CIE rats leads to altered astrocytic Ca^{2+} signaling. **A-J** Mean +/- SEM. * p <0.05, ** p<0.01, *** p<0.001, **** p<0.0001.

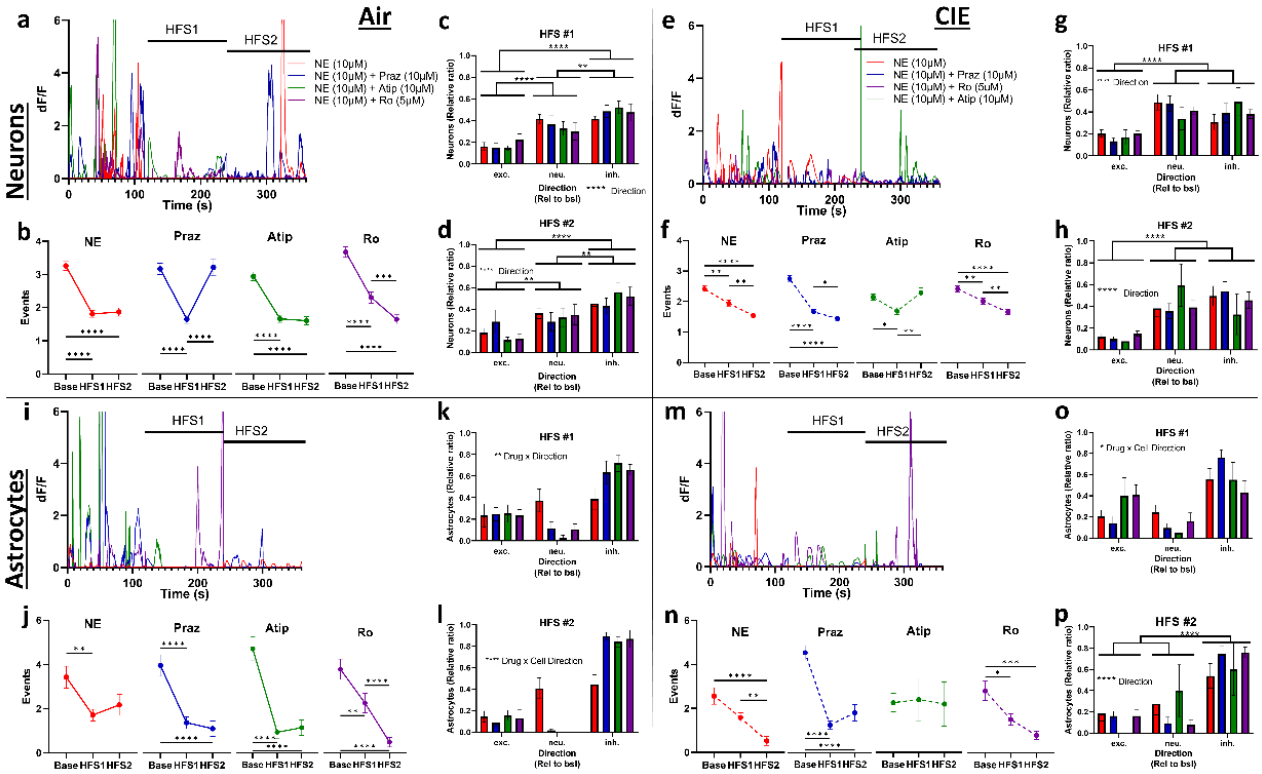

HFS-induced changes to Ca^{2+} signaling in PVN neurons are influenced by both αAR and CIE

Previous studies have documented a stress-dependent plasticity in PVN CRF neurons, whereby stimulation of afferents with 100Hz produces a short-term burst of glutamatergic signaling [17], which has been shown to be related to escape mechanisms in response to a looming

shadow *in-vivo* [19]. This metaplastic response in glutamate signaling is known to be disrupted following models of CIE exposure [11,110]. However, it remains unclear how unmasking this metaplastic response affects acute Ca^{2+} signals in neurons and astrocytes. On one hand, it has been shown that postsynaptic Ca^{2+} chelation through BAPTA unmasked HFS-induced STP in PNCs [17]. Seemingly paradoxically, both local glutamatergic signaling, and action potentials increase intracellular [Ca^{2+}] of the postsynaptic cell [204]. Thus, we sought to determine how HFS alters Ca^{2+} dynamics in neurons of Air and CIE rats. Following HFS#1 (HFS applied 3 minutes after last NE application), all neurons showed reduced event frequencies compared to baseline (Fig. 4-1 a-h). However, following HFS#2 (HFS applied 3 minutes after last DEX application), neurons in Air-treated groups showed a general decrease in event frequency compared to baseline (Fig. 4-1 a, b, d), except in PRAZ-treated cells that showed a significant increase from HFS#1 (Fig. 3b). In neurons of CIE-treated animals, event frequency was consistently further decreased in all groups during HFS#2 (Fig. 4-1 e, f, h), except Atip-treated cells (Fig. 4-1 f) which showed an increase compared to HFS#1.

CIE alters HFS-induced changes to Ca^{2+} signaling in astrocytic populations

HFS-induced changes to hypothalamic CRF neurons have been well-documented [13,17,66]. The effects of this stimulation-induced plasticity are not well understood, and no studies have reported a role of astrocytes in this phenomenon. This is despite the clear role astrocytes play in glutamate recycling [48]. We therefore sought to investigate how HFS can impact the frequency of Ca^{2+} events in astrocytes within the PVN. Astrocytes from Air rats decreased their events from basal levels during HFS#1 in all groups (Fig. 4-1 i, j, k). Events were also reduced during HFS#2 from baseline levels in all Air groups (Fig. 4-1 i, j, l) except just NE treated cells (Fig. 4-1 j). Astrocytes from CIE-treated rats only showed a decrease in frequency in those pretreated with PRAZ or Ro (Fig. 4-1 m, n, o). Astrocytes treated with NE or NE + Atip showed no change in frequency during HFS#1 (Fig. 4-1 m, n). All groups of CIE astrocytes (Fig. 4-1 m, n, p) showed a reduction from basal events during HFS#2, except following Atip pre-treatment (Fig. 4-1 n).

CIE causes astrocyte-specific shifts in Ca^{2+}-spike kinetics in response to HFS

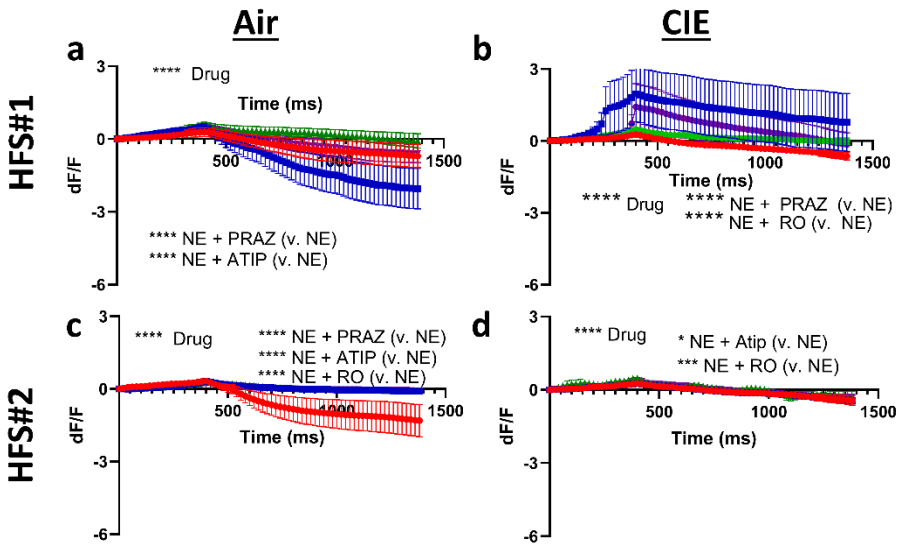

Figure 4-2: PVN astrocyte Ca^{2+} kinetics are robustly influenced by stimulation and neuroendocrine stress signaling in CIE rats. **A,B** CIE unmasks a greatly increased peak and anti-peak following α1AR and GluN2B blockade. **C,D** GR activation blocks HFS-induced peak and anti-peak increases in CIE astrocytes. **A-D** Mean +/- SEM. **** p<0.0001.

We next sought to determine if the kinetics of individual Ca^{2+} spikes were altered by either CIE, drug application, or HFS in neurons and astrocytes. We found that while the kinetics of neuronal Ca^{2+} spikes were relatively stable during all phases of the pharmacological stress protocol (Suppl. Fig. 4-1), astrocytes showed considerable treatment specific changes in Ca^{2+}-spike kinetics. HFS#1 had a very small effect on Air astrocytes post NE treatment (Fig 4-2 a). HFS#1 elicited unique and robust effects in the Ca^{2+} kinetics of CIE astrocytes (Fig. 4-2 b). Following washout of DEX and application of HFS#2, the anti-peak was eliminated in all groups except those cells previously treated with just NE (Fig. 4-2 c). There were subtle differences in the kinetics of astrocytic Ca^{2+} spikes from CIE rats following washout of Atip or Ro (Fig. 4-2 d). Collectively, these data suggest that increased function of α1AR and/or GluN2B following CIE may lead to a shift in the balance between protein kinase A and protein kinase C activation.

Discussion

Due to alcohol's ability to activate the HPA axis, CIE exposure results in dysregulation of the synaptic inputs that gate HPA axis responsivity. Afferents onto PVN CRF cells have a unique ability to rapidly facilitate local glutamate transmission (i.e., HFS-STP) in response to an imminent threat that helps to coordinate an adaptive behavioral response [19]. As this physiological feature is typically measured through whole-cell patch clamp recording [11,17,66,110], it is not yet determined how unmasking of this metaplastic response affects neuronal Ca^{2+} signaling. In all groups, HFS

following NE caused a decrease in neuronal Ca^{2+} event frequency. However, HFS following washout of DEX (HFS#2) caused a selective increase in the Ca^{2+} event frequency of Air neurons previously treated with Praz and CIE neurons previously treated with Atip. While it was previously known that NE and CRF contribute to metaplasticity formation within the PVN, our data suggest that GR function may interact with αAR function to gate STP formation.

The role of astrocytes in HFS-STP is completely unknown, despite the known crosstalk between neuronal and astrocytic populations and the critical role astrocytes play in glutamate shuttling [48]. We show here how HFS-evoked bursts of synaptic glutamatergic signals may influence astrocytic Ca^{2+} dynamics. All groups of astrocytes showed reduced events during HFS#1, except CIE astrocytes co-treated with Atip. Washout of DEX caused all groups except Air NE astrocytes to decrease their Ca^{2+} event frequency from baseline. Collectively, these data demonstrate that high-frequency stimulation modulates Ca^{2+} signaling in both neurons and astrocytes within the PVN. Further studies may assess the specific mechanisms by which astrocytic Ca^{2+} flux can influence neuronal signaling.

In multiple animal models, astrocytes have greater amplitude Ca^{2+} spike events than neurons [200,215]. We replicate this here, giving us increased confidence in the ability to distinguish between astrocytic and neuronal Ca^{2+} signals. EtOH exposure can trigger glutamate release, reactive oxygen species formation [216], amplify glucocorticoid induced Ca^{2+} accumulation [217] and induce gliosis in astrocytes of various brain regions, including the hypothalamus [218]. CIE caused a greatly amplified astrocytic basal Ca^{2+} peak. Previous reports showing that EtOH does not affect $[Ca^{2+}]_i$ [219] suggests that this is due to amplified Ca^{2+} release/influx, rather than through altered $[Ca^{2+}]_i$ [219]. There was also a greatly amplified anti-peak, which we took to indicate a refractory period between spikes. The Ca^{2+} spike kinetics of neurons were not particularly altered by drug treatments, stimulation, or CIE (Fig 4-2 a). However, astrocytes exhibited robust treatment-specific alterations to kinetics following HFS stimulation. Specifically, following treatment with NE and Praz or Ro, there was a complete reversal of the anti-peak of CIE astrocytes. This was temporary, as it was restored following DEX treatment. It is possible that the reversal in astrocytic Ca^{2+} spike kinetics may be due to the amplified glutamate release necessary for postsynaptic STP formation [17,209].

These mechanistic differences to astrocytic Ca^{2+} spike kinetics reflect known biochemical consequences of CIE exposure in the hypothalamus. We have previously shown that there is a selective increase in α1AR function following CIE and protracted withdrawal [110]. We and others have also shown that CIE causes a selective increase in the GluN2B subunit of NMDARs (reviewed in [220]), which can alter the formation of HFS-induced STP [11]. Both GluN2B and α1AR cause activation of protein kinase C (PKC) pathways [122,221], leading to increased autophagy [222] and shut down of translation through the integrated stress response [223]. Thus, chronic activation of PKC from these pathways may need to be inhibited (through Praz or Ro) to restore normal synaptic coupling between PNCs and astrocytes . Future studies may examine the necessity/sufficiency of PKA/PKC activity on the regulation of proteins necessary for modulating synaptic plasticity in hypothalamic PNCs [17] and other CNS synapses [224].

In conclusion, we provide evidence supporting the disruption of cooperative function between astrocytes and neurons following CIE vapor exposure and protracted withdrawal within the PVN. This may result in inappropriate stress-associated behaviors and an inability to cope with relapse-inducing stressors. α1AR and GluN2B antagonism was sufficient to reduce stimulation-induced changes to CIE astrocytic Ca^{2+} events following NE application. Thus, CIE-induced impairment of neuronal-astrocytic crosstalk likely involves co-dependent and/or redundant mechanisms involving hyperactivity of α1AR and GluN2B. Together, this provides key mechanistic insight towards pharmacotherapies that may ameliorate stress-associated behavioral maladaptations in those afflicted with AUD.

CHAPTER 5

Protracted withdrawal from chronic intermittent ethanol exposure causes distinct behavioral changes to stress-associated, anxiety-like, and consummatory behaviors in male Long-Evans rats

Abstract

Chronic exposure to ethanol induces broad neurophysiological effects that can result in long-lasting changes to behavior. As a complex disorder, interindividual differences in genetics, gene regulation, and environment may result in varied pharmaceutical efficacy for the treatment of AUD. To better understand how interindividual differences in behavior may reflect specific changes to the function of the hypothalamic tripartite synapse in response to stress, we conducted a behavioral battery of various behaviors shown to be pertinent to rodent models of AUD (such as grooming, rearing, open-field exploration, shock reactivity, and stress-enhanced fear learning to a normally innocuous stressor). We then related the features of Ca^{2+} signals in neurons and astrocytes to their recorded behaviors to evaluate how interindividual differences relate to pharmaceutical manipulation of neurophysiology. We identified marked differences in stress-associated, anxiety-like and exploratory behaviors between Air and CIE rats. We also identified both convergent and divergent relationships between physiological features and behaviors in CIE rats. For example, the grooming:rearing ratio showed a significant negative correlation to the fraction of excited astrocytes during HFS, suggesting that tripartite signaling dysfunction may underlie CIE-induced changes to the regulation of stress-coping and exploratory behaviors.

Introduction

AUD is a chronic relapsing disorder that has detrimental effects on those afflicted and loved ones. Attempts to pharmacologically treat AUD may be hindered by interindividual differences in the underlying cellular mechanisms underlying AUD [178,191]. Establishment of behavioral biomarkers as predictors of pharmacological efficacy can help clinicians understand the underlying mechanisms that contribute to variance in drug treatments and provide improved personalized treatment plans [191].

CIE exposure is a commonly employed preclinical model of AUD. Rodents subjected to CIE undergo behavioral changes which include loss of control over ethanol (EtOH) intake, anxiety-like behavior, and disruption of stress-coping behaviors [104,105]. Increased stress-induced grooming, which helps calm an animal after exposure to a stressor, is also lost following CIE [11]. However, even gold-standard preclinical models of AUD (such as CIE vapor exposure followed by protracted withdrawal) often result in a heterogeneity of drinking preference within each experimental group [105,225,226]. While exciting discoveries have started to uncover the neuronal underpinnings that contribute to compulsive escalation of alcohol intake leading to AUD [192], little is known about the broad consequences contributing to cellular dysfunction within the PVN following protracted withdrawal.

Appropriate preclinical models of behavioral pathologies should have face validity, theoretical rationale, and predictive validity [86]. This can be particularly troublesome when attempting to model psychiatric pathologies preclinically, as researchers are often tasked anthropomorphize instinctual behaviors in rodents without cross-conference [87]. For example, the elevated plus maze has been used extensively to measure anxiety-like behavior [87], but can also be impacted by the visual acuity of the strain of rodent at hand [88,89]. Humans with AUD and preclinical models of AUD both display increased anxiety-like behaviors [103,138,155,156,227–230]. However, it is not known how well anxiety-like behaviors can predict consummatory behavior, such as EtOH intake or preference, and whether they are symmetric in both species. The Long-Evans outbred strain of rat (generated with a Wistar female and wild male Grey Rat) retains many similar behaviors to wild rats [93], resulting in wide adoption by the behavioral neuroscience research

community. Importantly, Long-Evans rats have a more sensitive HPA axis response to passively and actively stressful assays than albino outbred Sprague-Dawley rats, potentially due to increased amygdalar and PVN CRF expression [80]. This suggests that this strain may be most appropriate when trying to understand behavioral consequences of CIE_{vapor} exposure.

Chronic exposure of rats to EtOH intoxication/withdrawal cycles results in behavioral changes, such as impaired flexibility, altered grooming, increased anxiety, increased EtOH seeking/consumption [11,104,105,231]. Interindividual differences in behavioral phenotypes may arise as a product of interaction between environmental factors and genetic predispositions [232,233]. Even "gold-standard" preclinical models of AUD, such as $CIE_{vapor,}$ results in considerable variability in the sought behavioral parameters (i.e., EtOH intake, EtOH preference, etc.) within experimental groups [105,225,226] likely reflecting phenotypes underling susceptibility to these traits [234,235]. Here, we opted for a behavioral battery to broadly assay stress-coping, exploratory, anxiety-like, reactivity, fear-learning and EtOH-related consummatory behaviors in adult Air and CIE-exposed Long-Evans male rats.

2. Methods

2.1 Animals

All experiments were performed in accordance with the guidance of the National Institutes of Health on animal care and use and the University of California, Los Angeles Animal Research Committee. Male Long-Evans rats (weighing 200-225 g) were pair-housed under 12-hr 6AM/6PM light/dark cycle with *ad libitum* access to food, water and environmental enrichment.

EtOH (Decon Laboratories, King of Prussia, PA) was administered via custom-built vapor chambers (La Jolla Alcohol Research, Inc.) for 12 hour on/off cycles (on at 10PM), referred to as CIE, as previously described [110] . Animals in their home cages passively consumed EtOH in gradually increasing doses throughout the 40-day experiment. Body weight was measured weekly to monitor potential adverse effects of EtOH exposure. Tail vein blood (30-50 μl) was collected into heparinized tubes (Microvette CB300, Starstedt, Germany) immediately following 12-hr vapor exposure during the last experimental week. Blood samples were centrifuged at 2,000 g for 10 min at room temperature and the EtOH content of each sample measured in duplicate along with EtOH standards using the alcohol oxidase reaction procedure (GM7 Micro-Stat, Analox,

Huntington Beach, CA). A cutoff of >150 mg/dl of EtOH in plasma was used to confirm that an intoxicating level of EtOH was reached in each rat [156]. Animals were subsequently withdrawn for a period of 30 days prior to behavioral assessment, which was employed to disentangle the persistent adaptations to the HPA axis seen previously [154,157], from the effects of acute withdrawal. Room air-exposed, weight- and age-matched rats were used as controls.

2.2 Behavioral Battery

Animals were given a behavioral battery to assess various stereotyped behaviors that have been associated with other preclinical models of AUD. First, animals were videotaped in a clean, bare Plexiglass cage for 15 minutes and behaviorally scored by a blinded recorder. Grooming, grooming transitions, rearing, and freezing were assessed as previously described [236]. Animals were allowed to acclimate to the room for 30 minutes following transfer and sessions started at 10AM. Three days later, animals were given a 10-minute open field test, digitally scored by EthoVision (Noldus, Leesburg, VA) software. The subsequent day, animals were exposed to 1 uncued foot-shock (1mA, 1s) during an 8-minute session with 2% Simple Green as an olfactory cue, blue polka dots as a visual cue, and metal bar flooring as a tactile cue. Animals were then reintroduced to the same context the next day to evaluate context-dependent freezing during a 15-minute session. Sessions were recorded using Video Freeze (Med Associates Fairfax, VT) software. Finally, animals were given an intermittent access 2-bottle choice between potable water and 10% w/w EtOH, as previously described [237].

2.3 Data Analysis

All data are expressed as mean ± SEM. For behavioral and basal event frequency data, student's t-test was used to evaluate differences between CIE and Air groups. Correlation was determined between behavioral variables using Pearson's correlation test. Correlation of behavioral variables with Ca^{2+} imaging parameters was evaluated using Spearman's correlation test. GraphPad Prism 9 and Python Jupyter notebook was used for all data analyses. Alpha cutoff of 0.05 was used.

Results

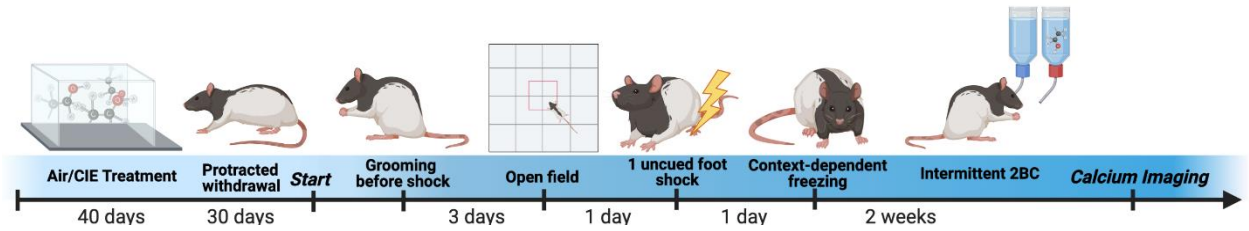

Timeline of experimental procedures to assess CIE-induced changes to stress-coping, anxiety-like and consummatory behaviors.

Figure 5-1: Timeline of experimental procedures to assess CIE-induced changes to stress-coping, anxiety-like and consummatory behaviors.. Following 40 days of exposure to gradually increasing doses of EtOH vapor or room-air, animals were removed from the vapor chamber for a period of 30 days. The behavioral battery consisted of a 15 minute video recording of grooming behavior. Three days later, animals were given an open field assay. Subsequently, animals received 1 uncued foot shock and were reintroduced to the same context without shock treatment to measure context-dependent freezing and startle reactivity. Finally, animals were given intermittent access to two-bottle choice between EtOH and potable tap water. Animals were withdrawn from EtOH exposure ~ 24 hours prior to conduction of Ca^{2+} imaging experiments.

CIE exposure alters hallmark behavioral traits and causes divergent relations between consummatory behaviors

Chronic exposure of rats to EtOH intoxication/withdrawal cycles results in behavioral changes, such as impaired flexibility, altered grooming, increased anxiety, increased EtOH seeking/consumption [11,104,105,231]. Still, it is appreciated that even "gold-standard" preclinical models of AUD have considerable variability in the sought behavioral parameters (i.e., EtOH intake, EtOH preference, etc.) within experimental groups [105,225,226] likely reflecting phenotypes underling susceptibility to these traits [234,235]. CIE rats showed lower grooming time (Fig. 5-2a), grooming:rearing ratio (Fig. 5-2c) and incorrect grooming transitions (Fig. 5-2d) and increased rearing time (Fig. 5-2b) during video recording. CIE animals also displayed increased anxiety measures through lower open field test velocity and time spent in the center (Fig. 5-2e, f). CIE animals displayed increased weight adjusted EtOH consumption and preference (Fig. 5-2g, h), with considerable variability within both groups (Fig 5-2j). When evaluating associated fear between Air and CIE groups, there was no detected statistical difference (Fig. 1j). However, if we collapsed CIE and Air animals and re-segregate them into groups based on whether their preference for 10% EtOH w/v was > 50% (drinker v. non-drinker), we then were able to detect a

difference in context-day fear, where non-drinkers spent significantly more time freezing (Fig. 5-2k).

Behavioral parameters were then mapped for correlations amongst Air and CIE rats. Divergent patterns of behavioral traits relating to drinking behavior were uncovered. In Air controls, reactivity to a single foot-shock was negatively correlated to cumulative EtOH consumption across the 2-week period (Fig. 5-2 l) and average EtOH preference was positively correlated to the latency to the center of the arena during the open field test (Fig. 5-2 m). Together, these data suggest that CIE alters the behavioral profile of rats, which can be predictors of consummatory EtOH behavior.

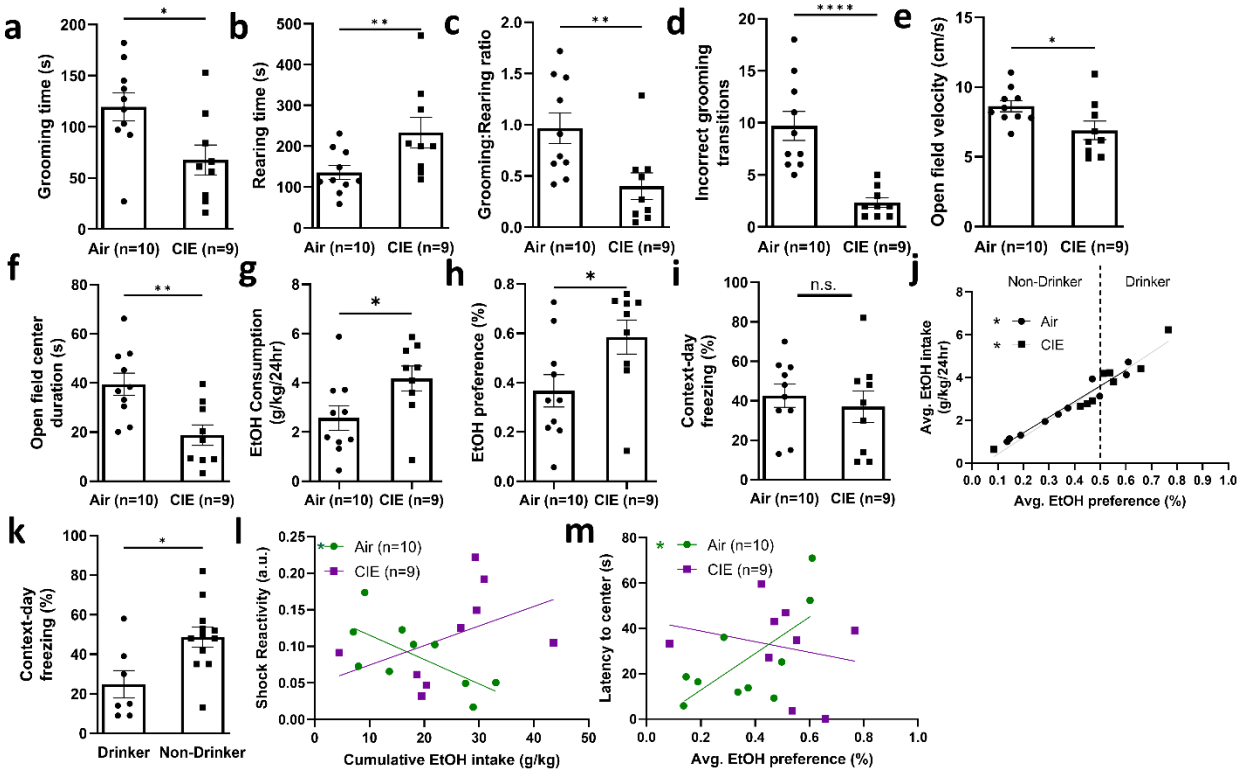

Figure 5-2: CIE exposure alters hallmark behavioral traits and causes divergent relations between consummatory behaviors.. **A** CIE decreases grooming time, **C** grooming:rearing ratio, **D** Incorrect grooming transitions, **E** open field velocity and **G** open field center duration. CIE increased **C** rearing, **F** EtOH consumption, and **G** preference over potable tap water. **H** No difference in context-dependent freezing between Air and CIE rats. **I** Average EtOH intake and preference are correlated in both Air and CIE rats. **J** Rats with >50% EtOH preference show enhanced context-dependent freezing. **K** Shock reactivity is negatively related to cumulative EtOH intake in Air rats. **L** Latency to the center of the open field is related to average EtOH preference in Air rats. Bar graphs represent mean +/- SEM. **A-H, J** Student's t-test. **I, K, L** Linear regression * p <0.05, ** p<0.01, **** p<0.0001.

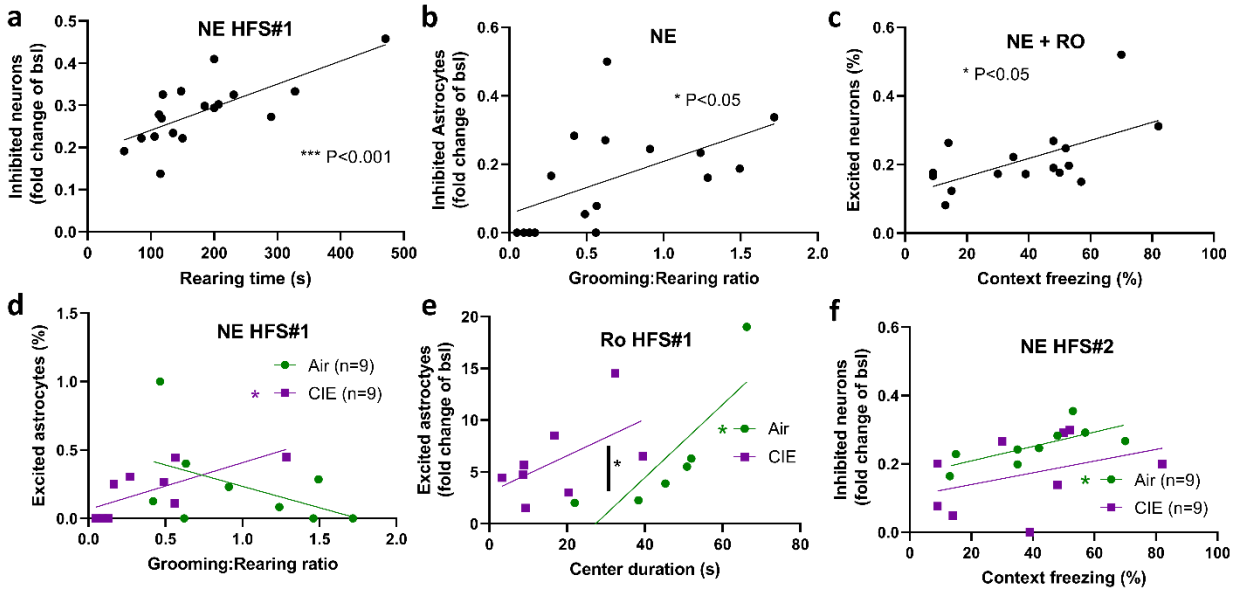

Figure 5-3: Convergent and divergent Ca^{2+} responses to stimulation. **A** Exploratory rearing behavior during open field is highly correlated to degree by which neurons were inhibited following NE HFS#1. **B** Relative time spent between exploratory and stress-relieving behaviors is positively correlated to the degree by astrocytes were inhibited by NE application. **C** Percentage of neurons excited by blockade of GluN2b-function is related to context-dependent freezing behavior. **D** Only CIE astrocyte excitation is an indicator of relative grooming:rearing ratio. **E** Classical anxiety-like measures are related to the degree of astrocyte excitation in only Air rats. **F** Degree of neuronal inhibition in positively correlated to context-dependent freezing percentage. **A-C** All rats. **D-F** Subjects stratified into treatment groups. **A-F** Linear regression. ***** **p<0.05,** ****** p<0.001.

Behavioral traits are both convergent and divergent predictors of drug-induced changes to neuronal activity within the PVN during a pharmacological stress

It is unknown how interindividual differences in astrocytic and neuronal signaling in response to stress may influence the behavioral variance observed during assays. Given the varied cell-type specific responses to various pharmacological and stimulation treatments (see Chapters 3 and 4), we performed nonparametric regressions of the individual behaviors examined during our behavioral battery against various the physiological Ca^{2+} imaging parameters. We identified some physiological features that corresponded to behavior, independent of CIE/Air treatment. For example, time spent rearing was significantly correlated to extent by which neurons were inhibited during HFS#1 following NE treatment (Fig. 5-3a). Further, we found that the grooming:rearing ratio was correlated to the extent to which astrocytes were inhibited during NE (Fig. 5-3b).

Additionally, the percent of neurons that were excited during NE + Ro was correlated to the percent of time spent freezing in the post-shock context test (Fig. 5-3c).

Other behavioral patterns showed divergence between CIE/Air treatments. For example, the percentage of astrocytes excited during NE HFS#1 was positively correlated to the grooming:rearing ratio only in CIE rats (Fig. 5-3 d). Further, during Ro HFS#1, the fold change by which astrocytes were excited was related to time spent in the center of the open field in air rats (Fig. 5-3 e). Additionally, after HFS#2 the fold change in neuronal inhibition was correlated to the context day percent time spent freezing in Air animals (Fig. 5-3 f).

Discussion

Alcohol has long been known as an acute activator of the HPA axis [26], whereas CIE exposure imposes a lasting toll on the resiliency of the HPA axis [11,107,110] and induces anxiety-like behaviors [105]. Our recent work showed that CIE exposure impairs PVN PNC's plastic and metaplastic glutamatergic synaptic transmission and responses to norepinephrine [11,110]. Consistent with previous reports [11], CIE animals exhibited decreased stress-coping behaviors, such as decreased time spent grooming. When CIE animals did groom, they showed more stereotyped patterning [236], as exhibited through decreased incorrect grooming transitions. Additionally, CIE animals increased exploratory behavior (rearing) [68], as well as increased anxiety-associated behaviors (decreases in center duration and velocity) in the open-field assay [238]. CIE animals also responded to intermittent-access two-bottle choice with both higher mean consumption and preference for EtOH [104,105]. While CIE did not alter context fear *per se*, those that had higher EtOH preference than 50% showed elevated levels of fear. The relationship of preference, anxiety and fear learning possibly supports previous evidence of CIE-induced alterations to hippocampal-amygdala circuitry [113,239,240], which mediates these affect-related behaviors [190,191]. Finally, the relation of anxiety (latency to the center) and startle responses were significantly correlated to drinking behaviors only in Air rats, suggesting that CIE causes a shift in the factors that drive increased EtOH salience.

We evaluated potential convergence and divergence in the relationship between behavioral traits and physiological features in Air and CIE rats First, we found a relationship between time spent rearing and the magnitude by which neurons were inhibited in response to HFS. Further, we

determined that the magnitude of astrocytic inhibition during NE was related to the grooming:rearing ratio. Together, these data suggest that the shift between stress-coping and exploratory behaviors may be a product of cooperative tripartite synaptic signaling *in vivo*. Additionally, we saw a correlation between the percent of excited neurons during NE + Ro to the magnitude of context-dependent freezing. Importantly, PVN neurons project to the central amygdala [241] and hippocampal CA2 [242,243]and receive direct inputs from the basolateral amygdala [54]. It remains an important question whether CIE-induced changes to PVN GluN2B function may be a mechanism by which CIE can augment amydala-hippocampal circuits that regulate context-dependent fear. [193]Given the observed link above between freezing to context-dependent cues and EtOH preference, our data suggests that pharmacologically reducing GluN2B levels in the PVN may also reduce EtOH preference in preclinical intermittent-access models.

Aside from the similarities, we also focused on identifying physiological biomarkers of behavioral traits specifically in Air and CIE animals to uncover mechanisms that may be manipulated by future pharmacotherapies. We determined only CIE animals showed a significant positive correlation between the percentage of astrocytes excited by NE HFS#1 and grooming:rearing ratio, suggesting that alterations in the behavioral choice between grooming and rearing in CIE rats may be due to differences in astrocytic responses to high-frequency afferent activity. Further, there was a significant co-variance in the magnitude of astrocytic excitement in response to HFS during co-application of NE + Ro with the center duration during open field, a hallmark indicator of anxiety-like behavior. Given the link of GluN2B upregulation to anxiety-like behaviors [244], this supports the notion that the anxiety displayed in CIE rats may be ameliorated by GluN2B antagonism, through action at astrocytes [122]. The specific relation of neuronal inhibition during HFS#2 to context dependent freezing suggests that CIE-induced changes to GR function in neurons may alter context-dependent fear. Recent reports show how CORT can regulate the endocytosis of α1AR [245]. It is possible that upregulation of α1AR as seen in CIE [113], or a CIE-specific impairment of this process leads to altered neuronal excitation during HFS#2. These correlations provide a fruitful groundwork for future mechanistic studies in preclinical models of AUD.

There are important limitations of our study that should be noted. We report here clear differences to behavioral changes imposed by CIE_{vapor} and protracted withdrawal in male Long-

Evans rats. We also identified potential behavioral biomarkers of altered hypothalamic tripartite signaling. We focused extensively on the role of glutamate (with the constant use of $GABA_A$ antagonist, picrotoxin) in this study to better investigate the neuroendocrine mechanisms that regulate the dynamic, stress-associated temporal changes in glutamate signaling within the PVN. However, $GABA_A$ plays a critical role in tonically constraining PVN PNC spiking and mediating a shift from infrequent bursting to repetitive single spikes *in-vivo* [15,52]. As CIE causes robust changes to GABAergic plasticity [246–248], future studies should examine the impact of CIE on $GABA_AR$ signaling and how this may relate to other stress-associated behaviors. Further, we focused primarily on comparing male Long-Evans rats, since female Long-Evans rats fail to escalate their EtOH consumption following CIE_{vapor} [105] and because we previously identified a Male sex × CIE interaction on CIE-induced alterations to noradrenergic signaling [110]. However, we plan to compare the behavioral and physiological consequences of CIE_{vapor} in males and females to identify potential sex-specific mechanisms that may affect vulnerability to $CIE_{vapor.}$

In summary, we provide firm evidence that the cooperative function between astrocytes and neurons is disrupted following CIE vapor exposure and protracted withdrawal within the PVN. These changes result in inadequate flexibility to respond to rapid increases in synaptic NE concentrations following exposure to a stressful stimulus, or other environmental factors that may activate the HPA axis, such as acute EtOH consumption [26]. This is likely due to increased neuronal α1AR function since this was reversed in both neurons and astrocytes during application of Praz. Further, α1AR and GluN2B antagonism was sufficient to reduce stimulation-induced changes to CIE astrocytic Ca^{2+} events following NE application. Thus, CIE-induced impairment of neuronal-astrocytic crosstalk likely involves co-dependent and/or redundant mechanisms involving hyperactivity of α1AR and GluN2B. Together, this provides key mechanistic insight towards pharmacotherapies that may ameliorate augmented anxiety-like behavioral responses to stressors in those afflicted with AUD.

GENERAL DISCUSSION

AUD is a chronic, relapsing disorder that imposes a large societal burden. Relapse rates for those afflicted by AUD are high, due to an inability to adequately cope with stressful stimuli. However, the neural mechanisms that contribute to altered behavioral hallmarks of AUD (negative emotional state, inability to cope with relapse-inducing stressors, loss of intake control) are poorly understood. In this dissertation, I utilized a preclinical model of CIE_{vapor} exposure followed by protracted withdrawal and employed whole-cell patch clamp electrophysiology and Ca^{2+} imaging techniques to assess the specific mechanisms by which hypothalamic neuronal and astrocytic signaling are altered in male rats. I determined that CIE alters PVN PNC responses to NE in a sex-dependent manner. I also determined that CIE-induced dysregulation of astrocytic-neuronal crosstalk that may be ameliorated through selective α1AR and/or GluN2B-containing NMDAR antagonism. Finally, we determined that CIE induces persistent changes to stress-related, anxiety-like and consummatory behaviors. There are divergences in the relation between anxiety-like and consummatory behaviors following EtOH treatment, and divergences in the relationship between astrocytic calcium signaling and behavior, suggesting that altered astrocytic responsivity may underlie stress-related differences to behavior seen following CIE.

Sex as a biological factor influences the neurophysiological and behavioral responses to stressors. Previous work has demonstrated that PVN CRF cells from females undergo changes to intrinsic excitability throughout the estrous cycle [249]. This may underlie sex differences seen previously in the ability of social isolation to gate HFS-STP[18]. We show here that CIE impacts the effects of NE on PNCs in a sex-dependent manner, such that female sex protects rats from the protracted neuroplastic consequences (impaired α1AR-mediated depolarizing, inward current and α2AR-mediated suppression of glutamate release) of CIE_{vapor} exposure [110]. We also demonstrate that co-application of NE with α1AR antagonist Praz, can restore CIE-induced loss of STP in stressed male rats. Our inability to recapitulate these results in females (our unpublished observations), suggests that known sex-differences to stress-associated GPCR internalization [136,153] may reflect differences in the pharmaceutical utility of drugs targeting noradrenergic receptors in AUD. These findings may additionally impact the treatment of other psychiatric diseases, as Praz is widely prescribed for PTSD despite mixed clinical efficacy [250,251]. Further, recent evidence suggests that one mechanism that CORT may act to negatively gate further HPA

axis activity is through GR-dependent endocytosis of α1AR [245]. Therefore, it is possible that sex differences in GR-dependent endocytosis may contribute to sex and CIE-dependent differences in α1AR to effect tripartite synaptic signal transmission. This could be examined closer in future studies using protein crosslinking [252] to determine membrane-bound (v. cytosolic) fractions of α1AR.

The tripartite synapse, composed of a presynaptic neuron, postsynaptic neuron and astrocyte, act cooperatively to orchestrate complex signal transmission. This is exemplified well by reports that α1AR activation in postsynaptic PVN CRF cells gates ATP release to amplify astrocytic dendritic release of glutamate, to provide a feed-forward mechanism by which NE can effect change on the HPA axis as a whole [123]. Here, we show that tripartite communication is disrupted in CIE males, by which increased neuronal a1AR can prevent NE-induced decrease in Ca^{2+} activity in both astrocytes and neurons. Antagonism of neuronal NMDAR subunit GluN2B can also ameliorate this NE-induced neurophysiological dysfunction, suggesting overlapping mechanisms. Future studies may use specific genetic Ca^{2+} indicators with non-overlapping emissions spectra to detail real-time alterations more precisely to tripartite communication *ex-vivo* or *in-vivo.* However, we note that this may require significant optimization as viruses can sometimes interfere in unintended manners [200].

After a long time in the shadow of excitable central nervous system cells, astrocytes are beginning to be recognized for their role in pathophysiology [46,47,120,253]. Astrocytes within the PVN are particularly important for modulating neighboring neuronal activity in a bidirectional manner in response to metabolic stress states [254]. This may be particularly insightful when considering that most pharmaceutical inventions targeting hypothalamic neurons have failed in clinical trials [254,255]. One particularly fruitful mechanism to consider in the future is the role of system X_c^-, which functions as a glutamate-cysteine exchanger in inflammosomogenic cells[256] (such as astrocytes) to synthesize antioxidant N-acetyl cysteine [257–259] enabling control over the mitochondrial redox state [260]. However, this transport consequently results in a linear release of glutamate from astrocytic stores [261]. Indeed, *Slc7a11* was identified as a epigenetic marker of alcohol consumption in those with AUD [262], suggesting a possible mechanistic link in AUD-associated pathologies. Understanding the mechanisms by which astrocytic remodeling from CIE exposure augments

neuronal excitability may bring us closer to translational acute and/or prophylactic treatments for AUD.

REFERENCES

1. Grant, B. F. *et al.* Epidemiology of DSM-5 Alcohol Use Disorder: Results From the National Epidemiologic Survey on Alcohol and Related Conditions III. *JAMA Psychiatry* **72**, 757–766 (2015).

2. Mokdad, A. H., Marks, J. S., Stroup, D. F. & Gerberding, J. L. Actual Causes of Death in the United States, 2000. *JAMA* **291**, 1238–1245 (2004).

3. Beynon, C. *et al.* Alcohol-related harm to others in England: a cross-sectional analysis of national survey data. *BMJ Open* **9**, e021046 (2019).

4. Haass-Koffler, C. L., Swift, R. M. & Leggio, L. Noradrenergic targets for the treatment of alcohol use disorder. *Psychopharmacology (Berl)* **235**, 1625–1634 (2018).

5. McKay, J. R., Franklin, T. R., Patapis, N. & Lynch, K. G. Conceptual, methodological, and analytical issues in the study of relapse. *Clin Psychol Rev* **26**, 109–127 (2006).

6. Yamashita, A. & Yoshioka, S. Chapter 40 - Relapse Risks in Patients With Alcohol Use Disorders. in (ed. Preedy, V. R. B. T.-N. of A.) 383–390 (Academic Press, 2019). doi:https://doi.org/10.1016/B978-0-12-813125-1.00040-4.

7. Tuithof, M., ten Have, M., van den Brink, W., Vollebergh, W. & de Graaf, R. Predicting persistency of DSM-5 alcohol use disorder and examining drinking patterns of recently remitted individuals: a prospective general population study. *Addiction* **108**, 2091–2099 (2013).

8. Wemm, S. E., Larkin, C., Hermes, G., Tennen, H. & Sinha, R. A day-by-day prospective analysis of stress, craving and risk of next day alcohol intake during alcohol use disorder treatment. *Drug Alcohol Depend* **204**, 107569 (2019).

9. Blaine, S. K. & Sinha, R. Alcohol, stress, and glucocorticoids: From risk to dependence and relapse in alcohol use disorders. *Neuropharmacology* **122**, 136–147 (2017).

10. McEWEN, B. S. Stress, Adaptation, and Disease: Allostasis and Allostatic Load. *Ann N Y Acad Sci* **840**, 33–44 (2006).

11. Marty, V. N., Mulpuri, Y., Munier, J. J. & Spigelman, I. Chronic alcohol disrupts hypothalamic responses to stress by modifying CRF and NMDA receptor function. *Neuropharmacology* **167**, 107991 (2020).

12. Smith, S. M. & Vale, W. W. The role of the hypothalamic-pituitary-adrenal axis in neuroendocrine responses to stress. *Dialogues Clin Neurosci* **8**, 383–395 (2006).

13. Bains, J. S., Cusulin, J. I. W. & Inoue, W. Stress-related synaptic plasticity in the hypothalamus. *Nat Rev Neurosci* **16**, 377–388 (2015).

14. Levy, B. H. & Tasker, J. G. Synaptic regulation of the hypothalamic–pituitary–adrenal axis and its modulation by glucocorticoids and stress. *Front Cell Neurosci* **6**, 1–13 (2012).

15. Colmers, P. L. W. & Bains, J. S. Balancing tonic and phasic inhibition in hypothalamic corticotropin-releasing hormone neurons. *J Physiol* **596**, 1919–1929 (2018).

16. Loewen, S. P., Baimoukhametova, D. & Bains, J. S. Sex-specific vasopressin signaling buffers stress-dependent synaptic changes in female mice. *Journal of Neuroscience* 2020.04.30.070532 (2020) doi:https://doi.org/10.1523/JNEUROSCI.1026-20.2020.

17. Kuzmiski, J. B., Marty, V., Baimoukhametova, D. v & Bains, J. S. Stress-induced priming of glutamate synapses unmasks associative short-term plasticity. *Nat Neurosci* **13**, 1257–1264 (2010).

18. Senst, L., Baimoukhametova, D., Sterley, T.-L. & Bains, J. S. Sexually dimorphic neuronal responses to social isolation. *Elife* **5**, e18726 (2016).

19. Daviu, N. *et al.* Paraventricular nucleus CRH neurons encode stress controllability and regulate defensive behavior selection. *Nat Neurosci* **23**, 398–410 (2020).

20. Iremonger, K. J., Benediktsson, A. M. & Bains, J. S. Glutamatergic synaptic transmission in neuroendocrine cells: Basic principles and mechanisms of plasticity. *Front Neuroendocrinol* **31**, 296–306 (2010).

21. da Silva, M. P., Merino, R. M., Mecawi, A. S., Moraes, D. J. & Varanda, W. A. In vitro differentiation between oxytocin- and vasopressin-secreting magnocellular neurons requires more than one experimental criterion. *Mol Cell Endocrinol* **400**, 102–111 (2015).

22. Hirasawa, M., Mouginot, D., Kozoriz, M. G., Kombian, S. B. & Pittman, Q. J. Vasopressin Differentially Modulates Non-NMDA Receptors in Vasopressin and Oxytocin Neurons in the Supraoptic Nucleus. *The Journal of Neuroscience* **23**, 4270–4277 (2003).

23. Itoh, S. *et al.* Attenuated stress-induced catecholamine release in mice lacking the vasopressin V $_{1b}$ receptor. *American Journal of Physiology-Endocrinology and Metabolism* **291**, E147–E151 (2006).

24. Gibbs, D. M. Oxytocin inhibits ACTH and peripheral catecholamine secretion in the urethane-anesthetized rat. *Regul Pept* **14**, 125–132 (1986).

25. Jamieson, B. B., Nair, B. B. & Iremonger, K. J. Regulation of hypothalamic corticotropin-releasing hormone neurone excitability by oxytocin. *J Neuroendocrinol* (2017) doi:10.1111/jne.12532.

26. Rivier, C. & Lee, S. Acute alcohol administration stimulates the activity of hypothalamic neurons that express corticotropin-releasing factor and vasopressin. *Brain Res* **726**, 1–10 (1996).

27. Scott, L. v & Dinan, T. G. Vasopressin and the regulation of hypothalamic-pituitary-adrenal axis function: Implications for the pathophysiology of depression. *Life Sci* **62**, 1985–1998 (1998).

28. Harper, K. M., Knapp, D. J., Criswell, H. E. & Breese, G. R. Vasopressin and alcohol: a multifaceted relationship. *Psychopharmacology (Berl)* **235**, 3363–3379 (2018).

29. Minhas, S., Liu, C., Galdamez, J., So, V. M. & Romeo, R. D. Stress-induced oxytocin release and oxytocin cell number and size in prepubertal and adult male and female rats. *Gen Comp Endocrinol* **234**, 103–109 (2016).

30. Cavanaugh, J., Carp, S. B., Rock, C. M. & French, J. A. Oxytocin modulates behavioral and physiological responses to a stressor in marmoset monkeys. *Psychoneuroendocrinology* (2016) doi:10.1016/j.psyneuen.2015.12.027.

31. Jurek, B. *et al.* Oxytocin Regulates Stress-Induced Crf Gene Transcription through CREB-Regulated Transcription Coactivator 3. *J Neurosci* **35**, 12248–12260 (2015).

32. Kudwa, A. E., McGivern, R. F. & Handa, R. J. Estrogen receptor β and oxytocin interact to modulate anxiety-like behavior and neuroendocrine stress reactivity in adult male and female rats. *Physiol Behav* **129**, 287–296 (2014).

33. Dabrowska, J. *et al.* Neuroanatomical evidence for reciprocal regulation of the corticotrophin-releasing factor and oxytocin systems in the hypothalamus and the bed nucleus of the stria terminalis of the rat: Implications for balancing stress and affect. *Psychoneuroendocrinology* **36**, 1312–1326 (2011).

34. Hernández, V. S. *et al.* Hypothalamic Vasopressinergic Projections Innervate Central Amygdala GABAergic Neurons: Implications for Anxiety and Stress Coping. *Front Neural Circuits* **10**, (2016).

35. Ma, X.-M., Lightman, S. L. & Aguilera, G. Vasopressin and Corticotropin-Releasing Hormone Gene Responses to Novel Stress in Rats Adapted to Repeated Restraint. *Endocrinology* **140**, 3623–3632 (1999).

36. Eliava, M. *et al.* A New Population of Parvocellular Oxytocin Neurons Controlling Magnocellular Neuron Activity and Inflammatory Pain Processing. *Neuron* **89**, 1291–1304 (2016).

37. Smith, A. S. *et al.* Local oxytocin tempers anxiety by activating GABAA receptors in the hypothalamic paraventricular nucleus. *Psychoneuroendocrinology* **63**, 50–58 (2016).

38. Neumann, I. D., Torner, L., Toschi, N. & Veenema, A. H. Oxytocin actions within the supraoptic and paraventricular nuclei: differential effects on peripheral and intranuclear vasopressin release. *American Journal of Physiology-Regulatory, Integrative and Comparative Physiology* **291**, R29–R36 (2006).

39. Dannenhoffer, C. A. *et al.* Oxytocin and vasopressin modulation of social anxiety following adolescent intermittent ethanol exposure. *Psychopharmacology (Berl)* **235**, 3065–3077 (2018).

40. Hansson, A. C. *et al.* Oxytocin Reduces Alcohol Cue-Reactivity in Alcohol-Dependent Rats and Humans. *Neuropsychopharmacology* **43**, 1235–1246 (2018).

41. Vena, A., King, A., Lee, R. & de Wit, H. Intranasal Oxytocin Does Not Modulate Responses to Alcohol in Social Drinkers. *Alcohol Clin Exp Res* **42**, 1725–1734 (2018).

42. Melby, K. *et al.* Actigraphy assessment of motor activity and sleep in patients with alcohol withdrawal syndrome and the effects of intranasal oxytocin. *PLoS One* **15**, e0228700 (2020).

43. Pedersen, C. A. *et al.* Intranasal Oxytocin Blocks Alcohol Withdrawal in Human Subjects. *Alcohol Clin Exp Res* **37**, 484–489 (2013).

44. Melby, K., Gråwe, R. W., Aamo, T. O., Salvesen, Ø. & Spigset, O. Effect of intranasal oxytocin on alcohol withdrawal syndrome: A randomized placebo-controlled double-blind clinical trial. *Drug Alcohol Depend* **197**, 95–101 (2019).

45. Melby, K., Gråwe, R. W., Aamo, T. O., Skovlund, E. & Spigset, O. Efficacy of Self-Administered Intranasal Oxytocin on Alcohol Use and Craving After Detoxification in Patients With Alcohol Dependence. A Double-Blind Placebo-Controlled Trial. *Alcohol and Alcoholism* **56**, 565–572 (2021).

46. Khakh, B. S. & Deneen, B. The Emerging Nature of Astrocyte Diversity. *Annu Rev Neurosci* **42**, 187–207 (2019).

47. Khakh, B. S. & Sofroniew, M. v. Diversity of astrocyte functions and phenotypes in neural circuits. *Nat Neurosci* **18**, 942–952 (2015).

48. Andersen, J. v *et al.* Glutamate metabolism and recycling at the excitatory synapse in health and neurodegeneration. *Neuropharmacology* **196**, 108719 (2021).

49. Wang, H. *et al.* Regulation of beta-amyloid production in neurons by astrocyte-derived cholesterol. *Proceedings of the National Academy of Sciences* **118**, (2021).

50. Lalo, U., Koh, W., Lee, C. J. & Pankratov, Y. The tripartite glutamatergic synapse. *Neuropharmacology* **199**, 108758 (2021).

51. English, K. *et al.* Astrocytes rescue neuronal health after cisplatin treatment through mitochondrial transfer. *Acta Neuropathol Commun* **8**, 36 (2020).

52. Ichiyama, A. *et al.* State-dependent activity dynamics of hypothalamic stress effector neurons. *Elife* **11**, e76832 (2022).

53. Huang, S.-T. *et al.* BNSTAVGABA-PVNCRF Circuit Regulates Visceral Hypersensitivity Induced by Maternal Separation in Vgat-Cre Mice. *Front Pharmacol* **12**, (2021).

54. Kim, T.-K. & Han, P.-L. Functional Connectivity of Basolateral Amygdala Neurons Carrying Orexin Receptors and Melanin-concentrating Hormone Receptors in Regulating Sociability and Mood-related Behaviors. *Exp Neurobiol* **25**, 307–317 (2016).

55. Kubota, N., Amemiya, S., Yanagita, S. & Kita, I. Neural pathways from the central nucleus of the amygdala to the paraventricular nucleus of the hypothalamus are involved in induction of yawning behavior due to emotional stress in rats. *Behavioural Brain Research* **436**, 114091 (2023).

56. Jhamandas, J. H., Harris, K. H., Petrov, T. & Krukoff, T. L. Characterization of the Parabrachial Nucleus Input to the Hypothalamic Paraventricular Nucleus in the Rat. *J Neuroendocrinol* **4**, 461–471 (1992).

57. Fawley, J. *et al.* PVN-projecting NTS neurons receive both direct and indirect inputs from solitary tract afferents. *The FASEB Journal* **34**, 1–1 (2020).

58. Flak, J. N. *et al.* Role of paraventricular nucleus-projecting norepinephrine/epinephrine neurons in acute and chronic stress. *European Journal of Neuroscience* **39**, 1903–1911 (2014).

59. Silverman, A. J., Hoffman, D. L. & Zimmerman, E. A. The descending afferent connections of the paraventricular nucleus of the hypothalamus (PVN). *Brain Res Bull* **6**, 47–61 (1981).

60. Larsen, P. & Mikkelsen, J. Functional identification of central afferent projections conveying information of acute 'stress' to the hypothalamic paraventricular nucleus. *The Journal of Neuroscience* **15**, 2609–2627 (1995).

61. Fenselau, H. *et al.* A rapidly acting glutamatergic ARC→PVH satiety circuit postsynaptically regulated by α-MSH. *Nat Neurosci* **20**, 42–51 (2017).

62. Martin, D. S. & Haywood, J. R. Hemodynamic responses to paraventricular nucleus disinhibition with bicuculline in conscious rats. *American Journal of Physiology-Heart and Circulatory Physiology* **265**, H1727–H1733 (1993).

63. Mendonça, M. M. *et al.* Involvement of GABAergic and Adrenergic Neurotransmissions on Paraventricular Nucleus of Hypothalamus in the Control of Cardiac Function. *Front Physiol* **9**, (2018).

64. Smith, A. S. *et al.* Local oxytocin tempers anxiety by activating GABAA receptors in the hypothalamic paraventricular nucleus. *Psychoneuroendocrinology* **63**, 50–58 (2016).

65. Page, M. C., Cassaglia, P. A. & Brooks, V. L. GABA in the paraventricular nucleus tonically suppresses baroreflex function: alterations during pregnancy. *American Journal of Physiology-Regulatory, Integrative and Comparative Physiology* **300**, R1452–R1458 (2011).

66. Marty, V., Kuzmiski, J. B., Baimoukhametova, D. v & Bains, J. S. Short-term plasticity impacts information transfer at glutamate synapses onto parvocellular neuroendocrine cells in the paraventricular nucleus of the hypothalamus. *J Physiol* **589**, 4259–4270 (2011).

67. Gouws, J. M., Sherrington, A., Zheng, S., Kim, J. S. & Iremonger, K. J. Regulation of corticotropin-releasing hormone neuronal network activity by noradrenergic stress signals. *J Physiol* **600**, 4347–4359 (2022).

68. Füzesi, T., Daviu, N., Wamsteeker Cusulin, J. I., Bonin, R. P. & Bains, J. S. Hypothalamic CRH neurons orchestrate complex behaviours after stress. *Nat Commun* **7**, 11937 (2016).

69. Daisuke, O. *et al.* The mammalian circadian pacemaker regulates wakefulness via CRF neurons in the paraventricular nucleus of the hypothalamus. *Sci Adv* **6**, eabd0384 (2021).

70. Kim, J. *et al.* Rapid, biphasic CRF neuronal responses encode positive and negative valence. *Nat Neurosci* **22**, 576–585 (2019).

71. Concetti, C. & Burdakov, D. Orexin/Hypocretin and MCH Neurons: Cognitive and Motor Roles Beyond Arousal. *Front Neurosci* **15**, (2021).

72. Aston-Jones, G. *et al.* Lateral hypothalamic orexin/hypocretin neurons: A role in reward-seeking and addiction. *Brain Res* **1314C**, 74 (2010).

73. Harris, G. C., Wimmer, M. & Aston-Jones, G. A role for lateral hypothalamic orexin neurons in reward seeking. *Nature* **437**, 556–559 (2005).

74. Koba, S. *et al.* Sympathoexcitation by hypothalamic paraventricular nucleus neurons projecting to the rostral ventrolateral medulla. *J Physiol* **596**, 4581–4595 (2018).

75. Ruyle, B. C., Martinez, D., Heesch, C. M., Kline, D. D. & Hasser, E. M. The PVN enhances cardiorespiratory responses to acute hypoxia via input to the nTS. *American Journal of Physiology-Regulatory, Integrative and Comparative Physiology* **317**, R818–R833 (2019).

76. Chen, Q.-H. & Toney, G. M. In Vivo Discharge Properties of Hypothalamic Paraventricular Nucleus Neurons With Axonal Projections to the Rostral Ventrolateral Medulla. *J Neurophysiol* **103**, 4–15 (2010).

77. Lee, S. K., Ryu, P. D. & Lee, S. Y. Differential distributions of neuropeptides in hypothalamic paraventricular nucleus neurons projecting to the rostral ventrolateral medulla in the rat. *Neurosci Lett* **556**, 160–165 (2013).

78. Tam, W. Y. & Cheung, K.-K. Phenotypic characteristics of commonly used inbred mouse strains. *J Mol Med* **98**, 1215–1234 (2020).

79. Ali Khan, A., Raess, M. & de Angelis, M. H. Moving forward with forward genetics: A summary of the INFRAFRONTIER Forward Genetics Panel Discussion. *F1000Res* **10**, 456 (2021).

80. Sanchís-Ollé, M. *et al.* Male long-Evans rats: An outbred model of marked hypothalamic-pituitary-adrenal hyperactivity. *Neurobiol Stress* **15**, (2021).

81. Armario, A., Gavaldà, A. & Martí, J. Comparison of the behavioural and endocrine response to forced swimming stress in five inbred strains of rats. *Psychoneuroendocrinology* **20**, 879–890 (1995).

82. Sternberg, E. M. *et al.* A central nervous system defect in biosynthesis of corticotropin-releasing hormone is associated with susceptibility to streptococcal cell wall-induced arthritis in Lewis rats. *Proceedings of the National Academy of Sciences* **86**, 4771–4775 (1989).

83. Crabbe, J. C., Merrill, C. M., Kim, D. & Belknap, J. K. Alcohol Dependence and Withdrawal: A Genetic Animal Model. *Ann Med* **22**, 259–263 (1990).

84. Colombo, G., Lobina, C., Carai, M. A. M. & Gessa, G. L. Phenotypic characterization of genetically selected Sardinian alcohol-preferring (sP) and -non-preferring (sNP) rats. *Addiction Biology* **11**, 324–338 (2006).

85. Lusis, A. J. *et al.* The Hybrid Mouse Diversity Panel: a resource for systems genetics analyses of metabolic and cardiovascular traits. *J Lipid Res* **57**, 925–942 (2016).

86. Sagvolden, T., Russell, V. A., Aase, H., Johansen, E. B. & Farshbaf, M. Rodent Models of Attention-Deficit/Hyperactivity Disorder. *Biol Psychiatry* **57**, 1239–1247 (2005).

87. Kraeuter, A.-K., Guest, P. C. & Sarnyai, Z. The Elevated Plus Maze Test for Measuring Anxiety-Like Behavior in Rodents. in *Pre-Clinical Models: Techniques and Protocols* (ed. Guest, P. C.) 69–74 (Springer New York, 2019). doi:10.1007/978-1-4939-8994-2_4.

88. Martínez, J. C., Cardenas, F., Lamprea, M. & Morato, S. The role of vision and proprioception in the aversion of rats to the open arms of an elevated plus-maze. *Behavioural Processes* **60**, 15–26 (2002).

89. Garcia, A. M. B., Cardenas, F. P. & Morato, S. Effect of different illumination levels on rat behavior in the elevated plus-maze. *Physiol Behav* **85**, 265–270 (2005).

90. Bockstal, V. *et al.* A comparative study between outbred and inbred rat strains for the use in in vivo IPV potency testing. *Vaccine* **36**, 2917–2920 (2018).

91. Binder, M. S., Shi, H. D. & Bordey, A. CD-1 Outbred Mice Produce Less Variable Ultrasonic Vocalizations Than FVB Inbred Mice, While Displaying a Similar Developmental Trajectory. *Front Psychiatry* **12**, (2021).

92. Bagley, J. R., Chesler, E. J., Philip, V. M. & Jentsch, J. D. Heritability of ethanol consumption and pharmacokinetics in a genetically diverse panel of collaborative cross mouse strains and their inbred founders. *Alcohol Clin Exp Res* **45**, 697–708 (2021).

93. Troy Harker, K. & Whishaw, I. Q. Place and matching-to-place spatial learning affected by rat inbreeding (Dark–Agouti, Fischer 344) and albinism (Wistar, Sprague–Dawley) but not domestication (wild rat vs. Long–Evans, Fischer–Norway). *Behavioural Brain Research* **134**, 467–477 (2002).

94. Nair, A. & Jacob, S. A simple practice guide for dose conversion between animals and human. *J Basic Clin Pharm* **7**, 27 (2016).

95. Smith, R. J. *et al.* Dynamic c-Fos changes in mouse brain during acute and protracted withdrawal from chronic intermittent ethanol exposure and relapse drinking. *Addiction biology* **25**, e12804 (2020).

96. Pettorelli, N., Coulson, T., Durant, S. M. & Gaillard, J.-M. Predation, individual variability and vertebrate population dynamics. *Oecologia* **167**, 305–314 (2011).

97. Fu, R. *et al.* Chronic intermittent voluntary alcohol drinking induces hyperalgesia in Sprague-Dawley rats. *Int J Physiol Pathophysiol Pharmacol* **7**, 136–44 (2015).

98. Hosová, D. & Spear, L. P. Voluntary elevated ethanol consumption in adolescent Sprague-Dawley rats: Procedural contributors and age-specificity. *Alcohol* **78**, 1–12 (2019).

99. Cederbaum, A. I. Alcohol Metabolism. *Clin Liver Dis* **16**, 667–685 (2012).

100. Wilson, D. F. & Matschinsky, F. M. Ethanol metabolism: The good, the bad, and the ugly. *Med Hypotheses* **140**, 109638 (2020).

101. Gubitosi-Klug, R. A. & Gross, R. W. Fatty Acid Ethyl Esters, Nonoxidative Metabolites of Ethanol, Accelerate the Kinetics of Activation of the Human Brain Delayed Rectifier K^+ Channel, Kv1.1 *. *Journal of Biological Chemistry* **271**, 32519–32522 (1996).

102. Jin, S. *et al.* Brain ethanol metabolism by astrocytic ALDH2 drives the behavioural effects of ethanol intoxication. *Nat Metab* **3**, 337–351 (2021).

103. Zhao, Y., Weiss, F. & Zorrilla, E. P. Remission and resurgence of anxiety-like behavior across protracted withdrawal stages in ethanol-dependent rats. *Alcohol Clin Exp Res* **31**, 1505–1515 (2007).

104. Kimbrough, A., Kim, S., Cole, M., Brennan, M. & George, O. Intermittent Access to Ethanol Drinking Facilitates the Transition to Excessive Drinking After Chronic Intermittent Ethanol Vapor Exposure. *Alcohol Clin Exp Res* **41**, 1502–1509 (2017).

105. Morales, M., McGinnis, M. M. & McCool, B. A. Chronic ethanol exposure increases voluntary home cage intake in adult male, but not female, Long-Evans rats. *Pharmacol Biochem Behav* **139**, 67–76 (2015).

106. Alele, P. E. & Devaud, L. L. Differential Adaptations in GABAergic and Glutamatergic Systems During Ethanol Withdrawal in Male and Female Rats. *Alcohol Clin Exp Res* **29**, 1027–1034 (2005).

107. Vendruscolo, L. F. *et al.* Corticosteroid-Dependent Plasticity Mediates Compulsive Alcohol Drinking in Rats. *The Journal of Neuroscience* **32**, 7563 (2012).

108. Herman, M. A., Contet, C. & Roberto, M. A Functional Switch in Tonic GABA Currents Alters the Output of Central Amygdala Corticotropin Releasing Factor Receptor-1 Neurons Following Chronic Ethanol Exposure. *J Neurosci* **36**, 10729–10741 (2016).

109. Repunte-Canonigo, V. *et al.* Nf1 regulates alcohol dependence-associated excessive drinking and gamma-aminobutyric acid release in the central amygdala in mice and is associated with alcohol dependence in humans. *Biol Psychiatry* **77**, 870–879 (2015).

110. Munier, J. J., Marty, V. N. & Spigelman, I. Sex differences in α-adrenergic receptor function contribute to impaired hypothalamic metaplasticity following chronic intermittent ethanol exposure. *Alcohol Clin Exp Res* (2022) doi:10.1111/acer.14900.

111. Marchesi, C., Chiodera, P., Brusamonti, E., Volpi, R. & Coiro, V. Abnormal plasma oxytocin and β-endorphin levels in alcoholics after short and long term abstinence. *Prog Neuropsychopharmacol Biol Psychiatry* **21**, 797–807 (1997).

112. Sizer, S. E., Parrish, B. C. & McCool, B. A. Chronic Ethanol Exposure Potentiates Cholinergic Neurotransmission in the Basolateral Amygdala. *Neuroscience* **455**, 165–176 (2021).

113. Varodayan, F. P. *et al.* The Amygdala Noradrenergic System Is Compromised With Alcohol Use Disorder. *Biol Psychiatry* **91**, 1008–1018 (2022).

114. Renteria, R., Maier, E. Y., Buske, T. R. & Morrisett, R. A. Selective alterations of NMDAR function and plasticity in D1 and D2 medium spiny neurons in the nucleus accumbens shell following chronic intermittent ethanol exposure. *Neuropharmacology* **112**, 164–171 (2017).

115. Loftén, A., Adermark, L., Ericson, M. & Söderpalm, B. An acetylcholine-dopamine interaction in the nucleus accumbens and its involvement in ethanol's dopamine-releasing effect. *Addiction Biology* **26**, e12959 (2021).

116. Liang, J., Marty, V. N., Mulpuri, Y., Olsen, R. W. & Spigelman, I. Selective modulation of GABAergic tonic current by dopamine in the nucleus accumbens of alcohol-dependent rats. *J Neurophysiol* **112**, 51–60 (2014).

117. Hade, A.-C. *et al.* Chronic Alcohol Use Induces Molecular Genetic Changes in the Dorsomedial Thalamus of People with Alcohol-Related Disorders. *Brain Sci* **11**, 435 (2021).

118. Agarwal, K. *et al.* Inflammatory Markers in Substance Use and Mood Disorders: A Neuroimaging Perspective. *Front Psychiatry* **13**, (2022).

119. Kelso, M. L., Liput, D. J., Eaves, D. W. & Nixon, K. Upregulated vimentin suggests new areas of neurodegeneration in a model of an alcohol use disorder. *Neuroscience* **197**, 381–393 (2011).

120. Moffat, J. J. & Ron, D. Astrocytes and alcohol: cortical astrocytes regulate alcohol consumption and intoxication. *Neuropsychopharmacology* (2020) doi:10.1038/s41386-020-0737-5.

121. Erickson, E. K. *et al.* Cortical astrocytes regulate ethanol consumption and intoxication in mice. *Neuropsychopharmacology* **46**, 500–508 (2021).

122. Hahn, J., Wang, X. & Margeta, M. Astrocytes increase the activity of synaptic GluN2B NMDA receptors. *Front Cell Neurosci* **9**, 117 (2015).

123. Chen, C. *et al.* Astrocytes Amplify Neuronal Dendritic Volume Transmission Stimulated by Norepinephrine. *Cell Rep* **29**, 4349-4361.e4 (2019).

124. Handa, R. J., Kudwa, A. E., Donner, N. C., McGivern, R. F. & Brown, R. Central 5-alpha reduction of testosterone is required for testosterone's inhibition of the hypothalamo-pituitary–adrenal axis response to restraint stress in adult male rats. *Brain Res* **1529**, 74–82 (2013).

125. Karkanias, G. B., Petitti, N. & Etgen, A. M. Progesterone attenuation of alpha 1-adrenergic receptor stimulation of phosphoinositol hydrolysis in hypothalamus of estrogen-primed female rats. *Endocrinology* **136**, 1993–1999 (1995).

126. González-Arenas, A., Aguilar-Maldonado, B., Avendaño-Vázquez, S. E. & García-Sáinz, J. A. Estrogens cross-talk to alpha1b-adrenergic receptors. *Mol Pharmacol* **70**, 154–162 (2006).

127. Weiser, M. J. & Handa, R. J. Estrogen impairs glucocorticoid dependent negative feedback on the hypothalamic-pituitary-adrenal axis via estrogen receptor alpha within the hypothalamus. *Neuroscience* **159**, 883–895 (2009).

128. Weiland, N. G. & Wise, P. M. Estrogen alters the diurnal rhythm of alpha 1-adrenergic receptor densities in selected brain regions. *Endocrinology* **121**, 1751–1758 (1987).

129. Sárvári, M. *et al.* Long-Term Estrogen Receptor Beta Agonist Treatment Modifies the Hippocampal Transcriptome in Middle-Aged Ovariectomized Rats . *Frontiers in Cellular*

Neuroscience vol. 10 149 Preprint at https://www.frontiersin.org/article/10.3389/fncel.2016.00149 (2016).

130. Arnold, A. P. & Chen, X. What does the 'four core genotypes' mouse model tell us about sex differences in the brain and other tissues? *Frontiers in Neuroendocrinology* vol. 30 1–9 Preprint at https://doi.org/10.1016/j.yfrne.2008.11.001 (2009).

131. Keyes, K. M., Grant, B. F. & Hasin, D. S. Evidence for a closing gender gap in alcohol use, abuse, and dependence in the United States population. *Drug Alcohol Depend* **93**, 21–29 (2008).

132. Cheng, H. G. & Anthony, J. C. Female–male differences in alcohol dependence levels: Evidence on newly incident adolescent and young-adult drinkers in the United States, 2002–2014. *Int J Methods Psychiatr Res* **27**, (2018).

133. Hingson, R. W., Zha, W. & White, A. M. Drinking Beyond the Binge Threshold: Predictors, Consequences, and Changes in the U.S. *Am J Prev Med* **52**, 717–727 (2017).

134. Guinle, M. I. B. The Role of Stress, Trauma, and Negative Affect in the Development of Alcohol Misuse and Alcohol Use Disorders in Women. *Alcohol Res* **40**, (2020).

135. Annis, H. M. & Graham, J. M. Profile types on the Inventory of Drinking Situations: Implications for relapse prevention counseling. *Psychology of Addictive Behaviors* **9**, 176–182 (1995).

136. Bangasser, D. A., Wiersielis, K. R. & Khantsis, S. Sex differences in the locus coeruleus-norepinephrine system and its regulation by stress. *Brain Res* **1641**, 177–188 (2016).

137. Bertholomey, M. L., Nagarajan, V. & Torregrossa, M. M. Sex differences in reinstatement of alcohol seeking in response to cues and yohimbine in rats with and without a history of adolescent corticosterone exposure. *Psychopharmacology (Berl)* **233**, 2277–2287 (2016).

138. Henricks, A. M. *et al.* Sex- and hormone-dependent alterations in alcohol withdrawal-induced anxiety and corticolimbic endocannabinoid signaling. *Neuropharmacology* **124**, 121–133 (2017).

139. Przybysz, K. R., Gamble, M. E. & Diaz, M. R. Moderate adolescent chronic intermittent ethanol exposure sex-dependently disrupts synaptic transmission and kappa opioid receptor function in the basolateral amygdala of adult rats. *Neuropharmacology* **188**, 108512 (2021).

140. Kirson, D. *et al.* Sex Differences in Acute Alcohol Sensitivity of Naïve and Alcohol Dependent Central Amygdala GABA Synapses. *Alcohol Alcohol* **56**, 581–588 (2021).

141. Koob, G. F. A role for brain stress systems in addiction. *Neuron* **59**, 11–34 (2008).

142. Centanni, S. W., Bedse, G., Patel, S. & Winder, D. G. Driving the Downward Spiral: Alcohol-Induced Dysregulation of Extended Amygdala Circuits and Negative Affect. *Alcohol Clin Exp Res* **43**, 2000–2013 (2019).

143. Fox, H. C., Milivojevic, V., Angarita, G. A., Stowe, R. & Sinha, R. Peripheral immune system suppression in early abstinent alcohol-dependent individuals: Links to stress and cue-related craving. *Journal of Psychopharmacology* **31**, 883–892 (2017).

144. Sinha, R. *et al.* Enhanced negative emotion and alcohol craving, and altered physiological responses following stress and cue exposure in alcohol dependent individuals. *Neuropsychopharmacology* **34**, 1198–208 (2009).

145. Schneider, J. E., Wise, J. D., Benton, N. A., Brozek, J. M. & Keen-Rhinehart, E. When do we eat? Ingestive behavior, survival, and reproductive success. *Hormones and Behavior* vol. 64 702–728 Preprint at https://doi.org/10.1016/j.yhbeh.2013.07.005 (2013).

146. McEwen, B. S. Physiology and Neurobiology of Stress and Adaptation: Central Role of the Brain. *Physiol Rev* **87**, 873–904 (2007).

147. Harbuz, M. S. & Lightman, S. L. Stress and the hypothalamo-pituitary-adrenal axis: acute, chronic and immunological activation. *J Endocrinol* **134**, 327–339 (1992).

148. Molinoff, P. B. Alpha- and beta-adrenergic receptor subtypes properties, distribution and regulation. *Drugs* **28 Suppl 2**, 1–15 (1984).

149. Daftary, S. S., Boudaba, C. & Tasker, J. G. Noradrenergic regulation of parvocellular neurons in the rat hypothalamic paraventricular nucleus. *Neuroscience* **96**, 743–751 (2000).

150. Boehm, S. & Huck, S. alpha 2-Adrenoreceptor-mediated inhibition of acetylcholine-induced noradrenaline release from rat sympathetic neurons: an action at voltage-gated Ca2+ channels. *Neuroscience* **69**, 221–231 (1995).

151. Martín, F. *et al.* Involvement of noradrenergic transmission in the PVN on CREB activation, TORC1 levels, and pituitary-adrenal axis activity during morphine withdrawal. *PLoS One* **7**, e31119–e31119 (2012).

152. Swift, R. M. & Aston, E. R. Pharmacotherapy for alcohol use disorder: current and emerging therapies. *Harv Rev Psychiatry* **23**, 122–133 (2015).

153. Petitti, N., Karkanias, G. B. & Etgen, A. M. Estradiol selectively regulates alpha 1B-noradrenergic receptors in the hypothalamus and preoptic area. *The Journal of Neuroscience* **12**, 3869 LP – 3876 (1992).

154. Richardson, H. N., Lee, S. Y., O'Dell, L. E., Koob, G. F. & Rivier, C. L. Alcohol self-administration acutely stimulates the hypothalamic-pituitary- adrenal axis, but alcohol dependence leads to a dampened neuroendocrine state. *European Journal of Neuroscience* **28**, 1641–1653 (2008).

155. Valdez, G. R. *et al.* Increased ethanol self-administration and anxiety-like behavior during acute ethanol withdrawal and protracted abstinence: regulation by corticotropin-releasing factor. *Alcohol Clin Exp Res* **26**, 1494–1501 (2002).

156. Getachew, B., Hauser, S. R., Taylor, R. E. & Tizabi, Y. Desipramine blocks alcohol-induced anxiety- and depressive-like behaviors in two rat strains. *Pharmacol Biochem Behav* **91**, 97–103 (2008).

157. Vendruscolo, L. F. *et al.* Corticosteroid-Dependent Plasticity Mediates Compulsive Alcohol Drinking in Rats. *Journal of Neuroscience* **32**, 7563–7571 (2012).

158. Luther, J. A. & Tasker, J. G. Voltage-gated currents distinguish parvocellular from magnocellular neurones in the rat hypothalamic paraventricular nucleus. *J Physiol* **523 Pt 1**, 193–209 (2000).

159. Sawchenko, P. & Swanson, L. The organization of noradrenergic pathways from the brainstem to the paraventricular and supraoptic nuclei in the rat. *Brain Res* **257**, 275–325 (1982).

160. Wang, B., Wang, Y., Wu, Q., Huang, H. & Li, S. Effects of α2A Adrenoceptors on Norepinephrine Secretion from the Locus Coeruleus during Chronic Stress-Induced Depression . *Frontiers in Neuroscience* vol. 11 243 Preprint at (2017).

161. Fitzgerald, P. J. Elevated Norepinephrine may be a Unifying Etiological Factor in the Abuse of a Broad Range of Substances: Alcohol, Nicotine, Marijuana, Heroin, Cocaine, and Caffeine. *Subst Abuse* **7**, 171–183 (2013).

162. Wallner, M. & Olsen, R. W. Physiology and pharmacology of alcohol: the imidazobenzodiazepine alcohol antagonist site on subtypes of GABAA receptors as an opportunity for drug development? *Br J Pharmacol* **154**, 288–298 (2008).

163. Yuan, Y. *et al.* Reward Inhibits Paraventricular CRH Neurons to Relieve Stress. *Current Biology* **29**, 1243-1251.e4 (2019).

164. Krugers, H. J., Karst, H. & Joels, M. Interactions between noradrenaline and corticosteroids in the brain: from electrical activity to cognitive performance. *Front Cell Neurosci* **6**, 15 (2012).

165. Petitti, N., Karkanias, G. B. & Etgen, A. M. Estradiol selectively regulates alpha 1B-noradrenergic receptors in the hypothalamus and preoptic area. *The Journal of Neuroscience* **12**, 3869 LP – 3876 (1992).

166. Gaidin, S. G. *et al.* Activation of alpha-2 adrenergic receptors stimulates GABA release by astrocytes. *Glia* **68**, 1114–1130 (2020).

167. Glover, E. J., Khan, F., Clayton-Stiglbauer, K. & Chandler, L. J. Impact of sex, strain, and age on blood ethanol concentration and behavioral signs of intoxication during ethanol vapor exposure. *Neuropharmacology* **184**, 108393 (2021).

168. Marsland, P. *et al.* Male, but not female, Sprague Dawley rats display enhanced fear learning following acute ethanol withdrawal (hangover). *Pharmacol Biochem Behav* **208**, 173229 (2021).

169. Sengupta, P. The Laboratory Rat: Relating Its Age With Human's. *Int J Prev Med* **4**, 624–630 (2013).

170. Rivier, C. Role of hypothalamic corticotropin-releasing factor in mediating alcohol-induced activation of the rat hypothalamic-pituitary-adrenal axis. *Front Neuroendocrinol* **35**, 221–233 (2014).

171. Rivier, C. & Rivest, S. Effect of stress on the activity of the hypothalamic-pituitary-gonadal axis: peripheral and central mechanisms. *Biol Reprod* **45**, 523–32 (1991).

172. Koob, G. F. Corticotropin-releasing factor, norepinephrine, and stress. *Biol Psychiatry* **46**, 1167–1180 (1999).

173. Koob, G. F. Alcoholism: allostasis and beyond. *Alcohol Clin Exp Res* **27**, 232–243 (2003).

174. Heilig, M. & Koob, G. F. A key role for corticotropin-releasing factor in alcohol dependence. *Trends in Neurosciences* vol. 30 399–406 Preprint at https://doi.org/10.1016/j.tins.2007.06.006 (2007).

175. Berridge, C. W. Noradrenergic modulation of arousal. *Brain Res Rev* **58**, 1–17 (2008).

176. Daviu, N. & Bains, J. S. Should I Stay or Should I Go? CRHPVN Neurons Gate State Transitions in Stress-Related Behaviors. *Endocrinology* **162**, (2021).

177. Froehlich, J. C., Hausauer, B. J., Federoff, D. L., Fischer, S. M. & Rasmussen, D. D. Prazosin Reduces Alcohol Drinking Throughout Prolonged Treatment and Blocks the Initiation of Drinking in Rats Selectively Bred for High Alcohol Intake. *Alcohol Clin Exp Res* **37**, 1552–1560 (2013).

178. Wilcox, C. E. *et al.* A Randomized, Placebo-controlled, Clinical Trial of Prazosin for the Treatment of Alcohol Use Disorder. *J Addict Med* **12**, 339–345 (2018).

179. Komatsu, S., Dobson, J. G. J., Ikebe, M., Shea, L. G. & Fenton, R. A. Crosstalk between adenosine A1 and β1-adrenergic receptors regulates translocation of PKCε in isolated rat cardiomyocytes. *J Cell Physiol* **227**, 3201–3207 (2012).

180. Vasudevan, N. T., Mohan, M. L., Gupta, M. K., Hussain, A. K. & Naga Prasad, S. V. Inhibition of Protein Phosphatase 2A Activity by PI3Kγ Regulates β-Adrenergic Receptor Function. *Mol Cell* **41**, 636–648 (2011).

181. Riedel, K. *et al.* Estrogen determines sex differences in adrenergic vessel tone by regulation of endothelial β-adrenoceptor expression. *American Journal of Physiology-Heart and Circulatory Physiology* **317**, H243–H254 (2019).

182. Costa-Mattioli, M. & Walter, P. The integrated stress response: From mechanism to disease. *Science* **368**, (2020).

183. Woo, C. W., Kutzler, L., Kimball, S. R. & Tabas, I. Toll-like receptor activation suppresses ER stress factor CHOP and translation inhibition through activation of eIF2B. *Nat Cell Biol* **14**, 192–200 (2012).

184. Brown, D. *et al.* The Beta-adrenergic agonist, Ractopamine, increases skeletal muscle expression of Asparagine Synthetase as part of an integrated stress response gene program. *Sci Rep* **8**, 15915 (2018).

185. Izumi, Y. & Zorumski, C. F. Inhibitors of cellular stress overcome acute effects of ethanol on hippocampal plasticity and learning. *Neurobiol Dis* **141**, 104875 (2020).

186. Lewis, M. Brain Change in Addiction as Learning, Not Disease. *N Engl J Med* **379**, 1551–1560 (2018).

187. Nielsen, C. K. *et al.* The delta opioid receptor antagonist, SoRI-9409, decreases yohimbine stress-induced reinstatement of ethanol-seeking. *Addiction biology* **17**, 224–234 (2012).

188. Sacks, J. J., Gonzales, K. R., Bouchery, E. E., Tomedi, L. E. & Brewer, R. D. 2010 National and State Costs of Excessive Alcohol Consumption. *Am J Prev Med* **49**, e73–e79 (2015).

189. Peltier, M. R. *et al.* Sex differences in stress-related alcohol use. *Neurobiol Stress* **10**, 100149 (2019).

190. Blanco, C. *et al.* Probability and predictors of treatment-seeking for substance use disorders in the U.S. *Drug Alcohol Depend* **149**, 136–144 (2015).

191. Heilig, M., Sommer, W. H. & Spanagel, R. The Need for Treatment Responsive Translational Biomarkers in Alcoholism Research. *Curr Top Behav Neurosci* **28**, 151–171 (2016).

192. Domi, E. *et al.* A neural substrate of compulsive alcohol use. *Sci Adv* **7**, (2021).

193. Hübel, N. & Ullah, G. Anions Govern Cell Volume: A Case Study of Relative Astrocytic and Neuronal Swelling in Spreading Depolarization. *PLoS One* **11**, e0147060 (2016).

194. Li, H., Lones, L. & DiAntonio, A. Bidirectional regulation of glial potassium buffering - glioprotection versus neuroprotection. *Elife* **10**, (2021).

195. Yang, W. & Yuste, R. In vivo imaging of neural activity. *Nat Methods* **14**, 349–359 (2017).

196. Hsiao, Y.-T., Wang, A. Y.-C., Lee, T.-Y. & Chang, C.-Y. Using Baseplating and a Miniscope Preanchored with an Objective Lens for Calcium Transient Research in Mice. *J Vis Exp* (2021) doi:10.3791/62611.

197. Schrank, S., Barrington, N. & Stutzmann, G. E. Calcium-Handling Defects and Neurodegenerative Disease. *Cold Spring Harb Perspect Biol* **12**, (2020).

198. Berridge, M. J. Neuronal calcium signaling. *Neuron* **21**, 13–26 (1998).

199. Aharoni, D., Khakh, B. S., Silva, A. J. & Golshani, P. All the light that we can see: a new era in miniaturized microscopy. *Nat Methods* **16**, 11–13 (2019).

200. Asrican, B. & Song, J. Extracting meaningful circuit-based calcium dynamics in astrocytes and neurons from adult mouse brain slices using single-photon GCaMP imaging. *STAR Protoc* **2**, 100306 (2021).

201. Liao, J. *et al.* A novel Ca2+ indicator for long-term tracking of intracellular calcium flux. *Biotechniques* **70**, 271–277 (2021).

202. Ravin, R. *et al.* Blast shockwaves propagate Ca2+ activity via purinergic astrocyte networks in human central nervous system cells. *Sci Rep* **6**, 25713 (2016).

203. Pachitariu, M. *et al.* Suite2p: beyond 10,000 neurons with standard two-photon microscopy. *bioRxiv* 061507 (2017) doi:10.1101/061507.

204. Tada, M., Takeuchi, A., Hashizume, M., Kitamura, K. & Kano, M. A highly sensitive fluorescent indicator dye for calcium imaging of neural activity in vitro and in vivo. *Eur J Neurosci* **39**, 1720–1728 (2014).

205. Lindberg, D., Ho, A. M. C., Peyton, L. & Choi, D.-S. Chronic Ethanol Exposure Disrupts Lactate and Glucose Homeostasis and Induces Dysfunction of the Astrocyte-Neuron Lactate Shuttle in the Brain. *Alcohol Clin Exp Res* **43**, 1838–1847 (2019).

206. Cole, R. L. & Sawchenko, P. E. Neurotransmitter regulation of cellular activation and neuropeptide gene expression in the paraventricular nucleus of the hypothalamus. *J Neurosci* **22**, 959–969 (2002).

207. Di, S., Malcher-Lopes, R., Halmos, K. Cs. & Tasker, J. G. Nongenomic Glucocorticoid Inhibition via Endocannabinoid Release in the Hypothalamus: A Fast Feedback Mechanism. *The Journal of Neuroscience* **23**, 4850 LP – 4857 (2003).

208. Manz, K. M. *et al.* Calcium-Permeable AMPA Receptors Promote Endocannabinoid Signaling at Parvalbumin Interneuron Synapses in the Nucleus Accumbens Core. *Cell Rep* **32**, 107971 (2020).

209. Kim, W. T., Rioult, M. G. & Cornell-Bell, A. H. Glutamate-induced calcium signaling in astrocytes. *Glia* **11**, 173–184 (1994).

210. Erickson, E. K., Blednov, Y. A., Harris, R. A. & Mayfield, R. D. Glial gene networks associated with alcohol dependence. *Sci Rep* **9**, 10949 (2019).

211. Lalo, U., Koh, W., Lee, C. J. & Pankratov, Y. The tripartite glutamatergic synapse. *Neuropharmacology* **199**, 108758 (2021).

212. Savtchouk, I. & Volterra, A. Gliotransmission: Beyond Black-and-White. *The Journal of Neuroscience* **38**, 14 LP – 25 (2018).

213. Wu, X. *et al.* A Modified Miniscope System for Simultaneous Electrophysiology and Calcium Imaging in vivo. *Front Integr Neurosci* **15**, 682019 (2021).

214. Du, H., Hou, P., Zhang, W. & Li, Q. Advances in CLARITY-based tissue clearing and imaging. *Exp Ther Med* **16**, 1567–1576 (2018).

215. Chen, J., Poskanzer, K. E., Freeman, M. R. & Monk, K. R. Live-imaging of astrocyte morphogenesis and function in zebrafish neural circuits. *Nat Neurosci* **23**, 1297–1306 (2020).

216. Salazar, M., Pariente, J. A., Salido, G. M. & González, A. Ethanol induces glutamate secretion by Ca2+ mobilization and ROS generation in rat hippocampal astrocytes. *Neurochem Int* **52**, 1061–1067 (2008).

217. Mulholland, P. J. *et al.* Corticosterone Increases Damage and Cytosolic Calcium Accumulation Associated With Ethanol Withdrawal in Rat Hippocampal Slice Cultures. *Alcohol Clin Exp Res* **29**, 871–881 (2005).

218. Villavicencio-Tejo, F., Flores-Bastías, O., Marambio-Ruiz, L., Pérez-Reytor, D. & Karahanian, E. Fenofibrate (a PPAR-α Agonist) Administered During Ethanol Withdrawal Reverts Ethanol-

Induced Astrogliosis and Restores the Levels of Glutamate Transporter in Ethanol-Administered Adolescent Rats. *Front Pharmacol* **12**, (2021).

219. Dildy-Mayfield, J. E. & Leslie, S. W. Mechanism of Inhibition of N-Methyl-d-Aspartate-Stimulated Increases in Free Intracellular Ca2+ Concentration by Ethanol. *J Neurochem* **56**, 1536–1543 (1991).

220. Naassila, M. & Pierrefiche, O. GluN2B Subunit of the NMDA Receptor: The Keystone of the Effects of Alcohol During Neurodevelopment. *Neurochem Res* **44**, 78–88 (2019).

221. Drouva, S. V, Faivre-Bauman, A., Loudes, C., Laplante, E. & Kordon, C. Alpha 1-adrenergic receptor coupling with phospholipase-C is negatively regulated by protein kinase-C in primary cultures of hypothalamic neurons and glial cells. *Endocrinology* **129**, 1605–1613 (1991).

222. Volpe, C. M. O., Villar-Delfino, P. H., Dos Anjos, P. M. F. & Nogueira-Machado, J. A. Cellular death, reactive oxygen species (ROS) and diabetic complications. *Cell Death Dis* **9**, 119 (2018).

223. Zhang, G. *et al.* Integrated Stress Response Couples Mitochondrial Protein Translation With Oxidative Stress Control. *Circulation* **144**, 1500–1515 (2021).

224. Irfan, M. *et al.* SNAP-25 isoforms differentially regulate synaptic transmission and long-term synaptic plasticity at central synapses. *Sci Rep* **9**, 6403 (2019).

225. Okhuarobo, A. *et al.* A novel mouse model for vulnerability to alcohol dependence induced by early-life adversity. *Neurobiol Stress* **13**, 100269 (2020).

226. Logrip, M. L. & Zorrilla, E. P. Stress history increases alcohol intake in relapse: relation to phosphodiesterase 10A. *Addiction Biology* **17**, 920–933 (2012).

227. Anker, J. Co-Occurring Alcohol Use Disorder and Anxiety: Bridging the Psychiatric, Psychological, and Neurobiological Perspectives. *Alcohol Res* **40**, (2019).

228. Moench, K. M. & Logrip, M. L. Housing Condition Differentially Impacts Escalation of Alcohol Intake, Relapse-Like Drinking, Anxiety-Like Behavior, and Stress History Effects by Sex. *Alcohol Clin Exp Res* **45**, 480–489 (2021).

229. Rylkova, D., Shah, H. P., Small, E. & Bruijnzeel, A. W. Deficit in brain reward function and acute and protracted anxiety-like behavior after discontinuation of a chronic alcohol liquid diet in rats. *Psychopharmacology (Berl)* **203**, 629–640 (2009).

230. Conway, K. P., Compton, W., Stinson, F. S. & Grant, B. F. Lifetime comorbidity of DSM-IV mood and anxiety disorders and specific drug use disorders: results from the National Epidemiologic Survey on Alcohol and Related Conditions. *J Clin Psychiatry* **67**, 247–257 (2006).

231. Fernandez, G. M., Lew, B. J., Vedder, L. C. & Savage, L. M. Chronic intermittent ethanol exposure leads to alterations in brain-derived neurotrophic factor within the frontal cortex and impaired behavioral flexibility in both adolescent and adult rats. *Neuroscience* **348**, 324–334 (2017).

232. Lin, Y. S., Thummel, K. E., Thompson, B. D., Totah, R. A. & Cho, C. W. Sources of Interindividual Variability. in *Enzyme Kinetics in Drug Metabolism: Fundamentals and Applications* (eds. Nagar,

S., Argikar, U. A. & Tweedie, D.) 481–550 (Springer US, 2021). doi:10.1007/978-1-0716-1554-6_17.

233. Genon, S., Eickhoff, S. B. & Kharabian, S. Linking interindividual variability in brain structure to behaviour. *Nat Rev Neurosci* **23**, 307–318 (2022).

234. Cloninger, C. R., Sigvardsson, S., Knorring, A.-L. & Bohman, M. The Swedish Studies of the Adopted Children of Alcoholics: A Reply to Littrell. *J Stud Alcohol* **49**, 500–509 (1988).

235. Tawa, E. A., Hall, S. D. & Lohoff, F. W. Overview of the Genetics of Alcohol Use Disorder. *Alcohol and Alcoholism* **51**, 507–514 (2016).

236. Kalueff, A. V, Aldridge, J. W., LaPorte, J. L., Murphy, D. L. & Tuohimaa, P. Analyzing grooming microstructure in neurobehavioral experiments. *Nat Protoc* **2**, 2538–2544 (2007).

237. Marty, V. N. *et al.* Long-Acting Glucagon-Like Peptide-1 Receptor Agonists Suppress Voluntary Alcohol Intake in Male Wistar Rats. *Front Neurosci* **14**, 599646 (2020).

238. Prut, L. & Belzung, C. The open field as a paradigm to measure the effects of drugs on anxiety-like behaviors: a review. *Eur J Pharmacol* **463**, 3–33 (2003).

239. Mira, R. G. *et al.* Alcohol impairs hippocampal function: From NMDA receptor synaptic transmission to mitochondrial function. *Drug Alcohol Depend* **205**, 107628 (2019).

240. Izumi, Y. & Zorumski, C. F. Inhibitors of cellular stress overcome acute effects of ethanol on hippocampal plasticity and learning. *Neurobiol Dis* **141**, 104875 (2020).

241. Ferretti, V. *et al.* Oxytocin Signaling in the Central Amygdala Modulates Emotion Discrimination in Mice. *Current Biology* **29**, 1938-1953.e6 (2019).

242. Cui, Z., Gerfen, C. R. & Young, W. S. Hypothalamic and other connections with dorsal CA2 area of the mouse hippocampus. *Journal of Comparative Neurology* **521**, 1844–1866 (2013).

243. Althammer, F. *et al.* Altered <scp>PVN-to-CA2</scp> hippocampal oxytocin pathway and reduced number of oxytocin-receptor expressing astrocytes in heart failure rats. *J Neuroendocrinol* **34**, (2022).

244. Fan, Y. *et al.* Intermittent Hypoxia Activates N-Methyl-D-Aspartate Receptors to Induce Anxiety Behaviors in a Mouse Model of Sleep-Associated Apnea. *Mol Neurobiol* **58**, 3238–3251 (2021).

245. Jiang, Z. *et al.* Stress-induced glucocorticoid desensitizes adrenoreceptors to gate the neuroendocrine response to somatic stress in male mice. *Cell Rep* **41**, 111509 (2022).

246. Lindemeyer, A. K. *et al.* α2 Subunit–Containing GABA_A Receptor Subtypes Are Upregulated and Contribute to Alcohol-Induced Functional Plasticity in the Rat Hippocampus. *Mol Pharmacol* **92**, 101 (2017).

247. Liang, J. *et al.* Plasticity of $GABA_A$ receptor-mediated neurotransmission in the nucleus accumbens of alcohol-dependent rats. *J Neurophysiol* **112**, 39–50 (2014).

248. Olsen, R. W. & Liang, J. Role of GABAA receptors in alcohol use disorders suggested by chronic intermittent ethanol (CIE) rodent model. *Mol Brain* **10**, 45 (2017).

249. Power, E. M. & Iremonger, K. J. Plasticity of intrinsic excitability across the estrous cycle in hypothalamic CRH neurons. *Sci Rep* **11**, 16700 (2021).

250. Raskind, M. A. *et al.* Trial of Prazosin for Post-Traumatic Stress Disorder in Military Veterans. *New England Journal of Medicine* **378**, 507–517 (2018).

251. Koola, M. M., Varghese, S. P. & Fawcett, J. A. High-dose prazosin for the treatment of post-traumatic stress disorder. *Ther Adv Psychopharmacol* **4**, 43–47 (2014).

252. Arora, B., Tandon, R., Attri, P. & Bhatia, R. Chemical Crosslinking: Role in Protein and Peptide Science. *Curr Protein Pept Sci* **18**, (2017).

253. Pacholko, A. G., Wotton, C. A. & Bekar, L. K. Astrocytes-The Ultimate Effectors of Long-Range Neuromodulatory Networks? *Front Cell Neurosci* **14**, 581075 (2020).

254. Herrera Moro Chao, D. *et al.* Hypothalamic astrocytes control systemic glucose metabolism and energy balance. *Cell Metab* **34**, 1532-1547.e6 (2022).

255. Ettaro, R., Laudermilk, L., Clark, S. D. & Maitra, R. Behavioral assessment of rimonabant under acute and chronic conditions. *Behavioural Brain Research* **390**, 112697 (2020).

256. Voet, S., Srinivasan, S., Lamkanfi, M. & Loo, G. Inflammasomes in neuroinflammatory and neurodegenerative diseases. *EMBO Mol Med* **11**, (2019).

257. Albano, R. & Lobner, D. Transport of BMAA into Neurons and Astrocytes by System xc-. *Neurotox Res* **33**, 1–5 (2018).

258. Parker, J. L. *et al.* Molecular basis for redox control by the human cystine/glutamate antiporter system xc−. *Nat Commun* **12**, 7147 (2021).

259. Jariyamana, N. *et al.* Effects of N-acetyl cysteine on mitochondrial ROS, mitochondrial dynamics, and inflammation on lipopolysaccharide-treated human apical papilla cells. *Clin Oral Investig* **25**, 3919–3928 (2021).

260. Handy, D. E. & Loscalzo, J. Redox Regulation of Mitochondrial Function. *Antioxid Redox Signal* **16**, 1323–1367 (2012).

261. Hung, C.-C., Lin, C.-H. & Lane, H.-Y. Cystine/Glutamate Antiporter in Schizophrenia: From Molecular Mechanism to Novel Biomarker and Treatment. *Int J Mol Sci* **22**, 9718 (2021).

262. Lohoff, F. W. *et al.* Epigenome-wide association study of alcohol consumption in N = 8161 individuals and relevance to alcohol use disorder pathophysiology: identification of the cystine/glutamate transporter SLC7A11 as a top target. *Mol Psychiatry* **27**, 1754–1764 (2022).